TECHNICAL REPORT STANDARD PAGE

1. Report No. **FHWA/LA.10/464**	**2. Government Accession No.**	**3. Recipient's Catalog No.**
4. Title and Subtitle **Application of Satellite Imagery for Surface Rain Rate Estimation**	**5. Report Date** March 31, 2010 **6. Performing Organization Code** **LTRC Project Number: 09-2TIRE** **State Project Number: 736-99-1643**	
7. Author(s) Shih A. Hsu and Brian W. Blanchard	**8. Performing Organization Report No.**	
9. Performing Organization Name and Address **Coastal Studies Institute** **Howe-Russell Geoscience Bldg.** **Louisiana State University** **Baton Rouge, LA 70803**	**10. Work Unit No.** **11. Contract or Grant No.**	
12. Sponsoring Agency Name and Address **Louisiana Department of Transportation and Development** **P.O. Box 94245** **Baton Rouge, LA 70804-9245**	**13. Type of Report and Period Covered** **Final Report** **April 2009 – May 2010** **14. Sponsoring Agency Code**	

15. Supplementary Notes
Conducted in Cooperation with the U.S. Department of Transportation, Federal Highway Administration

16. Abstract

As clouds grow through the troposphere, their upper surfaces cool with increasing altitude. An infrared sensor on board an orbiting satellite can detect these cloud top temperatures. Colder temperatures imply higher cloud tops, and these thicker clouds imply greater rain capacity. This simple relationship is the basis for estimating surface rainfall from satellite-derived cloud top temperatures. There are several computational methods in use and under development for generating these estimates. This study tests one basic rain-rate algorithm under various weather conditions in Louisiana. Hourly rain values calculated directly from the algorithm without atmospheric corrections were compared to near simultaneous surface rain gage measurements. Satellite data typically identify moderate to heavy rain events; however, calculated estimates can vary significantly from measured totals. Since many areas have no official rain gage measurement, or lie outside of reliable radar coverage, the satellite estimates as obtained here are still valuable as a first approximation.

17. Key Words Rain rate, GOES, infrared, water vapor, synoptic weather, Louisiana		**18. Distribution Statement** **Unrestricted. This document is available through the National Technical Information Service, Springfield, VA 21161.**	
19. Security Classif. (of this report)	**20. Security Classif. (of this page)**	21. No. of Pages 106	22. Price

Color Version Available

To view this report's graphs and tables in full color, please visit LTRC's Web site at **http://www.ltrc.lsu.edu/pdf/2010/fr_464.pdf** or use the CD provided (see back cover of printed report).

Application of Satellite Imagery for Surface Rain Rate Estimation

by

Shih A. Hsu and Brian W. Blanchard

Coastal Studies Institute
Louisiana State University
Baton Rouge, Louisiana 70803

LTRC Project No. 09-2TIRE
State Project No. 736-99-1643

conducted for

Louisiana Department of Transportation and Development
Louisiana Transportation Research Center

March 2010

ABSTRACT

As clouds grow through the troposphere, their upper surfaces cool with increasing altitude. An infrared sensor on board an orbiting satellite can detect these cloud top temperatures. Colder temperatures imply higher cloud tops, and these thicker clouds imply greater rain capacity. This simple relationship is the basis for estimating surface rainfall from satellite-derived cloud top temperatures. There are several computational methods in use and under development for generating these estimates. This study tests one basic rain-rate algorithm under various weather conditions in Louisiana. Hourly rain values calculated directly from the algorithm without atmospheric corrections were compared to near simultaneous surface rain gage measurements. Satellite data typically identify moderate to heavy rain events; however, calculated estimates can vary significantly from measured totals. Since many areas have no official rain gage measurement, or lie outside of reliable radar coverage, the satellite estimates as obtained here are still valuable as a first approximation.

IMPLEMENTATION STATEMENT

Satellite-derived rain rates can provide continuous surface rainfall estimates in areas without an official rain gage station as well as those outside of radar coverage. These estimates can be applied to modeling geophysical and hydrologic scenarios, such as surface runoff, flooding, streamflow, and scour.

The following are some potential applications of satellite-derived rainfall estimates for the Louisiana Department of Transportation and Development (LADOTD). At the request of the Louisiana Office of Risk Management, the authors performed numerous hydroplaning legal studies using methods as provided in this study. The Louisiana Transportation Research Center (LTRC) has funded Louisiana State University (LSU) a separate research project entitled "Evaluation of Design Methods to Determine Scour Depths for Bridge Structures" (Dr. Guoping Zang, PI, and Drs. Shih A. Hsu and Tim Tingzong Guo, Co-PIs). Satellite-derived rain estimates are an integral component for this scour research. Finally, LSU's agricultural weather stations provide near real-time evapotranspiration data. This data combined with satellite-derived rain estimates can yield regional soil moisture conditions. With this information, the safety and efficiency of highway maintenance scheduling may be enhanced.

TABLE OF CONTENTS

LIST OF TABLES

LIST OF FIGURES

INTRODUCTION

Rainfall events can directly affect the surface transportation infrastructure and disrupt routine operations. Extended periods of light to moderate rain can saturate the topsoil, leading to excessive runoff, inundation, and roadway damage. More intense events can cause widespread flooding that may ultimately increase flows in waterways, thereby impacting bridges and overpasses immediately from floating debris and, in the longer term, through potential scouring around supporting structures. Of course, highway safety during rain is a primary concern.

Traditionally, characteristics of rainfall events have been derived from rain gage data and radar observations. However, the number of official rain gage stations is relatively small, and their wide spatial distribution may not accurately represent a particular location of interest. Radar rain estimates are well accepted, but anomalous atmospheric propagation and the earth's curvature can introduce errors over distance.

More recently, infrared (IR) cloud top temperatures (CTTs) as observed by satellite are being employed to estimate a surface rain rate. A primary advantage of this method is the excellent spatial and temporal resolution of the imagery that is typically available in near real time. The Geostationary Operational Environmental Satellite (GOES) system provides IR imagery at 15- to 30-minute intervals with a resolution of 4 x 4 kilometers, or about 2.5 x 2.5 miles. Since the late 1970s, many algorithms and calibration techniques for relating CTT to surface rain rate have been developed and tested *[1]*, *[2]*, and *[3]*. The most current methods in use by the U.S. Federal government rely not only on GOES data, but also numerical model data, microwave rain rates, and other corrective factors to produce rain estimates (see www.star.nesdis.noaa.gov). An earlier method, the Automated Satellite Rainfall Rate Estimation technique, or Auto-Estimator, developed by Vincente et al. provided a formulation to directly estimate rain rate from IR CTT alone as one part of its computational process *[1]*.

The purpose of this brief study is to determine the applicability of this basic Vincente formulation for operational use in Louisiana. This will be accomplished by comparing the rain rates computed from GOES IR CTTs to actual rain gage measurements under a variety of synoptic weather situations.

OBJECTIVE

In response to the Request for Proposals issued by the Louisiana Transportation Research Center for Transportation Innovation for Research Exploration (TIRE) Awards, 2009, this study was developed to investigate and apply the burgeoning technology of satellite derived rain rates to Louisiana weather conditions. These conditions will be described by general synoptic weather type, and frequency of occurrence will be discussed. Hourly rain gage measurements from selected surface stations were acquired. Satellite image processing software was used to analyze GOES imagery recorded nearest coincident in space and time to the rain gage values. These values were then compared to the Vincente satellite rain-rate formulation.

SCOPE

This study only considers GOES satellite imagery, the basic Vincente rain rate formulation, and Louisiana rainfall events. Other more complex rain rate methods and calibration techniques are available and in use operationally, but only the direct CTT-rain rate relation is tested here.

METHODOLOGY

For this analysis, two primary sets of data were required. Five airport surface stations from across Louisiana were selected for hourly rainfall measurements (Figure 1). They were Shreveport (SHV, 32.45N 93.817W), Monroe (MLU, 32.517N 92.033W), Baton Rouge (BTR, 30.533N 91.15W), Lake Charles (LCH, 30.117N 93.233W), and New Orleans (MSY, 30.0N 90.25W). Given the importance of their airport setting, it was anticipated that these stations would be well maintained and yield the greatest data return. Actual precipitation values were obtained from *Hourly Precipitation Data Louisiana*, a publication issued monthly by the National Oceanic and Atmospheric Administration *[4]*.Total accumulated rainfall in inches is recorded for each hour in local standard time (CST). According to the Glossary of Meteorology, rain totals from a trace to 0.1 in. are considered as light; therefore, all hourly totals greater than or equal to 0.1 in. were retained to represent moderate to heavy rain conditions *[5]*.

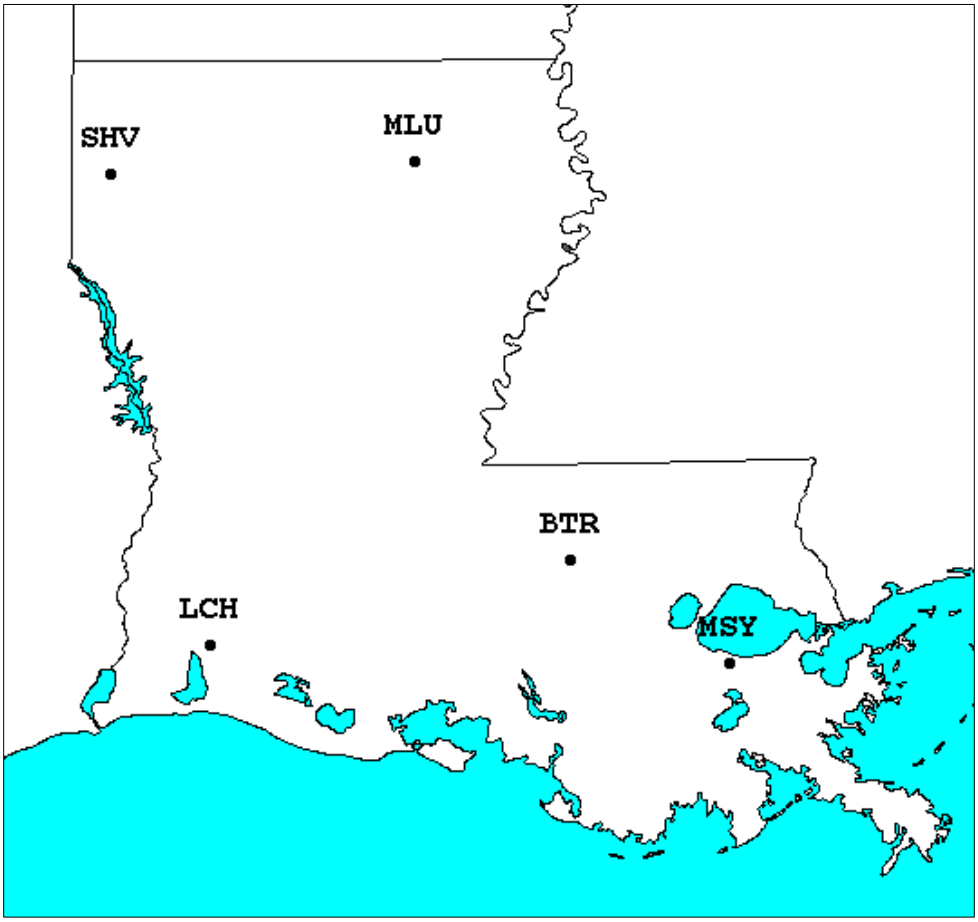

Figure 1
Location map of Louisiana surface weather stations used in this study

With the Earth Scan Lab, Louisiana State University maintains an archive of approximately 10 years of digital GOES data. Images are saved at 30-minute intervals and include visible (daytime), water vapor, and IR spectral channels. The data were processed using XVU and Terrascan software packages. For each hour with recorded surface rainfall, the corresponding two 30-minute satellite images (15 and 45 minutes past the hour) were examined and the IR CTT values over the affected stations obtained and averaged for an hourly IR temperature. This IR value was then input into the Vincente formulation, and an hourly rain rate computed for comparison to the measured value.

Several considerations led to the selection of year 2008 for analysis. Being the most recent complete year at project start, the satellite data return was high and of the best quality. In September 2008, Hurricane Gustav traveled across Louisiana, providing an ideal tropical rain situation. On the other hand, La Nina conditions also prevailed throughout most of 2008, causing drier than normal rain totals. From Figure 2, only the Monroe station total was near the 30-year average, with the other stations approximately 10-25 percent below average. Nevertheless, 589 samples of moderate to heavy rain were available for study.

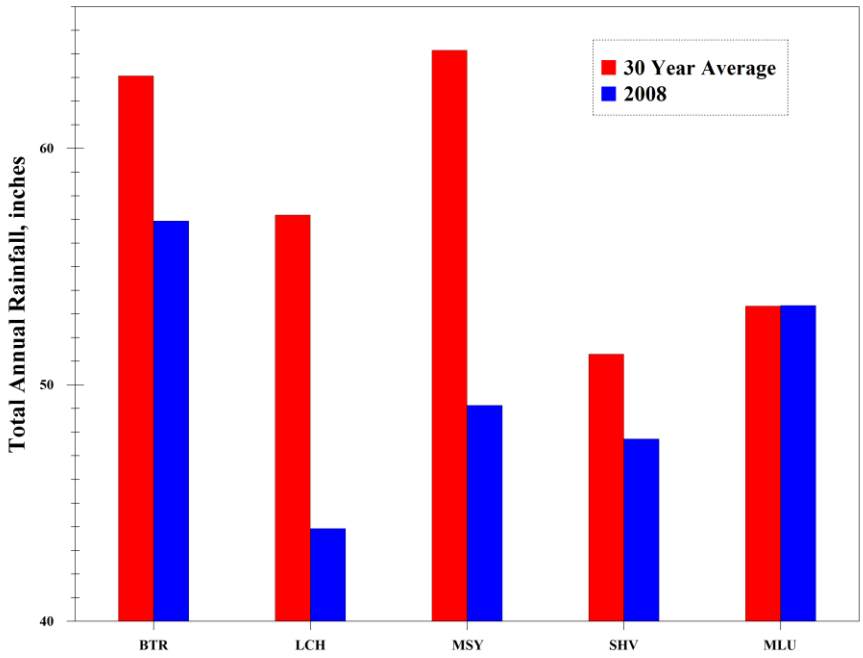

Figure 2
30-year normal precipitation and 2008 totals for selected stations (data source: Louisiana Office of State Climatology [LOSC] and Southern Regional Climate Center [SRCC] *[6]*, *[7]*)

DISCUSSION OF RESULTS

Dominant Weather Patterns Affecting Louisiana

Precipitation occurs when the tiny water droplets or ice crystals composing a cloud grow large enough that gravity causes them to fall. Reaching the ground in liquid form, it is termed rain and may be classified by intensity and duration. Generally, steady, lighter rain is associated with widespread stratiform, or layered, clouds. Intermittent, heavier rain, or showers, is observed mostly with cumuliform clouds, which grow vertically through the troposphere due to convection and instability *[8]*.

As weather patterns change over time, a variety of cloud types, and in turn precipitation patterns, may be observed. Muller used 0600 CST daily weather maps to classify the atmospheric circulation patterns into one of eight all-inclusive synoptic weather types for the New Orleans, Louisiana region (Figures 3 – 6) *[9]*. Brief descriptions of each type are as follows (for more detail, see *[10]* and *[11]*):

- Pacific High (PH): After a "Pacific" cold front, the weather is normally fair and mild with west to northwest winds. Prior to the frontal passage, stronger southerly flow prevails.

- Continental High (CH): Associated with polar or Arctic outbreaks. North and northeasterly winds prevail. Fair weather.

- Frontal Overrunning (FOR): This cloudy and rainy type occurs frequently in the fall and winter when cold fronts become stationary near the Gulf coast. Cooler continental air at surface on northern side of front is overrun by warmer tropical air.

- Coastal Return (CR): Wind around high pressure centered over eastern Canada brings easterly, southerly, and southeasterly winds. In summer includes the Bermuda High pattern.

- Gulf Return (GR): Similar to CR but has stronger winds due to developing low pressure system over Texas.

- Frontal Gulf Return (FGR): Cold front approaching from the west-northwest generates strong southerly return flow and stormy conditions.

- Gulf High (GH): High center near Louisiana coast, calm and clear conditions.

- Gulf Tropical Disturbance (GTD): The influence of tropical weather systems such as easterly waves and hurricanes.

Table 1 lists the frequency of occurrence of each weather type affecting the New Orleans region for a 30-year normal period (1961 – 1990). Four of the types are plotted in Figure 7. A strong seasonal signature is evident; for example, FOR conditions peak in the winter and GH in the summer.

Table 1
Synoptic weather type frequency (in percentage) at New Orleans, Louisiana from 1961 through 1990

Month	PH	CH	FOR	CR	GR	FGR	GH	GTD
Jan	4	23	37	7	11	13	5	0
Feb	6	23	31	7	11	16	6	0
Mar	6	21	24	9	21	16	3	0
Apr	5	20	13	10	31	15	6	0
May	4	20	13	12	28	15	7	1
Jun	0	17	7	15	27	11	19	5
Jul	0	6	4	16	20	8	36	10
Aug	0	14	7	21	16	8	25	9
Sep	1	29	13	19	14	7	6	12
Oct	3	42	16	16	10	8	3	2
Nov	4	30	23	12	15	13	2	1
Dec	4	26	32	6	12	16	4	0
Annual	3	23	18	13	18	12	10	3

PH: Pacific High; CH: Continental High; FOR: Frontal Overrunning; CR: Coastal Return; FGR: Frontal Gulf Return; GH: Gulf High; GTD: Gulf Tropical Disturbance (see Muller and Wax, *[12]*).

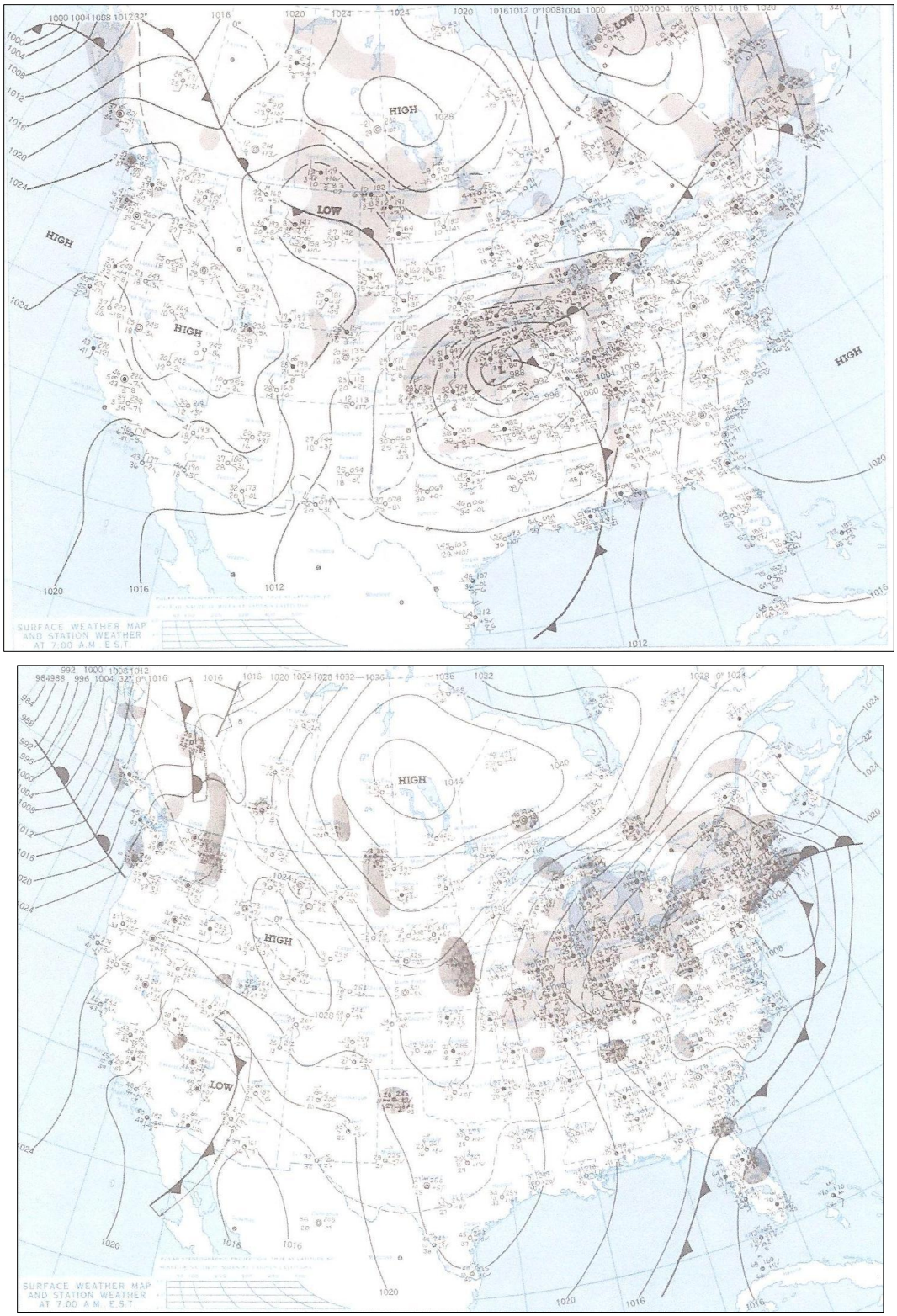

Figure 3
Examples of Pacific high (top) and continental high (bottom) synoptic weather types

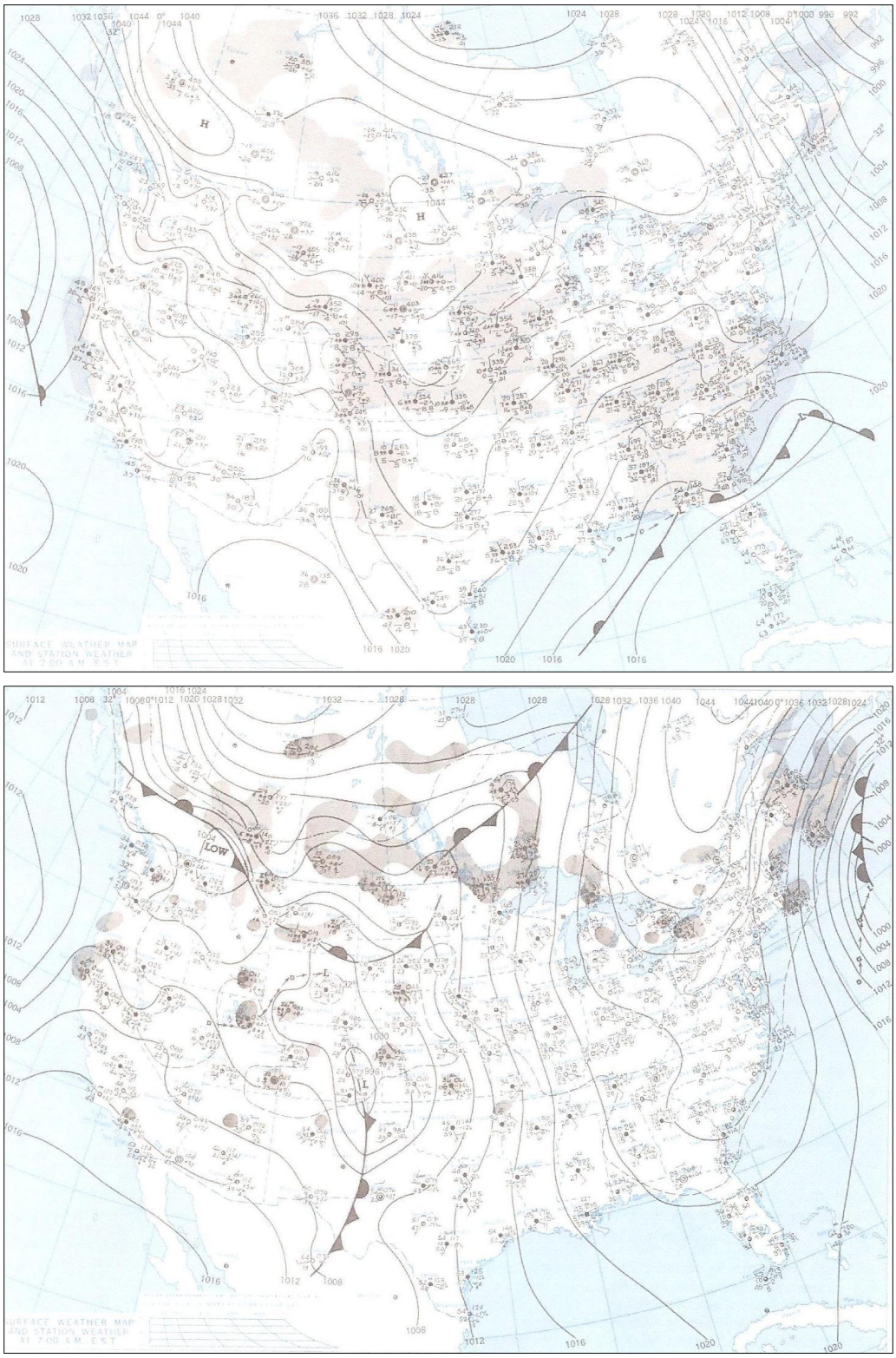

Figure 4
Examples of frontal overrunning (top) and coastal return (bottom) synoptic weather types

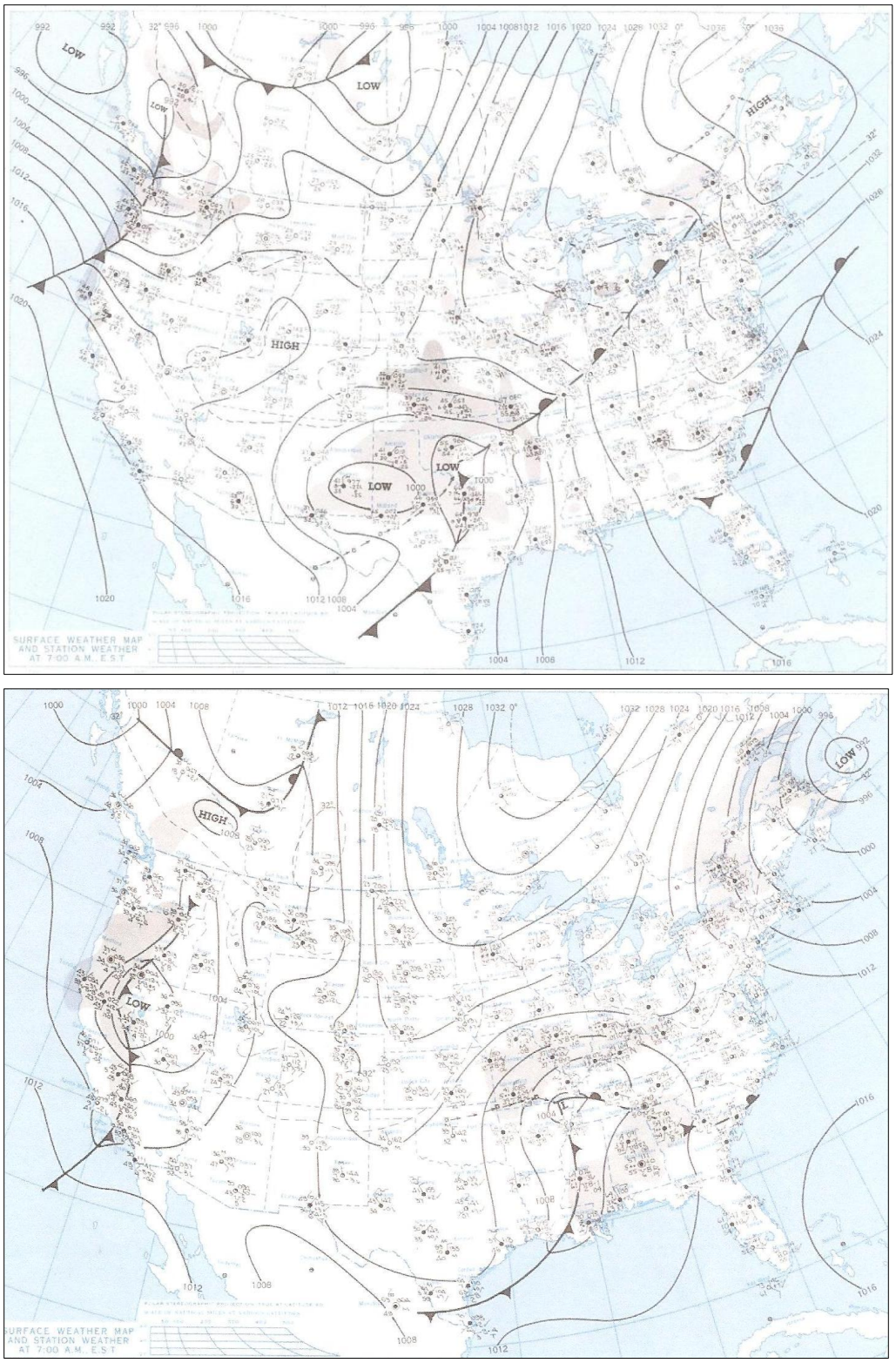

Figure 5
Examples of Gulf return (top) and frontal Gulf return (bottom) synoptic weather types

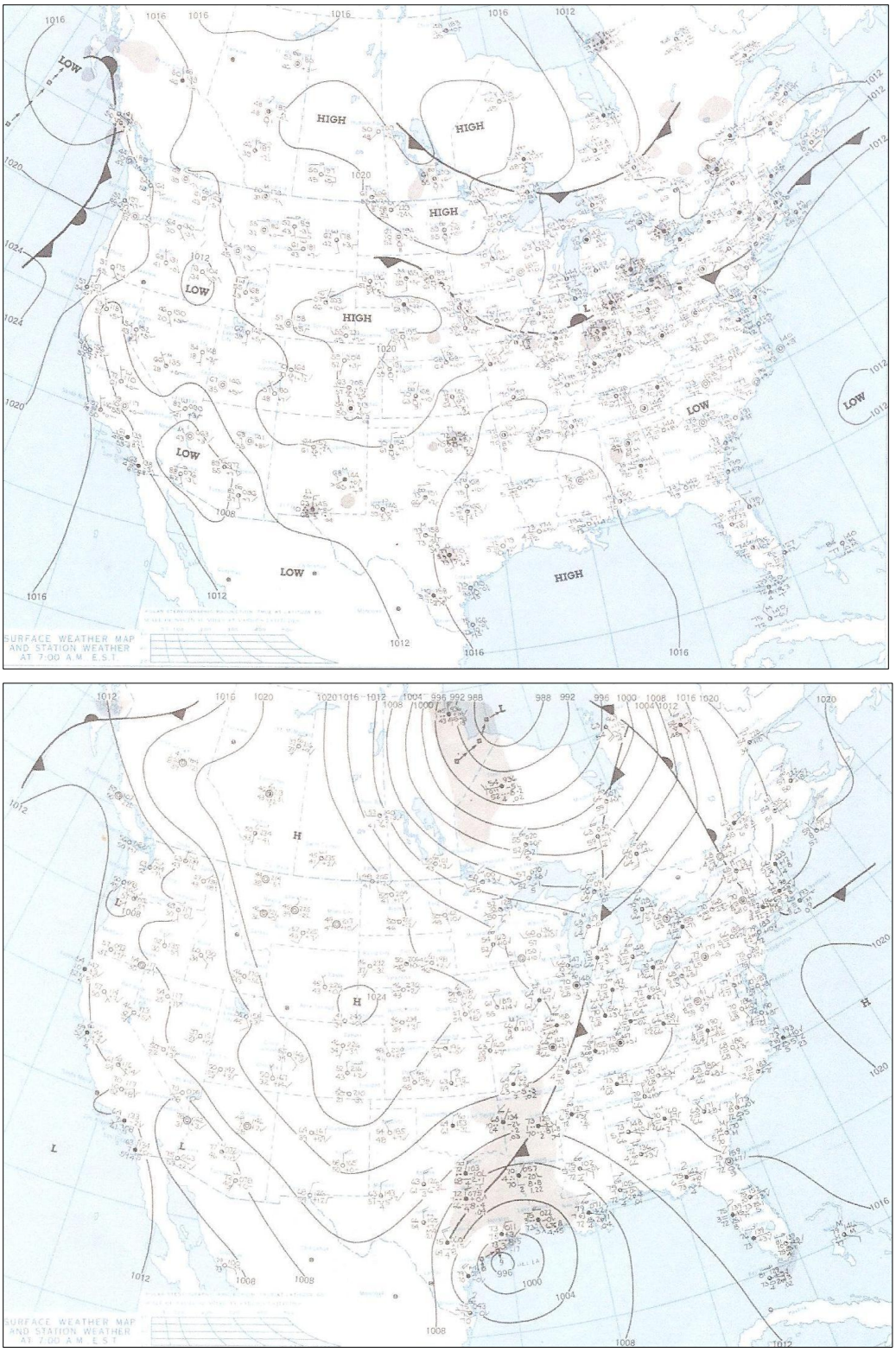

Figure 6
Examples of Gulf high (top) and Gulf tropical disturbance (bottom) synoptic weather types

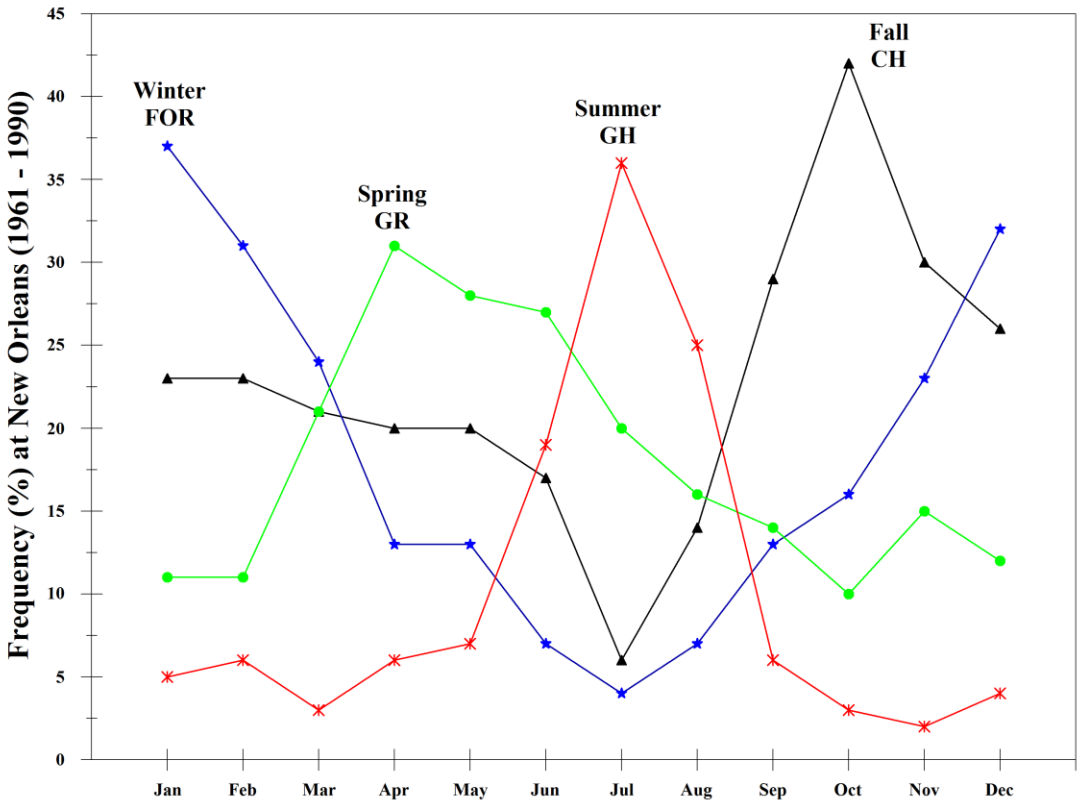

Figure 7
Frequency of occurrence for four weather types over New Orleans

According to Muller and Wax, precipitation across southern Louisiana is mostly associated with the FGR and FOR patterns, followed by GTD and GR *[12]*. During FOR, warm moist Gulf air rises northward across the stationary front and over the cooler, more continental air at the surface. This gentle lifting produces a broad area of mostly stratiform clouds, which can bring light to moderate steady rain for extended periods of time. The other synoptic patterns likely generate more cumuliform cloud and rain due to rapid frontal forcing and atmospheric instability. A developing low pressure system moving toward Louisiana from the west is usually preceded by a warm front that moves northward from the Gulf across the state. The warm front can bring stratiform rain and is followed by unstable maritime air from the south. The low center and trailing cold front then sweeps in from the west, causing rapid lifting of the moist air leading to cumulus development, often in the form of a squall line. Storm cells along the squall line and subsequent frontal zone can cause torrential rain and extensive damages (due to winds, lightning, hail, etc.). During summer months, CR and GR patterns promote southerly flow and a continuous influx of moist Gulf air. Daytime heating of this unstable air mass spurs widespread cumulus formation. Under favorable conditions, these individual cloud masses can grow into scattered afternoon thunderstorms (“popcorn”

storms). Tropical systems, including easterly waves and tropical storms, occasionally produce heavy convective rain during hurricane season.

Figure 8 illustrates the 100-year rainfall patterns for 3-, 12-, and 24-hour accumulations. A similar pattern emerges for all three, with maximum accumulations along the Gulf coast, particularly in southeast and southwest Louisiana, decreasing in magnitude to the north. The smaller values centered over southeastern Louisiana may be due to the stabilizing effect of the Lake Pontchartrain system *[13]*.

2008 Data Analysis

Geosynchronous IR satellite imagery is derived from emissions by the Earth and atmosphere at thermal infrared wavelengths (10 – 12 μm). IR provides information on the temperature of the underlying surface or cloud. Since temperature normally decreases with height, the IR radiation with the lowest intensity is emitted by the highest and coldest clouds. Hence, good contrast is seen amongst clouds of varying heights *[14]*. The application of IR imagery for estimating surface participation rates is based on the basic assumption that clouds with cold tops are higher and thicker and will therefore produce more rainfall than those with warmer tops. For example, convective thunderstorms are characterized by very low CTTs and rapid spatial and temporal changes in the cloud top structure *[1]*. Enhancement of the GOES sensor platform now allows near-continuous monitoring of cloud systems at a resolution (field of view) of four km, making it suitable for nowcasting, river forecasting, and land surface modeling (after corrections) *[15]*.

Several computational techniques have been developed for estimating surface rain rate from satellite IR imagery. In general, each begins with an empirical relationship between GOES IR temperature and surface rainfall estimates (radar or gage derived). For this study, the basic formulation developed by Vincente et al. is employed such that *[1]*:

$$R = 4.4027\ x\ 10^{9}\ e^{\left(-3.6382\ x\ 10^{-2}(T+273.16)^{1.2}\right)} \quad (1)$$

where, R is the rain rate in in/hr and T is the CTT in °C. No corrections or calibrations were applied as the goal was to compare the computed R derived from CTT directly to measured rain gage data.

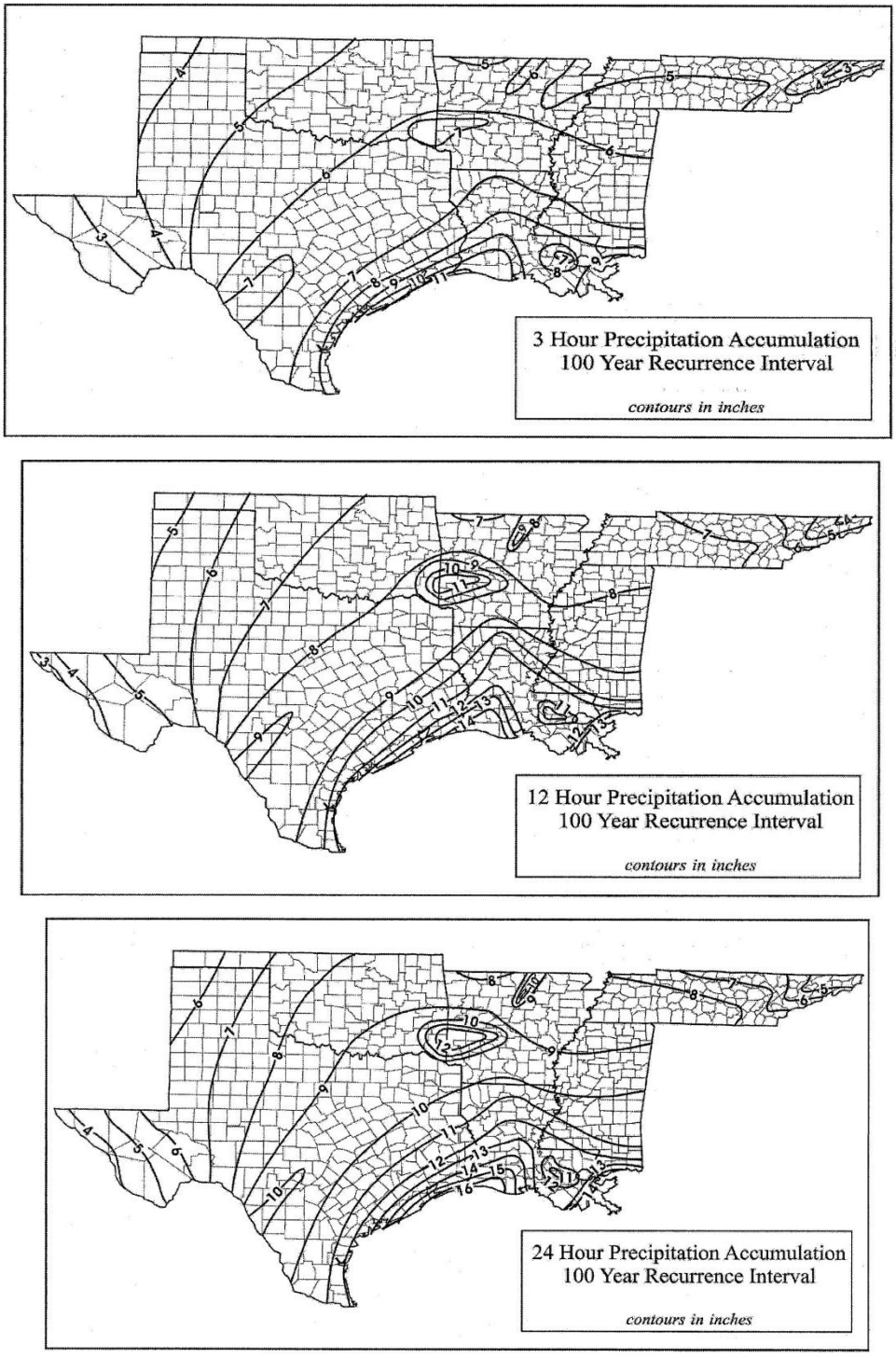

Figure 8
Three-, 12-, and 24-hour 100-year rainfall patterns (from *[13]*)

Hourly raingage measurements and GOES IR data for 2008 were processed as described in the Methodology section. The majority of all hourly rain samples were well below 0.5 in., with heavy rain events occurring most frequently in the spring and summer (Figure 9). The distribution of satellite and raingage values is provided in Figure 10. Recall that the minimum raingage value selected was 0.1 in. in order to exclude light rain and drizzle events. IR temperatures range from nearly -75°C to 25°C, with considerable scatter throughout. The bottom panel of Figure 10 is a comparison between GOES spectral channel 4 (IR) and channel 3 (water vapor, WV) values. Water vapor imagery is observed at 6.7 μm, where water vapor tends to absorb radiation. A dark pixel (warm) indicates strong radiation sensed, implying little water vapor (dry). Conversely, a bright pixel (moist) suggests that radiation was absorbed by water vapor (weaker radiation sensed). Water vapor imagery only works in the mid- to upper-troposphere *[16]*. From Figure 10, there is a near one-to-one agreement between channels 3 and 4 below about -45°C. Therefore, it can be inferred that these extremely cold temperatures are associated with a very moist troposphere and deep convection. This is significant because IR rain rate techniques are most applicable for cold convective clouds, while poor results are common for stratiform clouds with warm CTT *[1]*, *[2]*. Substituting an R value of 0.1 in./hr into equation (1) yields an IR CTT of approximately -45°C. Based on these discussions and because we are primarily interested in moderate to heavy rain events, we set the maximum value for our IR data to -45°C, leaving 257 values.

For better visualization, the remaining data were separated into 12 class intervals of 2.5°C and mean values derived. There is reasonable agreement between these class means and equation (1) within the IR range of -45° to approximately -61°C; however, the measured values mostly fall well below the computed curve towards the lower end of the data range (Figure 11). This is due in part to the small number of samples available at these extreme temperatures, as depicted in Figure 12. Furthermore, Vincente et al. note that the rain estimation technique overestimates the area of rainfall amounts that are associated with slow-moving cold topped mesoscale convective systems (MCSs) with large cirrus cloud shields *[1]*. The cloud tops of mature convective thunderstorms can reach or exceed the tropopause level. At these heights the temperature is well below freezing, and the cloud top is composed of ice crystals (the cirrus anvil), which produces little or no precipitation. Afternoon radiosonde data from the National Weather Service Slidell station was analyzed and the mean and standard deviation of the tropopause temperature was found to be -67°C ± 5.7°C (Figure 13). Since the first quartile value of the temperature data is about -59°C and one deviation of the tropopause -61°C, the data comparison was concentrated within the range of -45°C to -61°C.

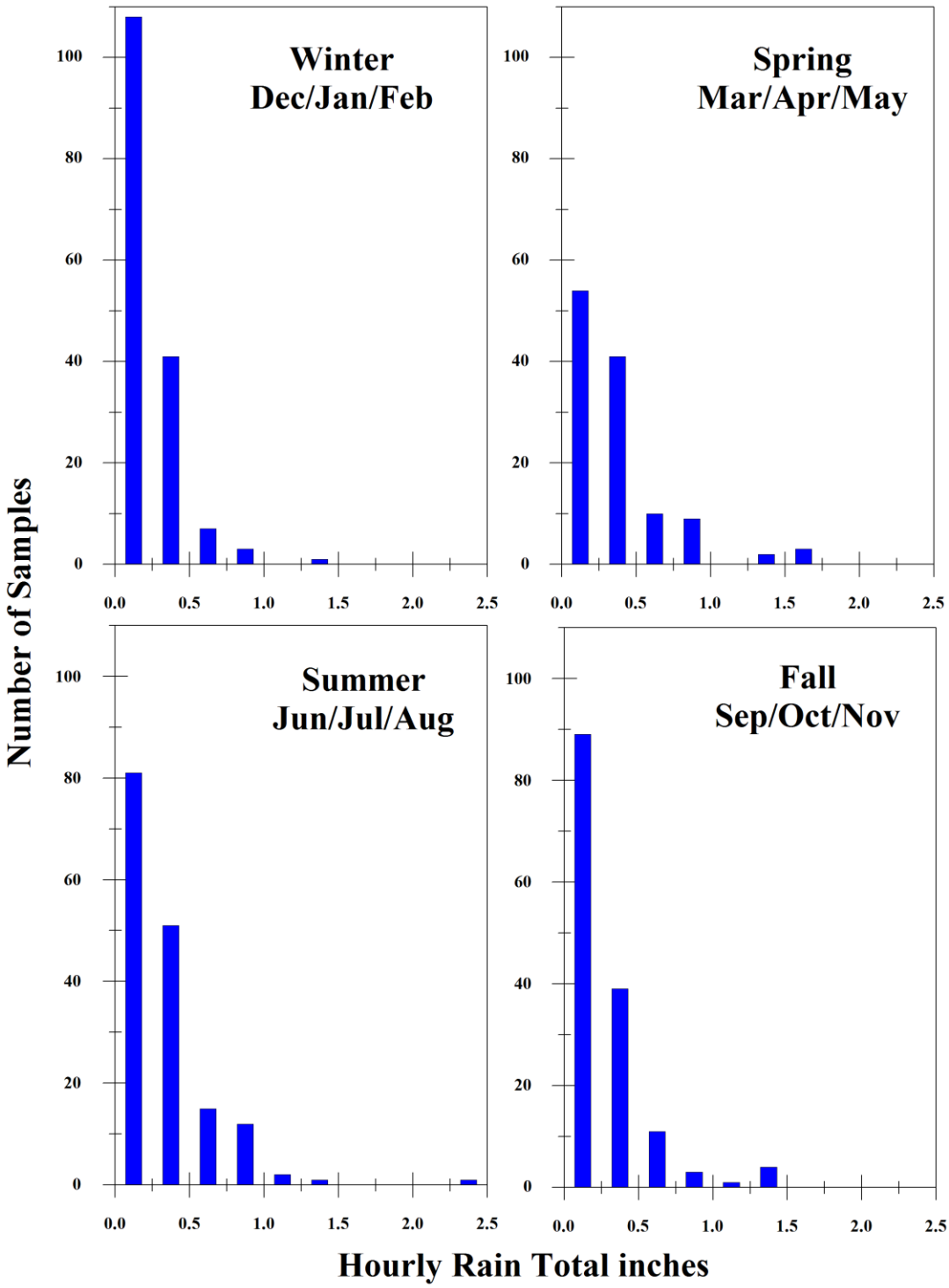

Figure 9
Seasonal distribution of hourly rainfall intensities from selected stations during 2008

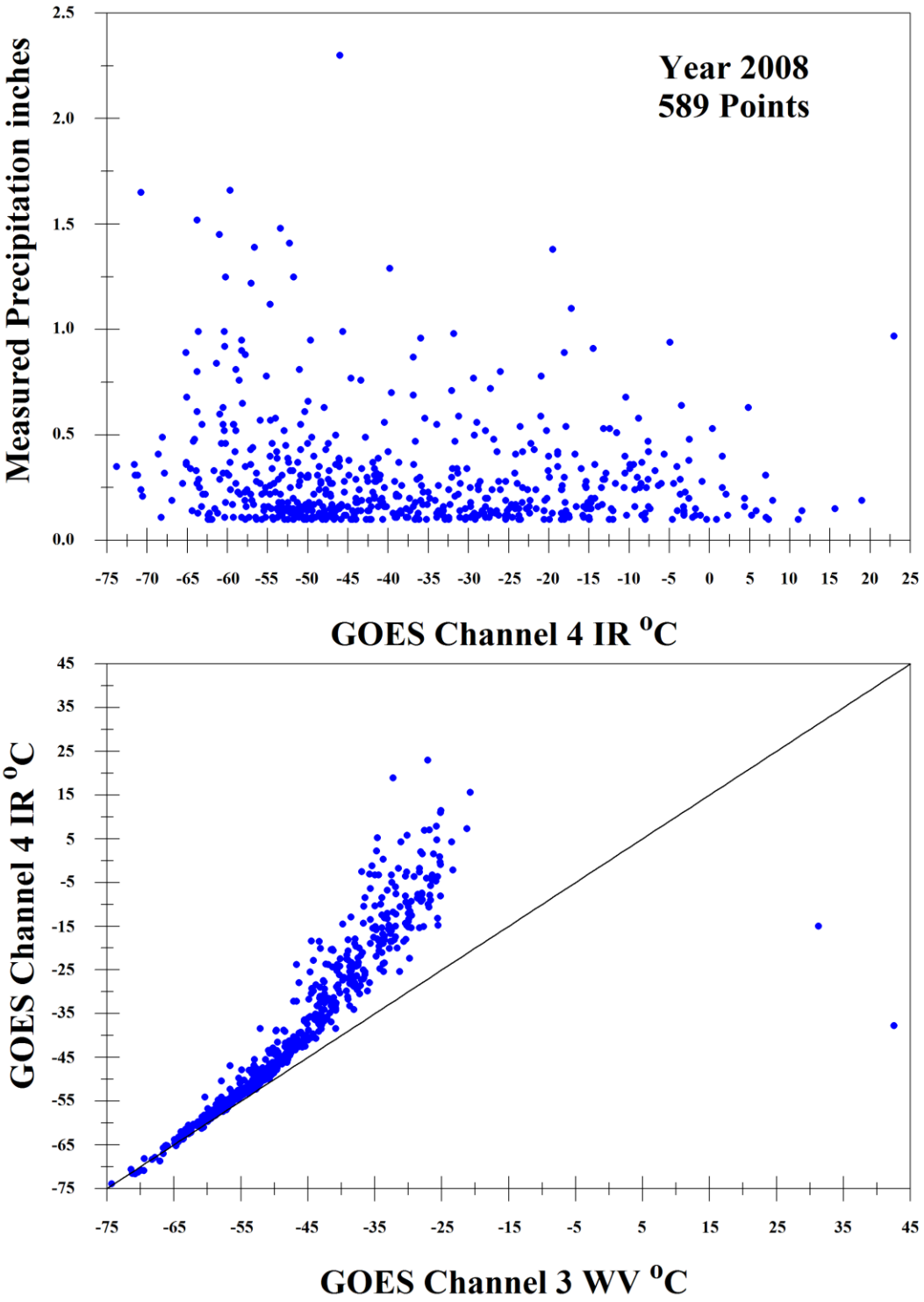

Figure 10
Distribution of measured hourly rainfall with GOES IR temperatures (top) and one-to-one comparison of simultaneous GOES IR and water vapor values (bottom)

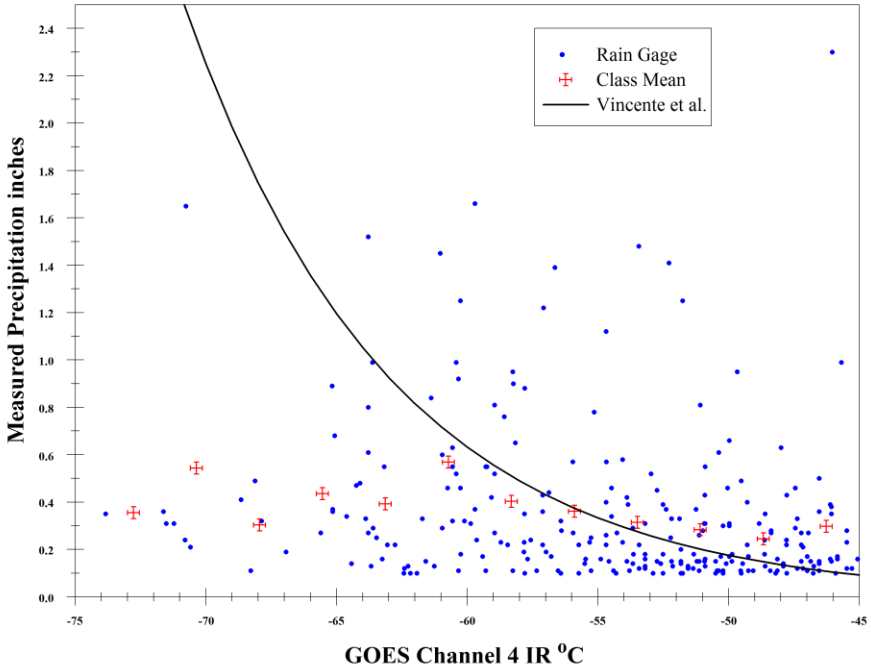

Figure 11
Distribution of measured hourly rainfall and class means with GOES IR; solid line is equation (1)

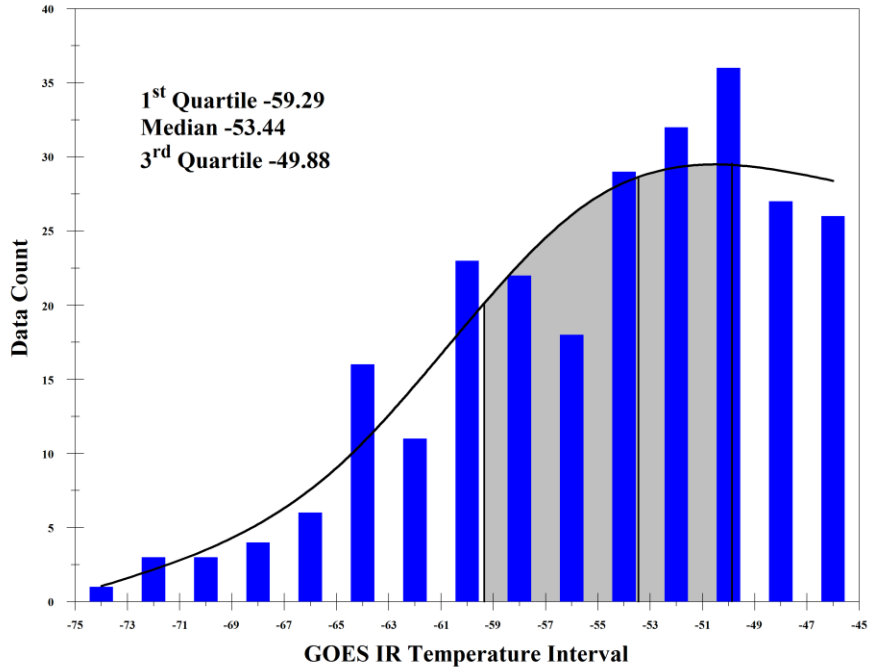

Figure 12
Frequency of occurrence of GOES IR data values

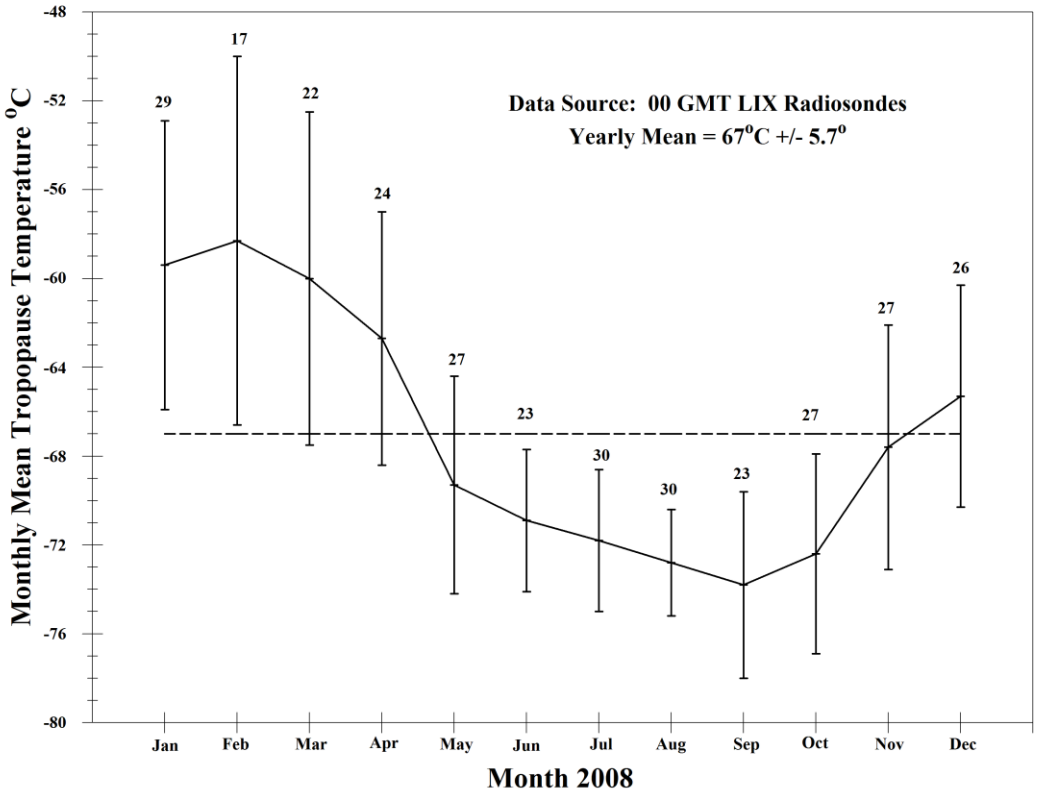

Figure 13
Mean and standard deviation of monthly 00 UTC (1800 CST) tropopause temperatures from the National Weather Service Slidell station

A box plot diagram of the remaining data is provided in Figure 14. Median values are clearly below the means, reflecting the greater number of smaller magnitude values. A third-order polynomial provided the best fit to the mean values such that:

$$DR = -4.497462 - 0.364705T - 0.008889T^2 - 0.00007T^3 \quad (2)$$

with a correlation coefficient of 0.97. Both the Vincente formulation [equation (1)] and the derived equation (2) fall within the first and third quartiles of the measured data (Figure 15), and extending to the mean tropopause temperature shows reasonable agreement in trend (Figure 16). Note that Vincente et al. recommend that the rain rate be limited to 2.84 in/hr for IR temperatures less than -73°C *[1]*.

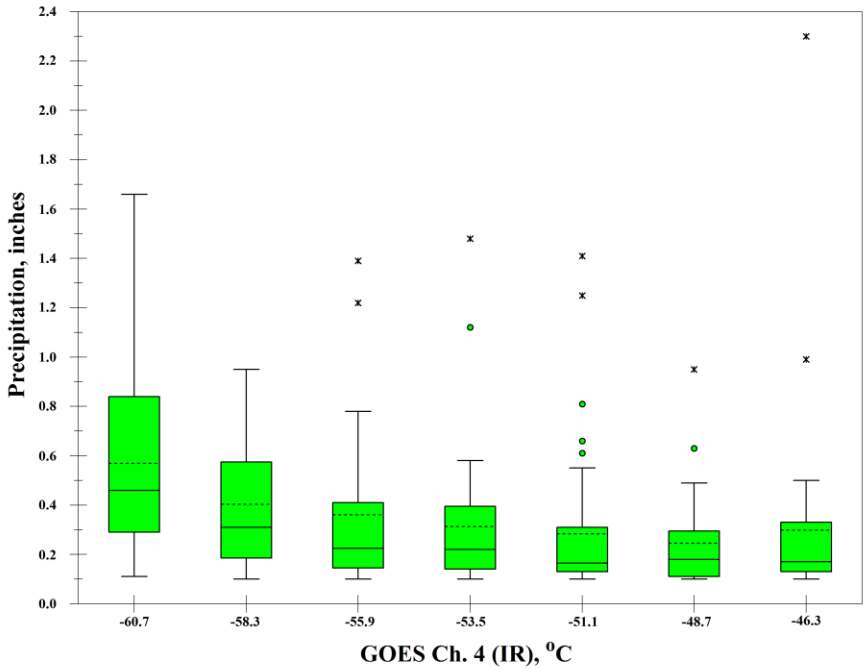

Figure 14
Box diagram of rainfall data. Lower and upper limits of box are first and third quartiles, solid line is second quartile (median), and dashed line is class mean

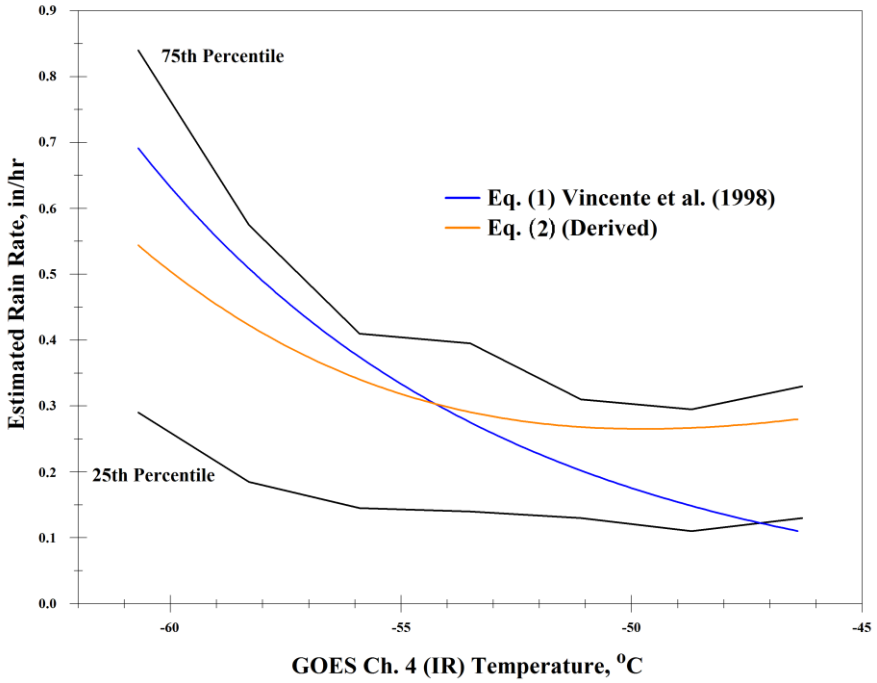

Figure 15
Distribution of Vincente algorithm [equation (1), blue] and derived formula [equation (2), orange]

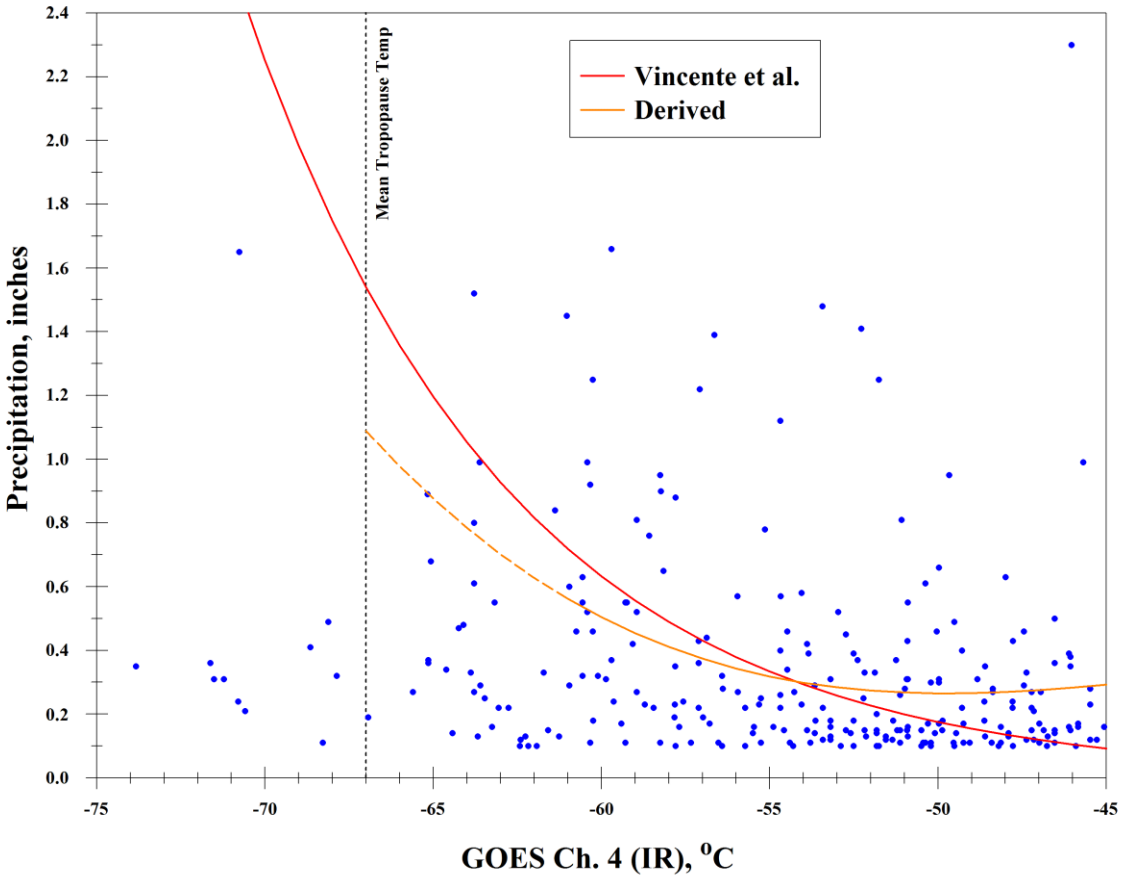

Figure 16
Distribution of data with rain-rate formulations

Case Studies

Case studies of moderate to heavy rain events were selected from the 2008 hourly raingage data in order to test the performance of the satellite IR rain estimations. Multiple events from each station throughout the year were chosen so that a variety of prevailing weather conditions could be examined. For each event, a surface weather map, a time series of GOES IR temperature (point and area average) and hourly rainfall, and selected contoured GOES IR images are presented. The contour lines in the satellite images are for -45°C (yellow), -55°C (orange), and -65°C (cyan).

January 31, Baton Rouge (BTR) (Table 2, Figures 17 - 19)

An occluded low system and cold front moved from west to east across Louisiana, Frontal Gulf Return becoming Pacific High. Probable squall line and heavy rain with the front, cumulonimbus (CB) and thunder were reported. Figure 19 shows a cold convective cell (less than -55°C) moving over the observing station. Good agreement existed between CTT and measured rain, however computed a very low total.

Table 2
Selected surface observations from BTR on January 31, 2008 CST

Time	Sky Condition	Visibility	Weather Type
1353	SCT030CB BKN045 OVC060	9	-RA
1401	SCT020CB BKN030 OVC060	6	TSRA
1416	BKN020CB BKN040 OVC060	2	TSRA
1453	BKN010 BKN020CB OVC030	2	+TSRA BR
1553	FEW003 BKN017CB OVC034	2	TSRA BR
1627	FEW005 OVC034	6	-RA BR

Sky Conditions:
FEW—> 0/8 to 2/8 sky cover
SCT—Scattered, 3/8 to 4/8 cover
BKN—Broken, 5/8 to 7/8 cover
OVC—Overcast, 8/8 cover
VV—indefinite ceiling with vertical visibility in hundreds of feet agl
CB—Cumulonimbus
TCU—Towering Cumulus
Numbers following sky cover are base heights in hundreds of feet agl, (for example, 030 is 3000 feet)

Visibility in statute miles

Weather Type:
RA—Rain
TSRA—Thunderstorm/Rain
BR—Mist
FG—Fog
TS—Thunderstorm
VC—Vicinity
+ is Heavy, - is light, no sign is moderate

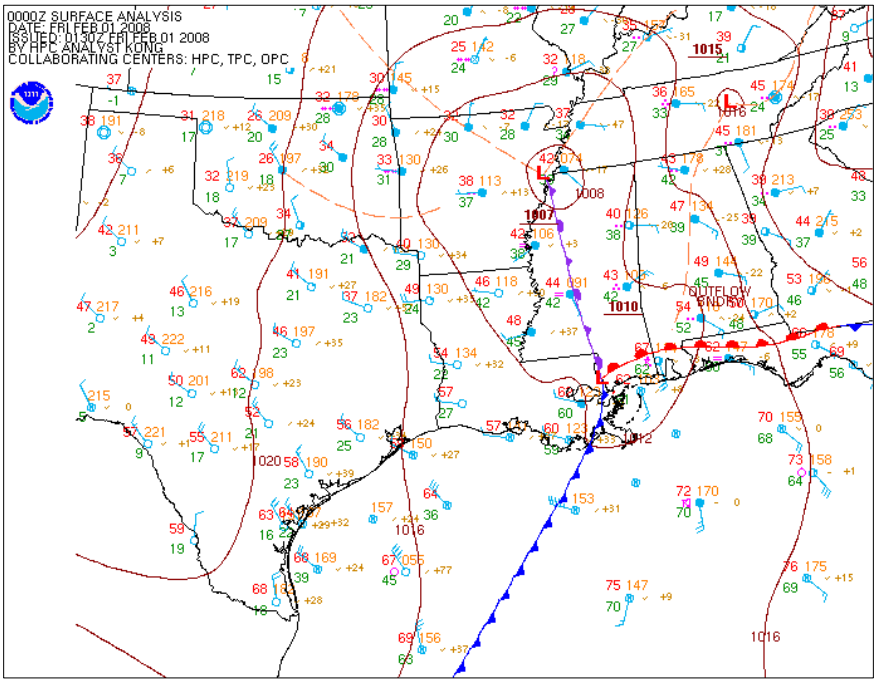

Figure 17
February 1, 2008 00 UTC (January 31, 1800 CST) surface weather map

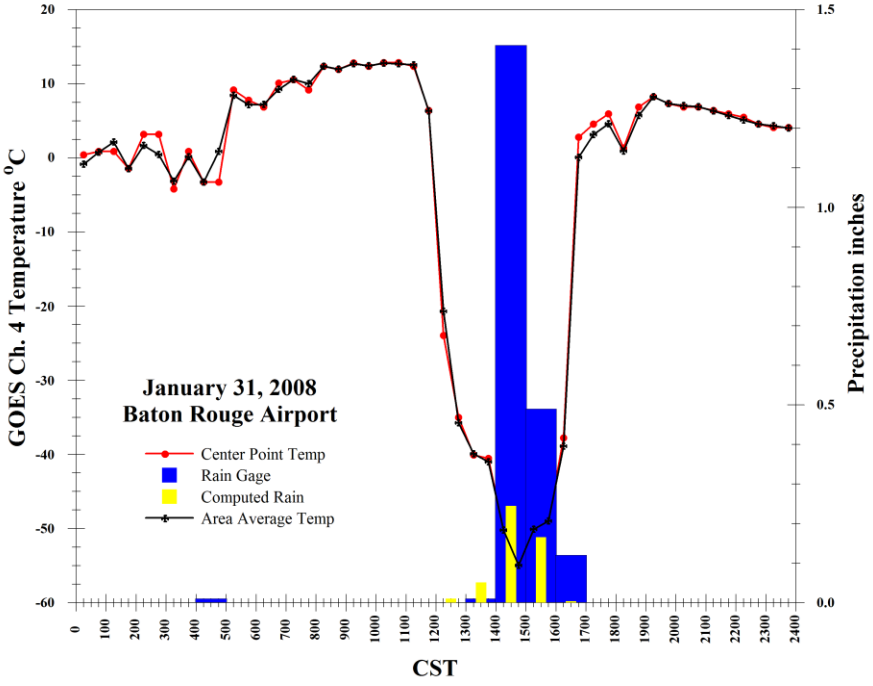

Figure 18
Time series of IR temperature along with measured and estimated rainfall totals for January 31, 2008 at BTR

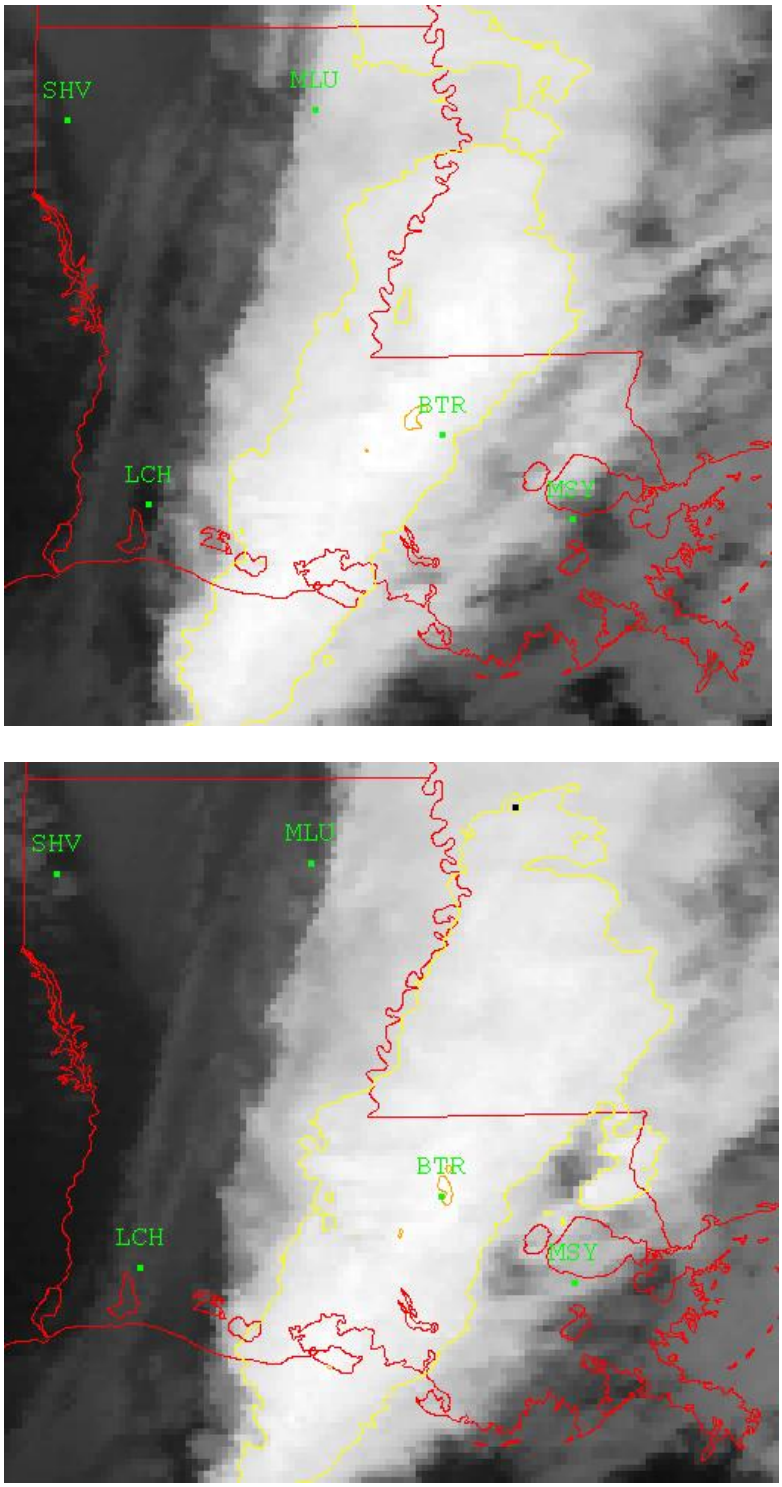

Figure 19
GOES IR image at 2015 UTC (1415 CST) (top) and 2045 UTC (1445 CST) (bottom) on January 31, 2008. Yellow contour is -45°C and orange is -55°C

February 12, Lake Charles (LCH) (Table 3, Figures 20 – 22)

A cold front extended to the southwest across Louisiana from a low over Kentucky, Coastal Return becoming Continental High. A large, cold cloud mass covered most of the state. Figure 22 shows the very cold MCS affecting the observing station with minimum CTTs less than -65°C. No CB reported, but likely embedded as thunderstorms were noted. Good agreement existed between temperatures and recorded rain, estimates much higher than measured values.

Table 3
Selected surface observations from LCH on February 12, 2008 CST
(coded as in Table 2)

Time	Sky Condition	Visibility	Weather Type
1323	FEW024 BKN038 OVC047	2.5	TSRA
1331	FEW016 BKN038 OVC047	1.5	TSRA BR
1336	FEW016 SCT039 OVC047	3	TSRA BR
1345	FEW018 SCT024 OVC047	1.75	TSRA BR
1353	SCT018 BKN033 OVC047	1	TSRA BR
1403	SCT017 BKN022 OVC047	1.25	TSRA BR
1420	FEW016 BKN024 OVC075	2.5	TSRA BR
1431	FEW016 BKN026 OVC075	1.75	TSRA BR
1451	FEW014 SCT024 OVC030	2	TSRA BR
1453	FEW014 SCT024 OVC036	2	TSRA BR
1503	FEW011 OVC040	3	RA BR
1553	FEW039 BKN049 OVC100	5	RA BR
1646	SCT011 BKN019 OVC075	6	RA BR
1653	SCT011 OVC019	9	RA
1714	SCT015 BKN022 OVC027	10	RA
1730	FEW005 BKN015 OVC022	10	RA

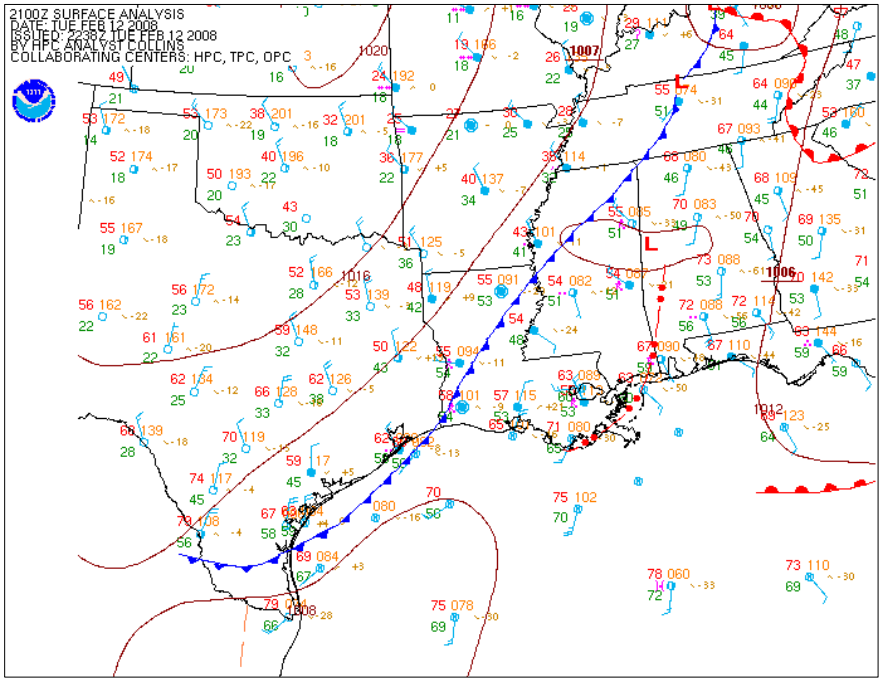

Figure 20
February 12, 2008 2100 UTC (1500 CST) surface weather map

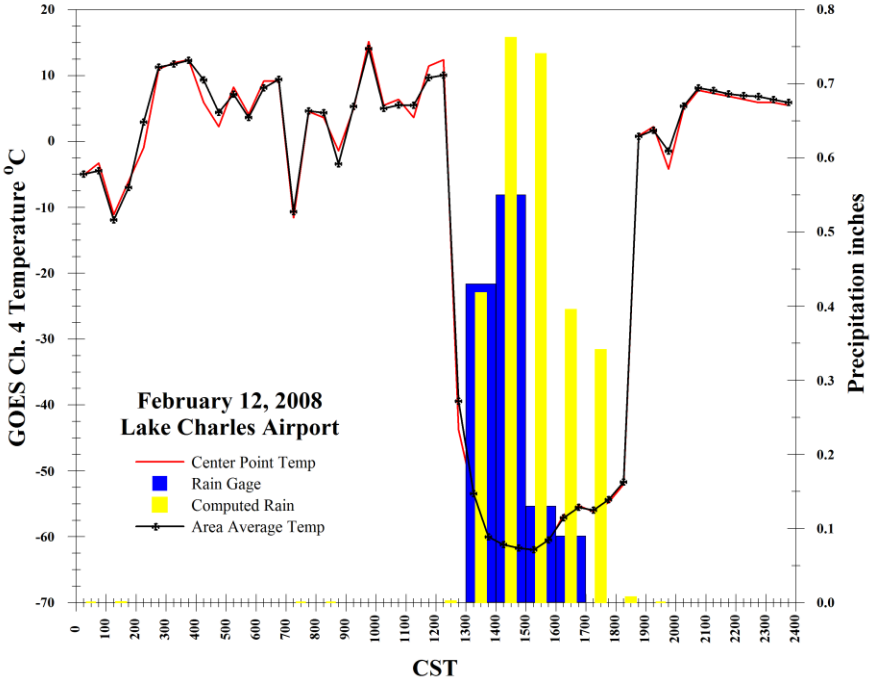

Figure 21
Time series of IR temperature along with measured and estimated rainfall totals on February 12, 2008 at LCH

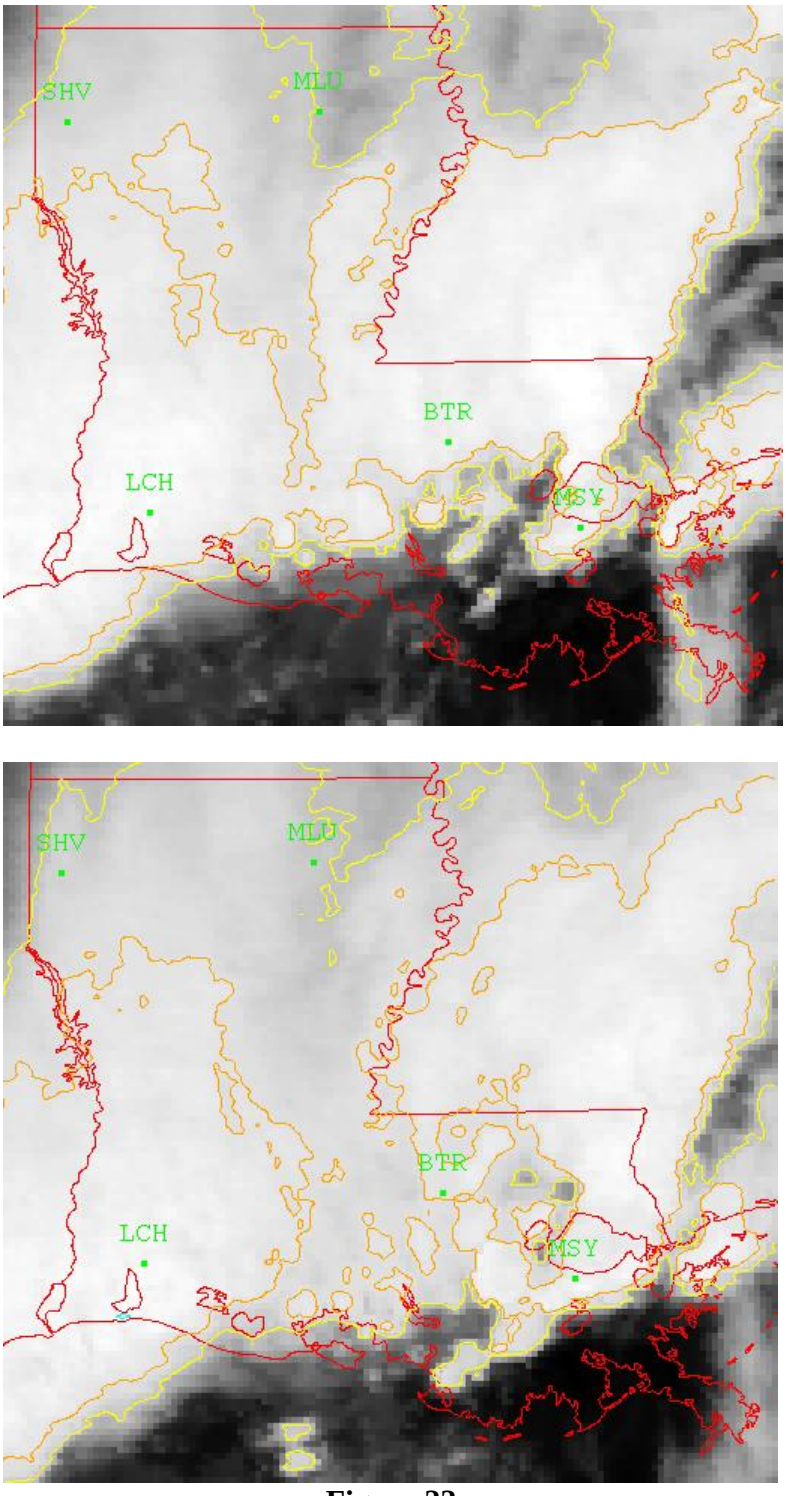

Figure 22
GOES IR image at 2015 UTC (1415 CST) (top) and 2045 UTC (1445 CST) (bottom) on February 12, 2008. Cyan contour is -65°C

February 16, Shreveport (SHV) (Table 4, Figures 23 – 26)

A stationary front extended across northern Louisiana from a weak low over eastern Texas. The front eventually moved to the north. A secondary low frontal system developed over south-central Texas and then moved eastward across Louisiana after merging with the earlier system; Gulf Return and Frontal Gulf Return. There were two periods of rain recorded, in the morning and the late evening CST. The cloud mass during the later rain exhibited colder CTTs, and CB and thunder were reported throughout the day. The onset of recorded rain appeared delayed from the CTT time series. Daily total amounts were within about 0.5 in. despite the timing difference.

Table 4
Selected surface observations from SHV on February 16, 2008 CST
(coded as in Table 2)

Time	Sky Conditions	Visibility	Weather Type
256	OVC004	7	-RA
303	OVC004CB	8	-TSRA
356	OVC004	9	-RA
507	OVC009CB	10	-TSRA
556	OVC012CB	10	-TSRA
603	FEW007 OVC012CB	8	-TSRA
656	SCT005 BKN020CB OVC055	1	+TSRA BR
703	SCT008 BKN017CB OVC044	3	+TSRA BR
724	BKN005 OVC013CB	6	-TSRA BR
756	BKN005 OVC011	2	RA BR
840	OVC005	1.5	-RA BR
856	BKN007 OVC012	1.5	RA BR
956	BKN005 OVC016	3	-RA BR
1015	BKN005 OVC021	4	-RA BR
1056	BKN005 OVC008	2	BR
1156	OVC003	3	BR
1319	OVC004	2.5	RA BR
1356	OVC005	4	BR
1456	BKN010 OVC030	6	-RA BR
1826	OVC024	10	TS
1856	OVC024	10	-TSRA
1956	OVC024	10	-TSRA
2044	BKN005 OVC0202	1	+TSRA BR
2056	FEW007 OVC014	7	+TSRA
2156	FEW007 BKN019 OVC030	3	+TSRA BR
2256	SCT009 BKN032 OVC080	10	RA
2356	SCT038 OVC090	10	RA

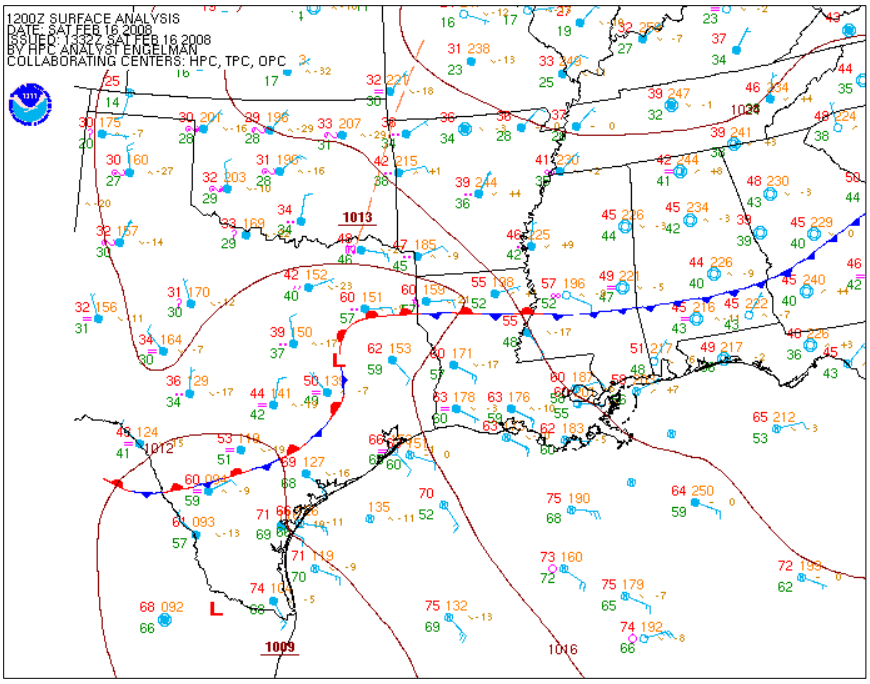

Figure 23
February 16, 2008 1200 UTC (0600 CST) surface weather map

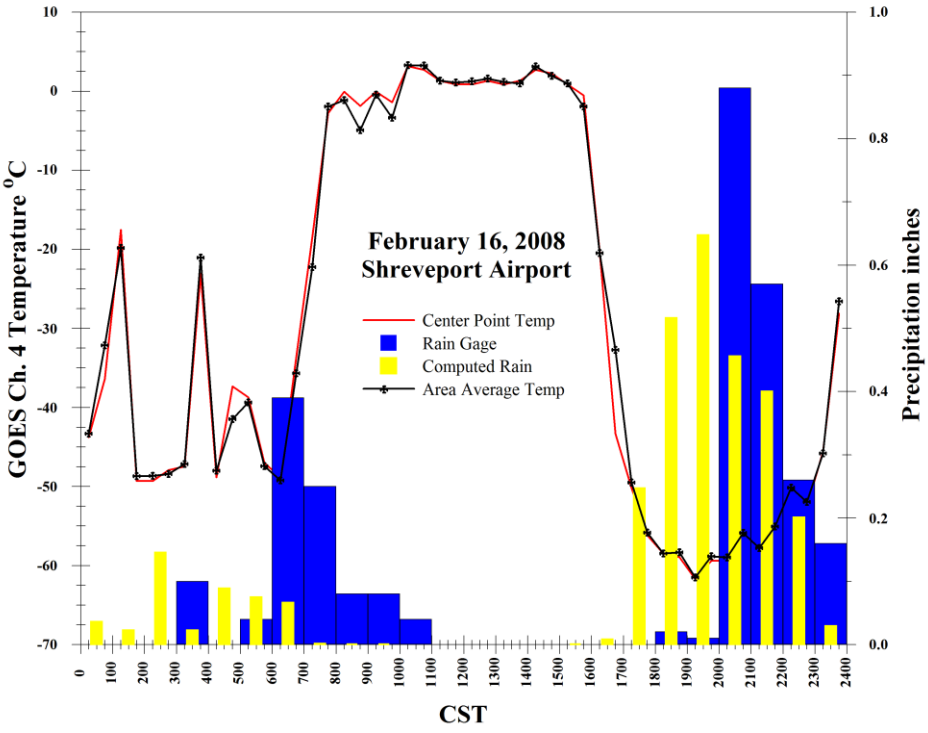

Figure 24
Time series of IR temperature along with measured and estimated rainfall totals on February 16, 2008 at SHV

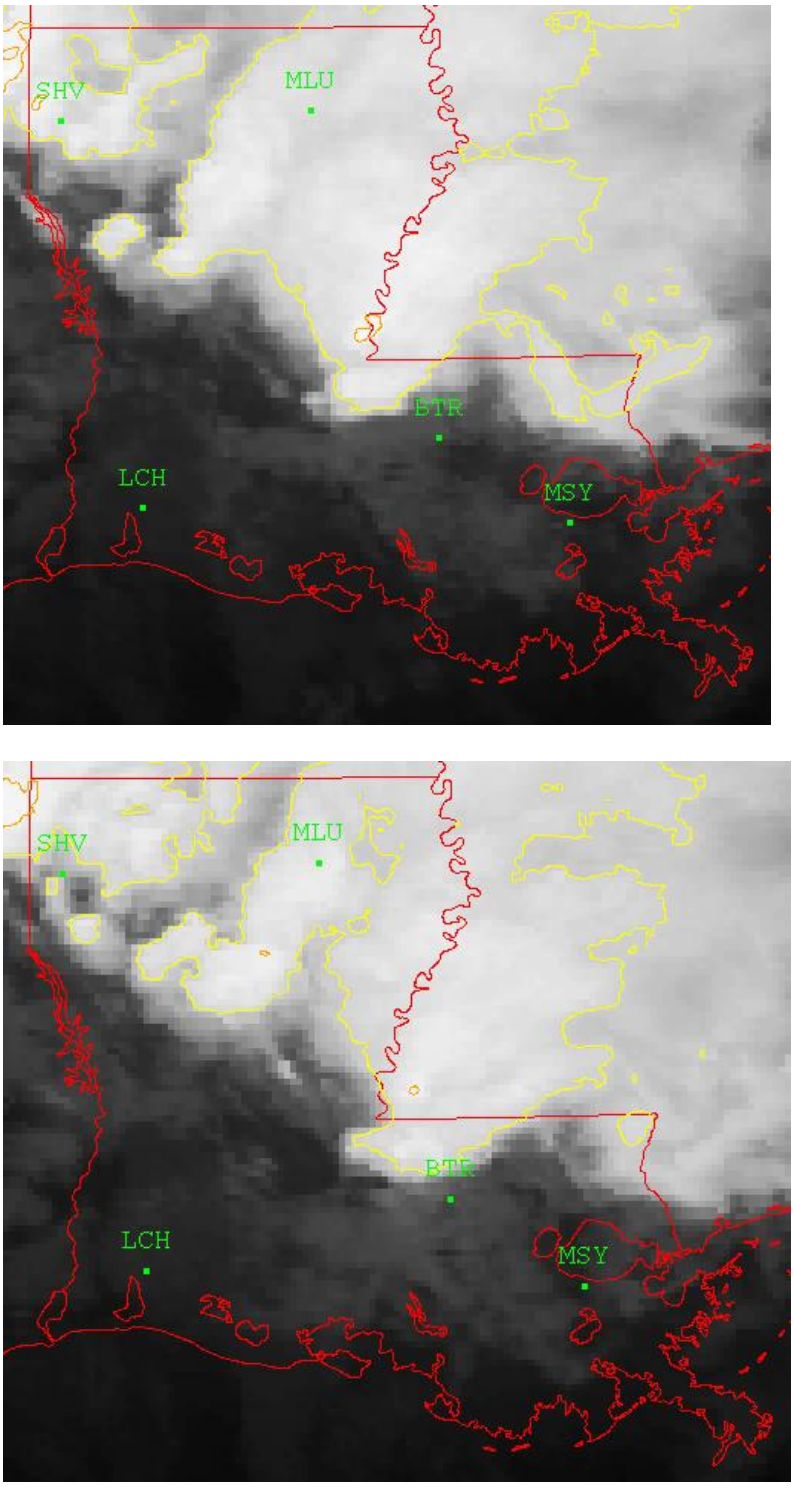

Figure 25
GOES IR image at 1215 UTC (0615 CST) (top) and 1245 UTC (0645 CST) (bottom) on February 16, 2008

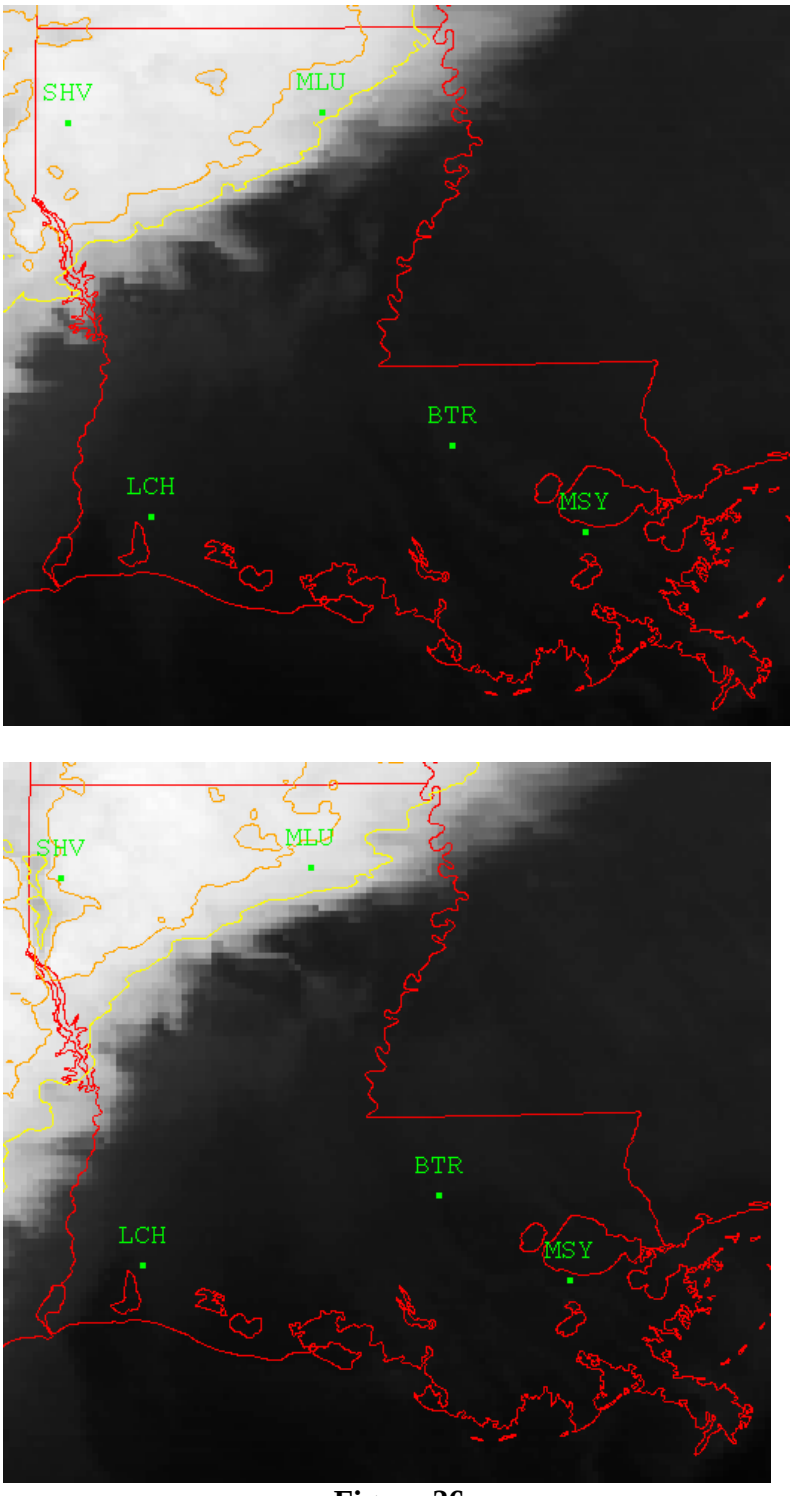

Figure 26
GOES IR images on February 17, 2008 at 0215 UTC (February 16 2015 CST) (top) and 0245 UTC (February 16 2045 CST) (bottom)

February 21, Monroe (MLU) (Table 5, Figures 27 – 29)

Complex pattern with a warm front over southeastern Louisiana and a cold front spread over the north; Coastal Return and Frontal Gulf Return. Widespread rain, fog, and overcast conditions prevailed. Broken cloud cover with embedded MCSs were observed with thunderstorms throughout the day. The maximum recorded rainfall was slightly delayed from the CTT time series, and the estimated daily total was off by about 1 in.

Table 5
Selected surface observations from MLU on February 21, 2008 CST
(coded as in Table 2)

Time	Sky Condition	Visibility	Weather Type
106	BKN020	10	-RA
153	OVC016	10	-RA
253	OVC012	8	-RA
453	OVC008	8	-RA
553	OVC008	6	RA BR
653	OVC008	5	RA BR
753	OVC006	4	-RA BR
853	OVC004	3	-TSRA BR
900	OVC004	1.75	+TSRA BR
953	OVC004	1.5	RA BR
1053	BKN004 OVC060	1.5	+RA BR
1153	BKN004 OVC016	1.5	VCTS +RA BR
1229	FEW002 BKN006 OVC024	0.5	+TSRA FG
1253	SCT003 BKN014 OVC070	4	RA BR
1414	SCT004 OVC033	1.25	+RA BR
1653	OVC022	6	-RA BR
1853	BKN006 OVC011	10	-RA
1953	BKN007 BKN029 OVC065	7	RA
2053	BKN007 BKN029 OVC065	10	-RA
2114	OVC007	7	-TSRA
2253	OVC003	3	BR
2353	OVC001	1.25	-TSRA BR

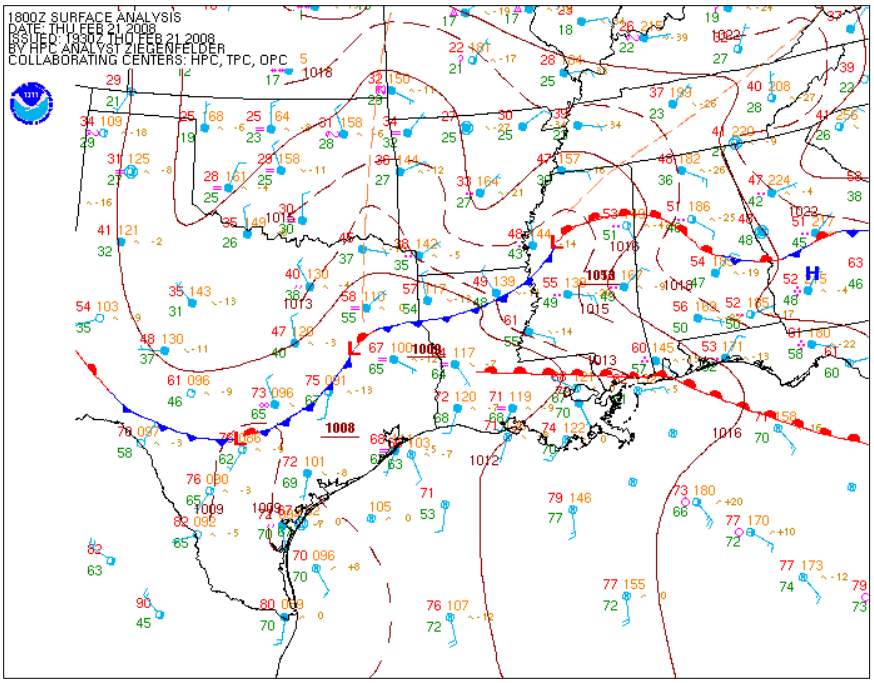

Figure 27
February 21, 2008 1800 UTC (1200 CST) surface weather map

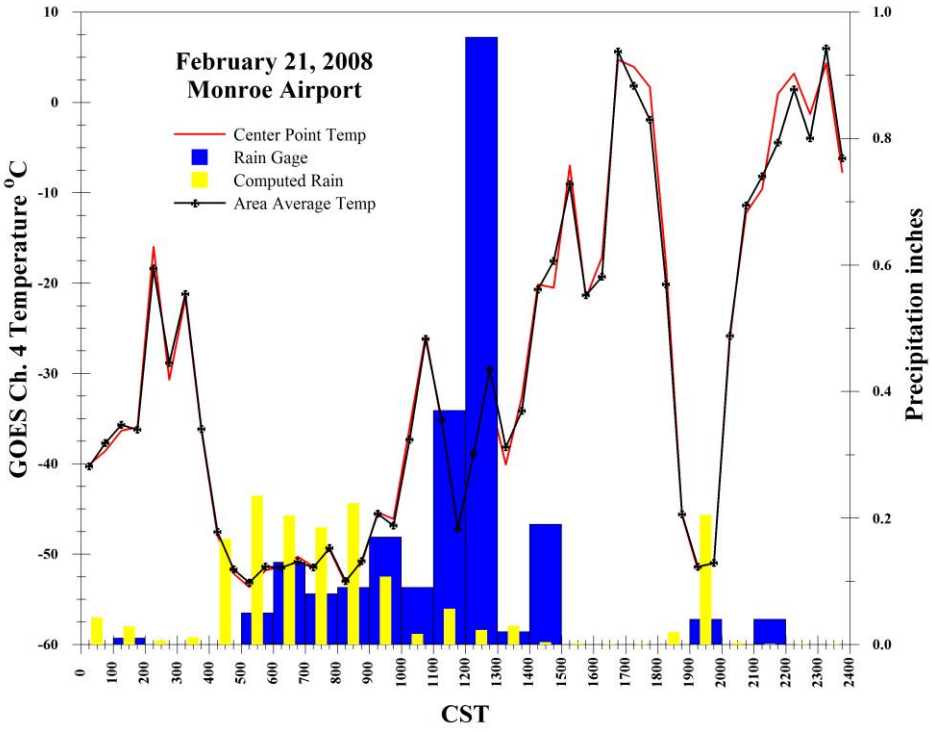

Figure 28
Time series of IR temperature along with measured and estimated rainfall totals on February 21, 2008 at MLU

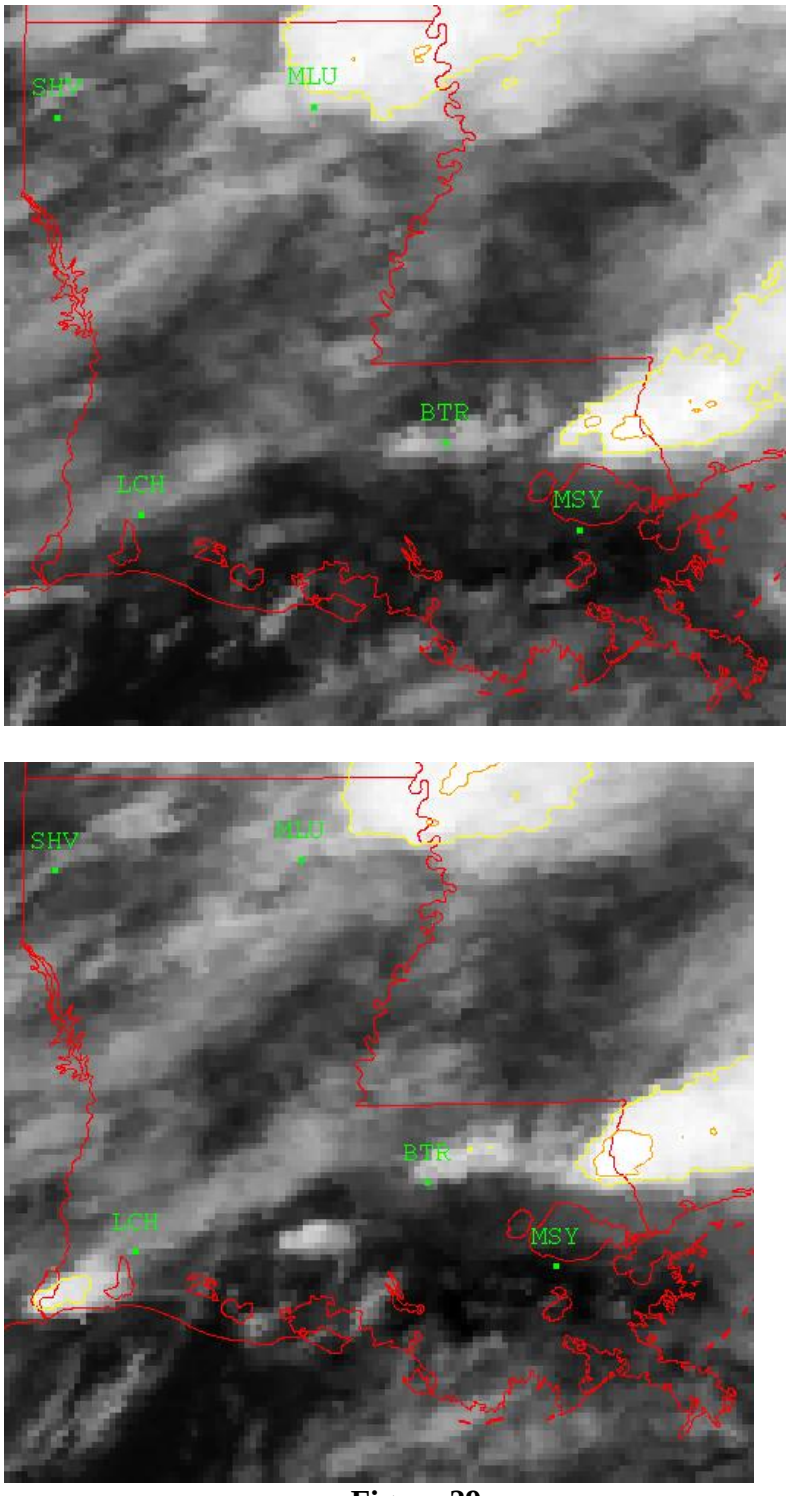

Figure 29
GOES IR images for 1815 UTC (1215 CST) (top) and 1845 UTC (1245 CST) (bottom) on February 21, 2008

March 10, Lake Charles (LCH) (Table 6, Figures 30 – 32)

Low center and cold frontal passage progressed from west to east across Louisiana, Gulf Return and Frontal Gulf Return. Prior to passage, a squall line developed over southeastern Texas, but weakened considerably before entering the state. No CB or thunder reported. Clouds covered the western half of the state with embedded MCSs. Recorded rain continued even though CTTs warmed; likely more stratus clouds. Estimated rain totals were lower than measured.

Table 6
Selected observations from LCH on March 10, 2008 CST (coded as in Table 2)

Time	Sky Conditions	Visibility	Weather Type
1053	OVC030	8	-RA
1126	BKN015 BKN030 OVC037	0.75	+RA
1153	BKN018 BKN033 OVC042	3	-RA
1253	BKN026 OVC049	10	-RA
1415	BKN031 OVC050	10	-RA
1453	FEW008 BKN014 OVC031	6	BR
1527	SCT007 SCT016 OVC031	1.25	+RA
1553	FEW007 OVC033	2	+RA BR
1653	BKN006 OVC029	7	-RA
1753	FEW008 SCT012 OVC023	2.5	+RA BR
1853	BKN022 OVC030	7	-RA
1920	FEW007 OVC028	3	+RA BR
1953	BKN006 OVC032	7	-RA
2053	BKN036 OVC044	5	RA BR
2153	FEW027 BKN050 OVC085	8	-RA

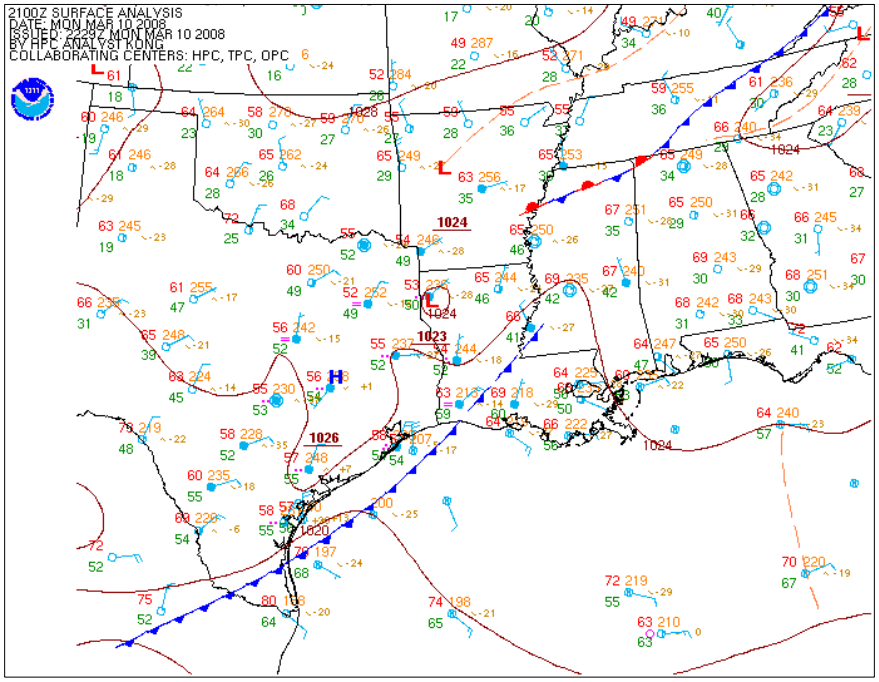

Figure 30
March 10, 2008 2100 UTC (1500 CST) surface weather map

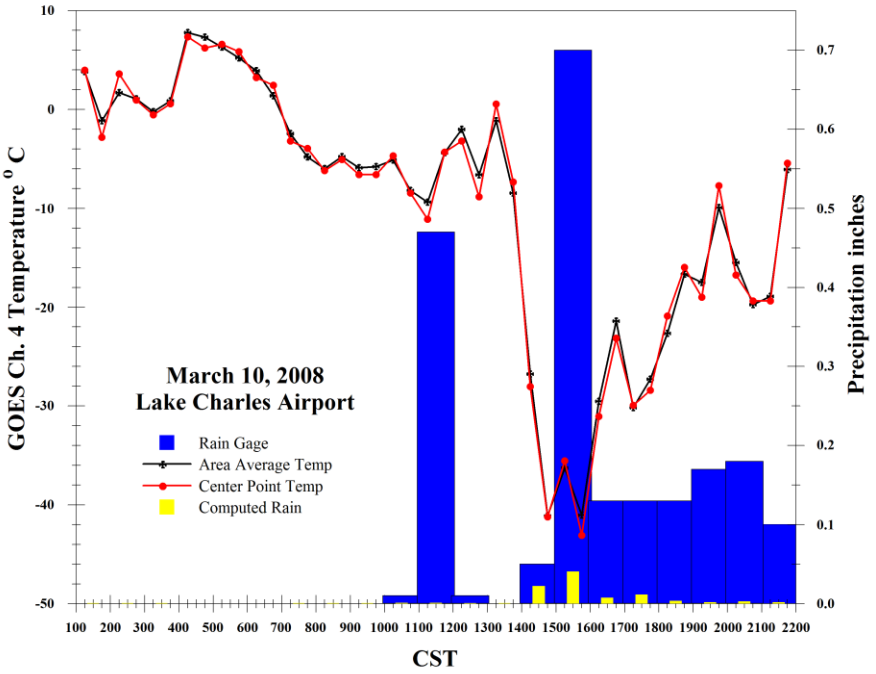

Figure 31
Time series of IR temperature along with measured and estimated rainfall on March 10, 2008 at LCH

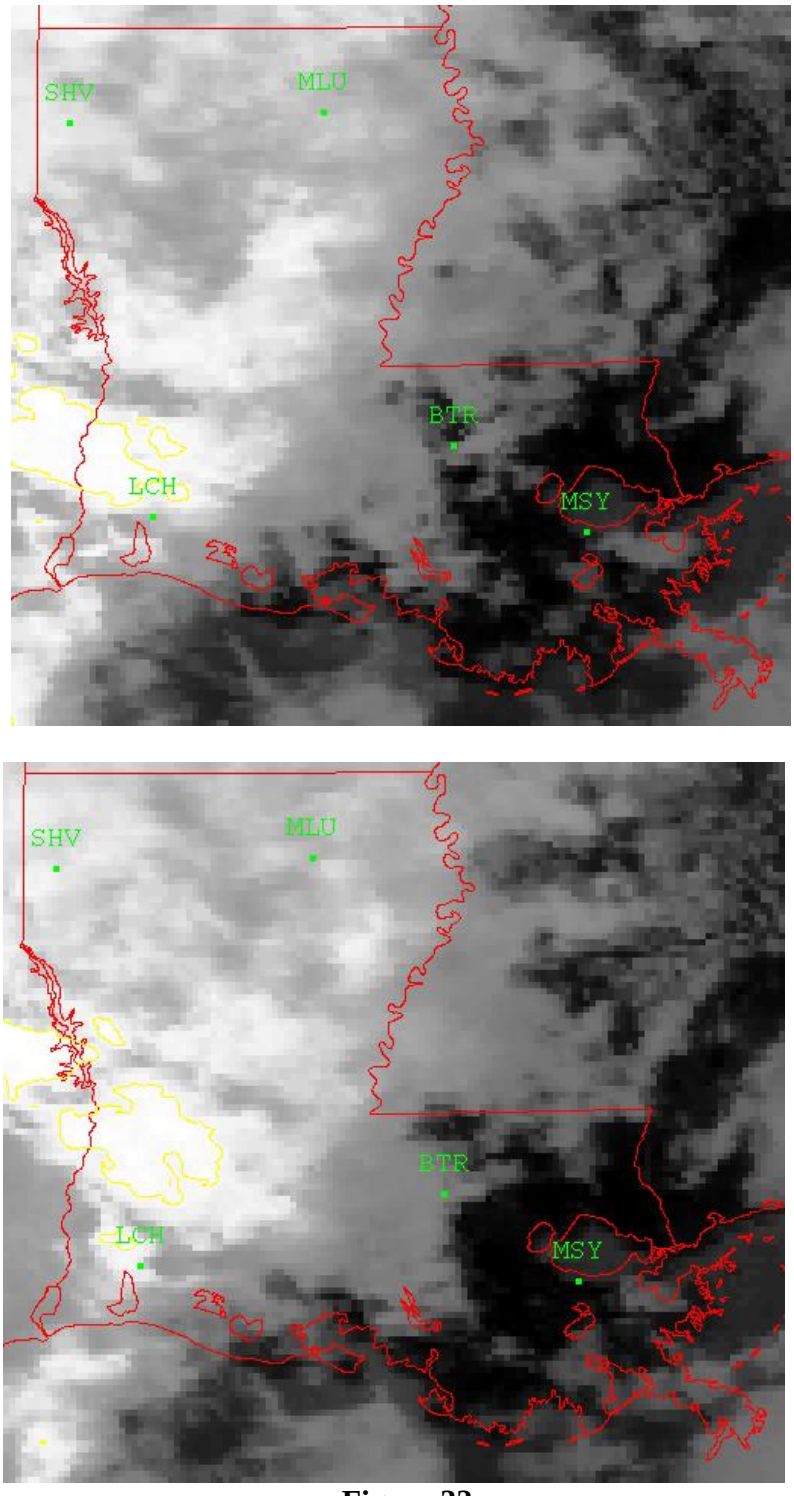

Figure 32
GOES IR image for 2115 UTC (1515 CST) (top) and 2145 UTC (1545 CST) (bottom) on March 10, 2008

April 4, Lake Charles (LCH) (Table 7, Figures 33 – 35)

Cold frontal passage observed with Coastal Return becoming Continental High condition. An extremely cold cloud mass was associated with the frontal zone and was oriented roughly north-south through the state, however no CB reported. Estimated totals were below measured values.

Table 7
Selected surface observations from LCH on April 4, 2008 CST (coded as in Table 2)

Time	Sky Conditions	Visibility	Weather Type
1753	SCT019 BKN024 OVC048	9	VCTS –RA
1805	BKN015 BKN024 OVC033	3	TSRA
1824	BKN004 BKN009 OVC015	0.5	+TSRA FG
1853	SCT010 SCT035 OVC041	5	+TSRA BR
1915	BKN006 BKN012 OVC041	8	-RA
1953	OVC008	6	+TSRA BR
2013	BKN008 BKN014 OVC027	3	TSRA BR
2053	BKN033 OVC060	10	TS
2123	FEW011 BKN015 OVC055	10	-RA
2153	SCT011 BKN016 OVC065	10	VCTS

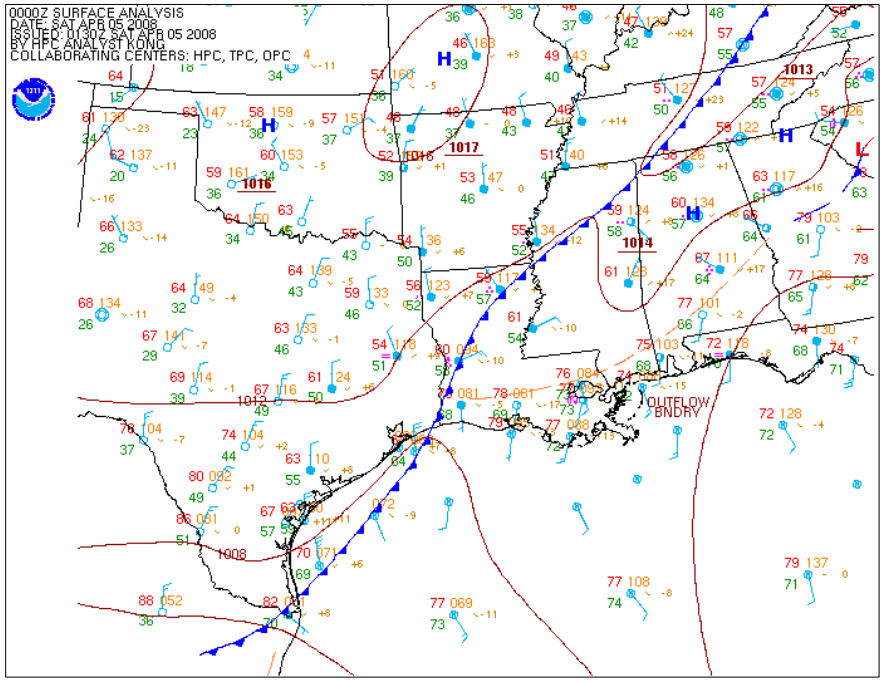

Figure 33
April 5, 2008 0000 UTC (April 4 1800 CST) surface weather map

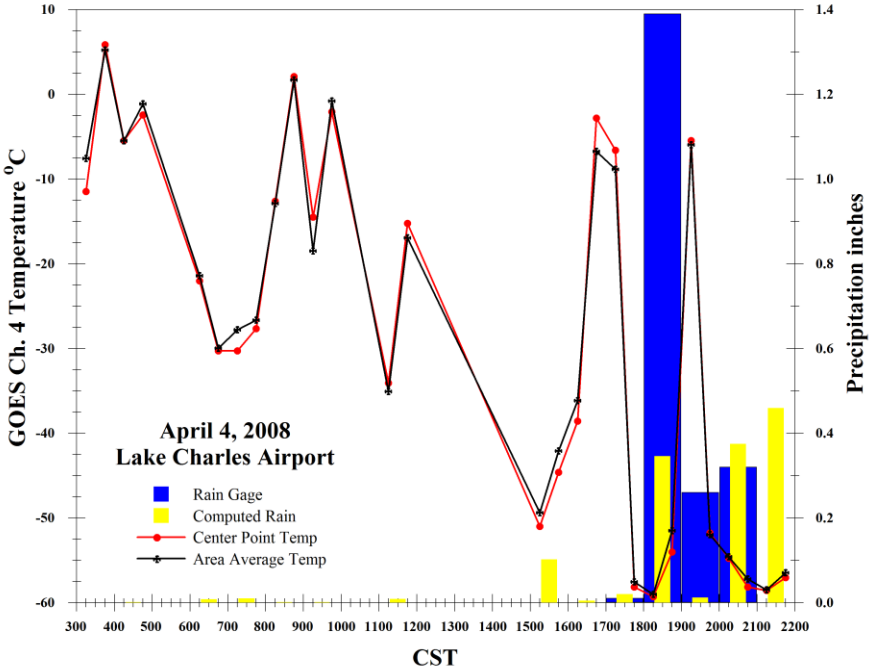

Figure 34
Time series of IR temperature along with measured and estimated rainfall on April 4, 2008 at LCH

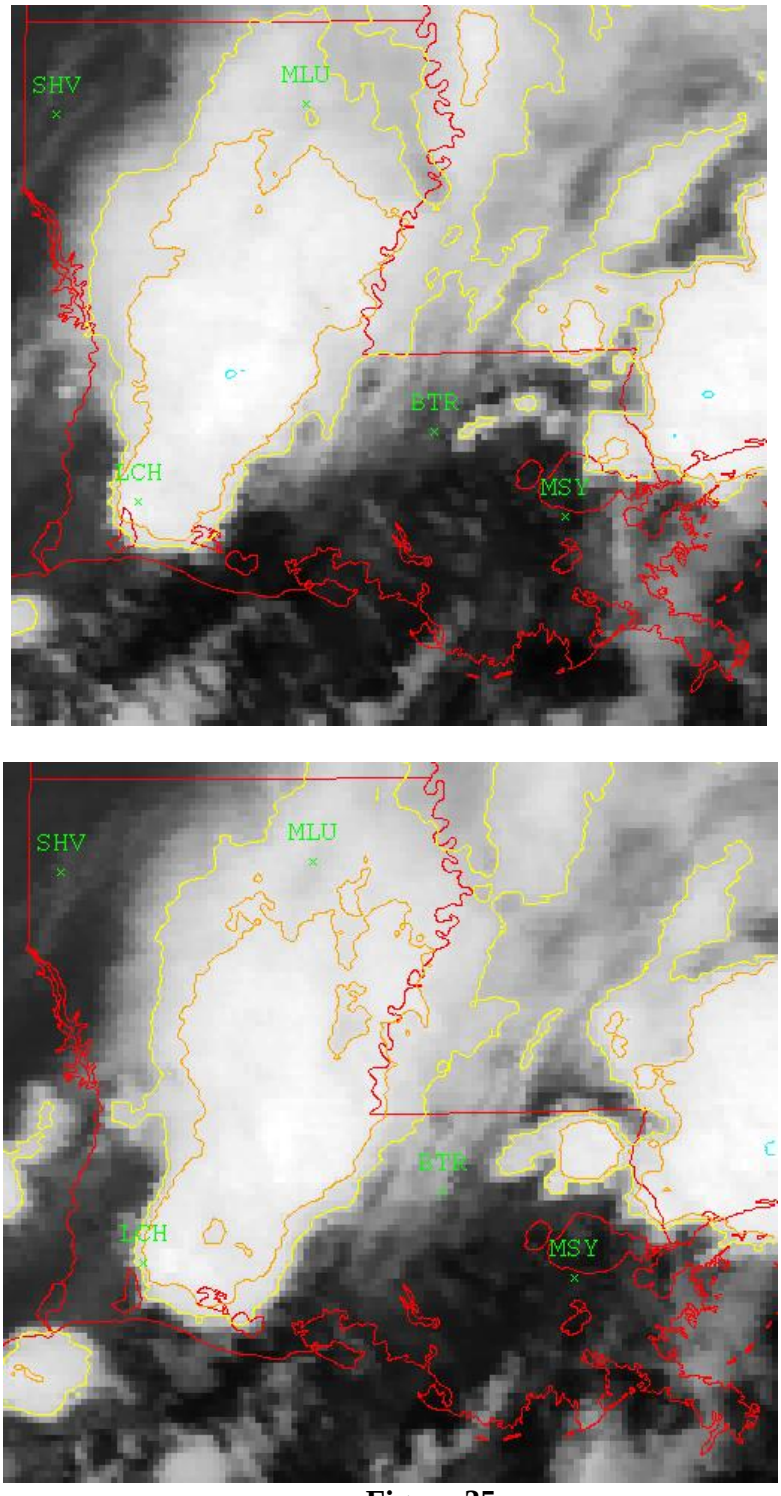

Figure 35
GOES IR image for April 5, 2008 0015 UTC (April 4 1815 CST) (top) and 0045 UTC (April 4 1845 CST) (bottom)

May 22, New Orleans (MSY) (Table 8, Figures 36 – 38)

Strong Coastal Return flow behind warm front situated over southern Arkansas. Widespread cloud cover with embedded extremely cold MCSs existed. Note the cells near MSY at 1845 UTC (1245 CST) and 2145 UTC (1545 CST) in Figure 38. Multiple reports of CBs and thunder were associated with these airmass storms. There was reasonable agreement between measured rain and CTT time series; daily total from Vincente [equation (1)] was lower than measured while the total from derived equation (2) was within 0.1 in.

Table 8
Selected surface observations from MSY on May 22, 2008 CST (coded as in Table 2)

Time	Sky Conditions	Visibility	Weather Type
948	SCT023CB BKN100 OVC250	6	-TSRA BR
953	SCT023CB BKN100 OVC250	6	-TSRA BR
1019	SCT019CB BKN031 OVC060	5	-TSRA BR
1053	SCT019CB BKN031 OVC060	3	-TSRA BR
1153	SCT019CB BKN034	8	TS
1253	SCT022CB BKN046 OVC100	7	-TSRA
1330	FEW017 BKN033CB OVC090	2	-TSRA BR
1353	FEW017 BKN033CB OVC090	3	TSRA BR
1439	FEW015 BKN031CB OVC060	1.75	+TSRA BR
1453	SCT022 BKN031CB OVC060	1.5	+TSRA BR
1526	FEW022 BKN031 OVC060	1.5	+RA BR
1553	FEW016 BKN033CB OVC065	1.25	+TSRA BR
1653	FEW027 BKN095 BKN110	10	-RA
1753	FEW020 SCT049 OVC090	7	-RA
1853	FEW020CB SCT070	8	-TSRA
1953	FEW020 BKN070 OVC110	5	-RA BR
2053	FEW020 OVC090	10	-RA
2153	SCT031CB BKN080 OVC110	10	-TSRA
2253	BKN010 BKN026CB OVC035	1.25	+TSRA BR
2329	BKN023CB OVC085	1.75	+TSRA BR
2346	FEW016 BKN032CB OVC110	4	+TSRA BR

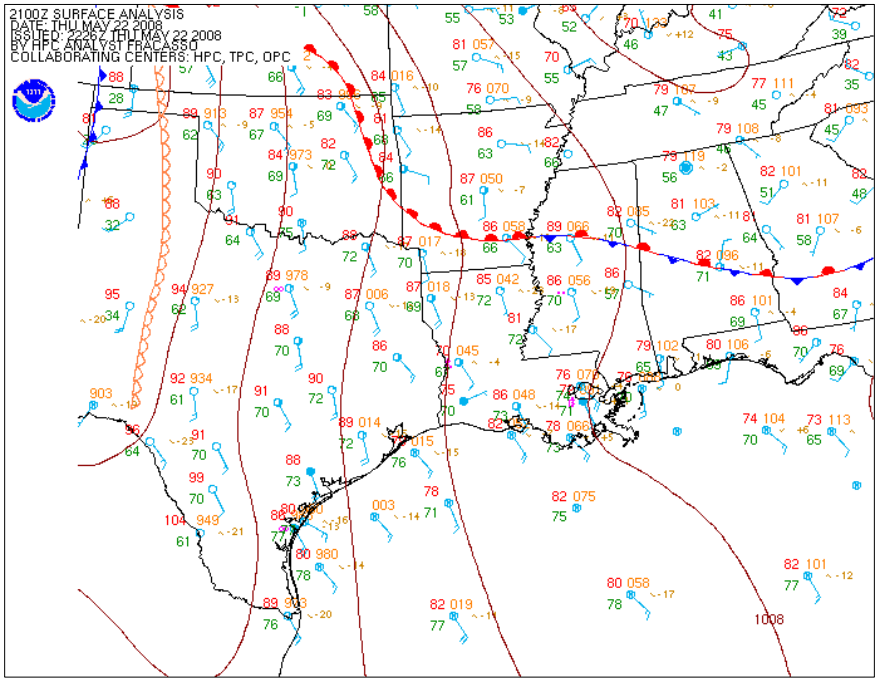

Figure 36
May 22, 2008 2100 UTC (1500 CST) surface weather map

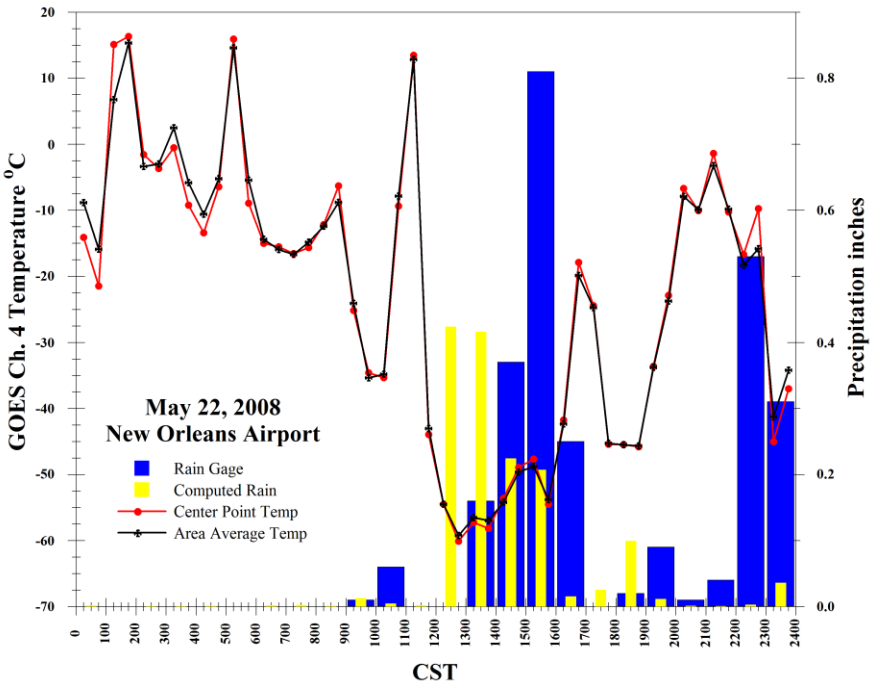

Figure 37
Time series of IR temperature along with measured and estimated rainfall on May 22, 2008 at MSY

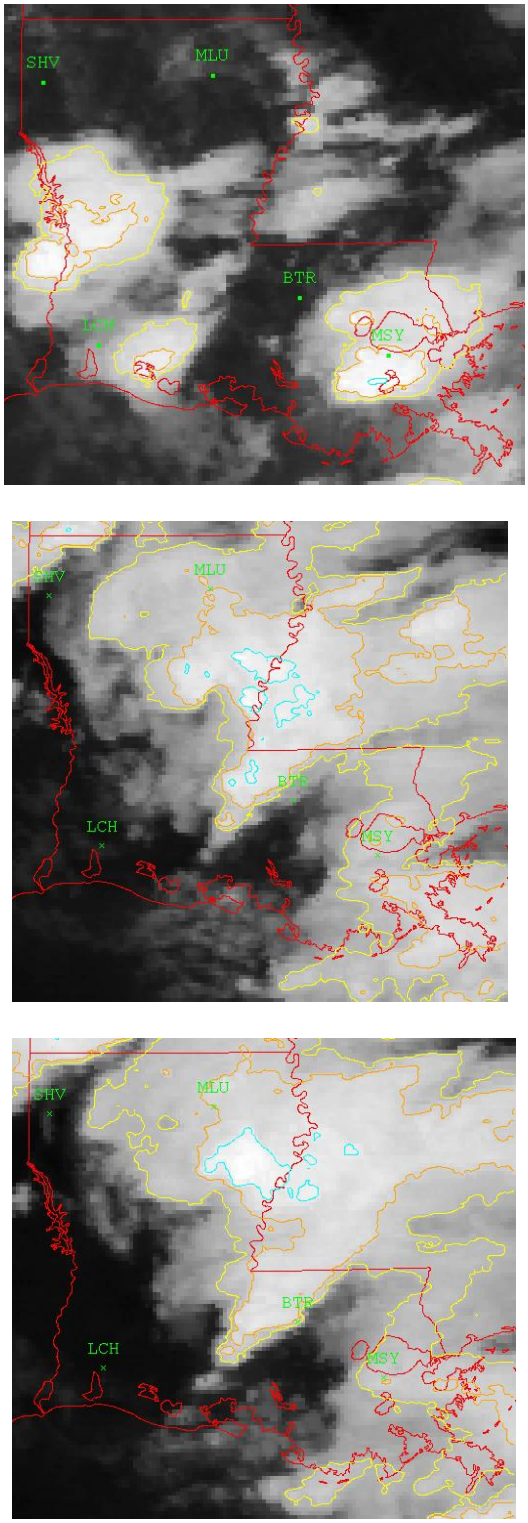

Figure 38
GOES IR image for 1845 UTC (1245 CST) (top), 2115 UTC (1515 CST) (middle), and 2145 UTC (1545 CST) (bottom) on May 22, 2008

June 9 – 10, Shreveport (SHV) (Table 9, Figures 39 – 41)

A weak stationary front over northwest Louisiana eventually moved northward as a warm front producing Gulf Return conditions; significant instability occurred along the front and extremely cold MCSs developed. Multiple reports of CB, towering cumulus (TCU), and thunder were reported. Reasonable agreement existed between measured rain and CTT time series with maximum rain accumulation occurring at coldest CTT. Estimated totals for this event were greater than measured amounts.

Table 9
Selected surface observations from SHV on June 9 – 10, 2008 CST (coded as in Table 2)

Day	Time	Sky Conditions	Visibility	Weather Type
9	1742	FEW060CB SCT075	10	TS
	1756	FEW060CB SCT075	10	TS
	1856	FEW040TCU SCT070	10	-RA
	1913	FEW040CB SCT080	10	-TSRA
	1956	FEW040TCU SCT080	7	-RA
	2056	FEW012 BKN030CB OVC038	3	-TSRA
	2156	FEW020 BKN030CB OVC038	10	-TSRA
	2226	FEW005 OVC032CB	2	+TSRA BR
	2256	SCT005 BKN017CB OVC030	1.5	+TSRA BR
	2325	SCT011 BKN031CB OVC039	0.75	+TSRA
	2353	SCT004 BKN022CB OVC041	4	TSRA
10	29	FEW004 BKN018CB OVC047	0.5	+TSRA
	56	FEW004 SCT009 OVC034CB	6	-TSRA
	128	FEW004 BKN032 OVC050	7	-RA
	210	BKN022 OVC029CB	7	+TSRA
	256	SCT024 BKN030 OVC055	7	-RA
	337	FEW008 BKN028 OVC065	7	-RA
	359	FEW008 BKN033CB OVC050	7	TSRA
	431	FEW010 BKN014 OVC036CB	3	TSRA
	456	FEW010 BKN014 OVC036CB	1	-TSRA
	556	BKN065 OVC085	7	-RA

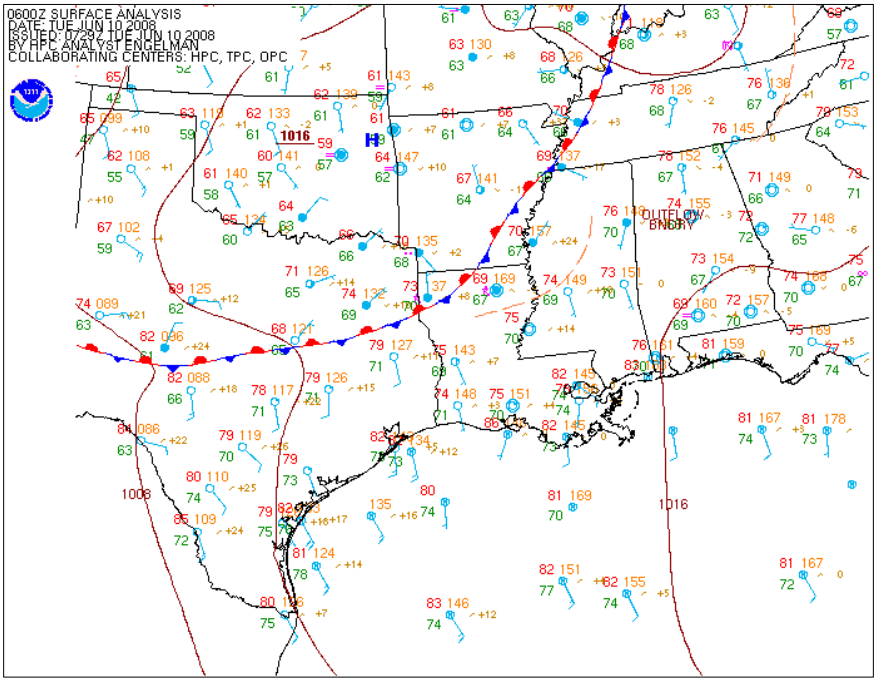

Figure 39
June 10, 2008 0600 UTC (0000 CST) surface weather map

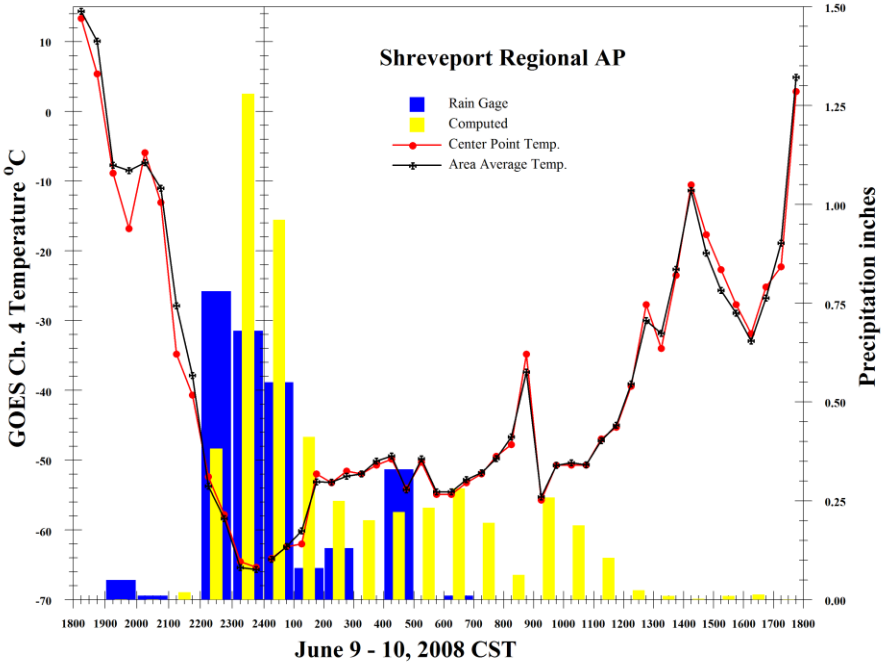

Figure 40
Time series of IR temperature along with measured and estimated rainfall on June 9 and 10, 2008 at SHV

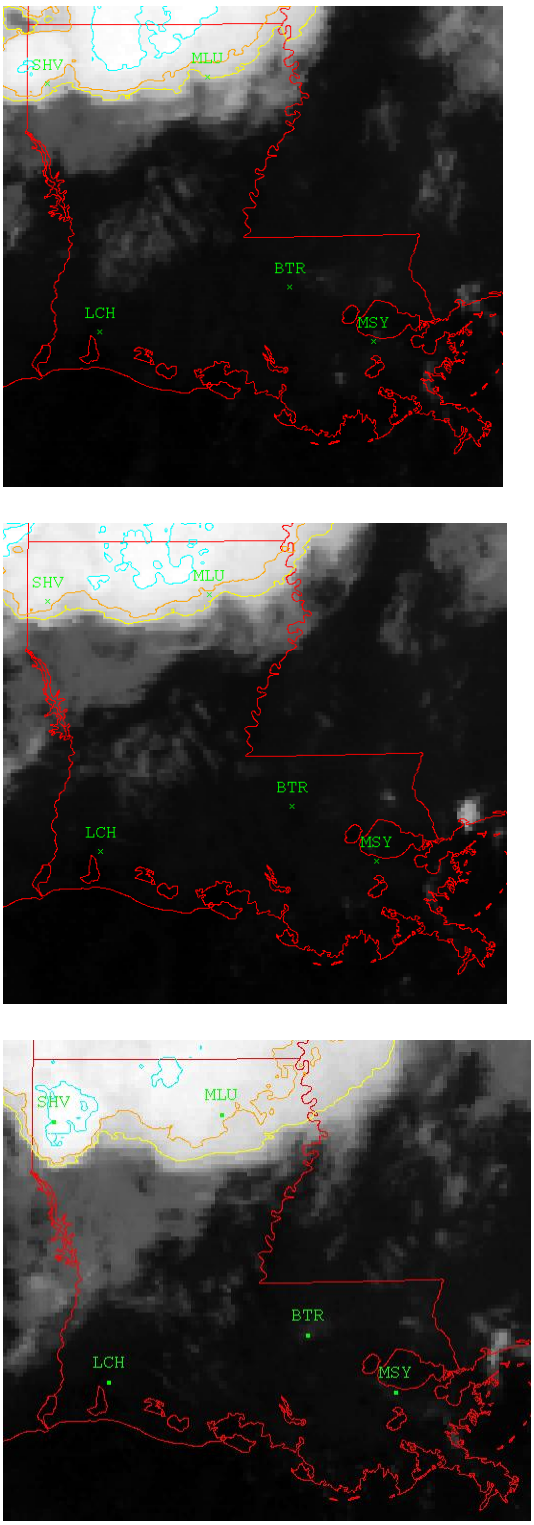

Figure 41
GOES IR image for June 10, 2008 0415 UTC (June 9 2215 CST) (top), 0445 UTC (2245 CST) (middle), and 0545 UTC (2345 CST) (bottom)

July 15, Lake Charles (LCH) (Table 10, Figures 42 – 44)

A stationary front extended across southern Louisiana, separating Continental High conditions to the north from weak Coastal Return to the south. An area of MCSs appeared to be moving northward into the LCH area from the Gulf. Note the developing cell over the station at 1245 UTC (0645 CST) in Figure 44. Thunderstorms were reported. Reasonable agreement existed between measured rain and CTT time series; estimated totals were much lower than the recorded amount.

Table 10
Selected surface observations from LCH on July 15, 2008 CST (coded as in Table 2)

Time	Sky Conditions	Visibility	Weather Type
453	SCT017 OVC022	5	VCTS RA BR
536	BKN022 OVC036	5	VCTS –RA BR
553	SCT005 BKN022 OVC026	1.75	+TSRA BR
621	BKN005 OVC026	0.25	+RA FG
653	VV006	0.5	+TSRA FG
720	BKN011 OVC041	0.25	+TSRA FG
753	VV015	0.75	+TSRA BR
823	OVC027	3	VCTS RA BR
853	FEW022 BKN055 OVC065	6	VCTS –RA BR
953	OVC035	3	RA BR
1048	SCT025 BKN090	10	-RA

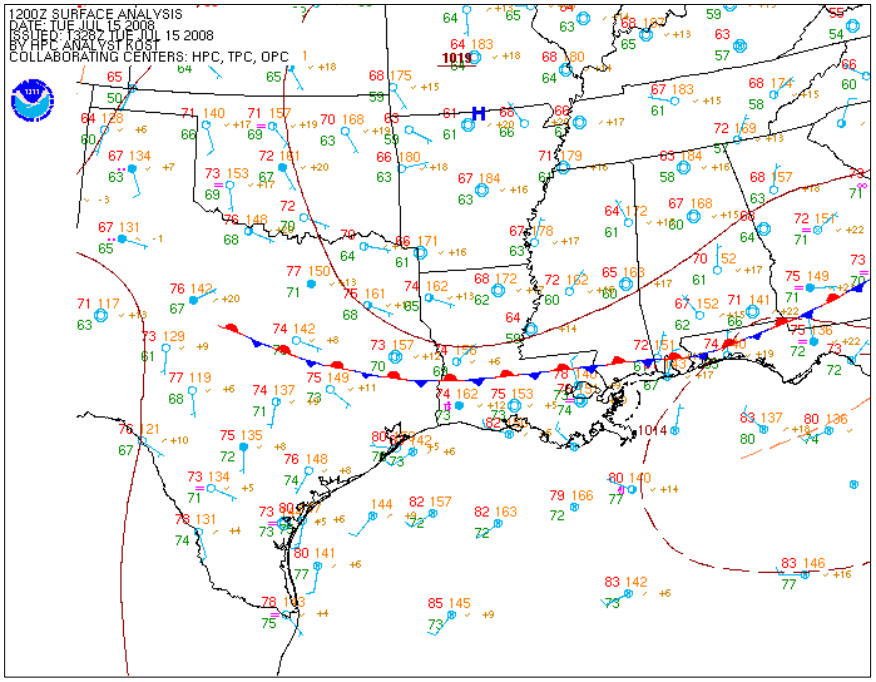

Figure 42
July 15, 2008 1200 UTC (0600 CST) surface weather map

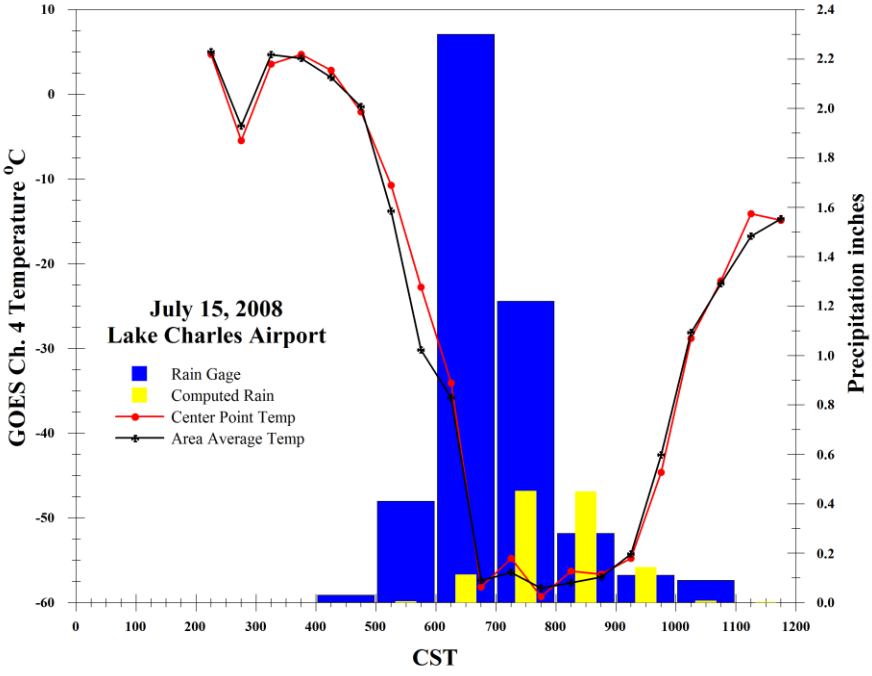

Figure 43
Time series of IR temperature along with measured and estimated rainfall on July 15, 2008 at LCH

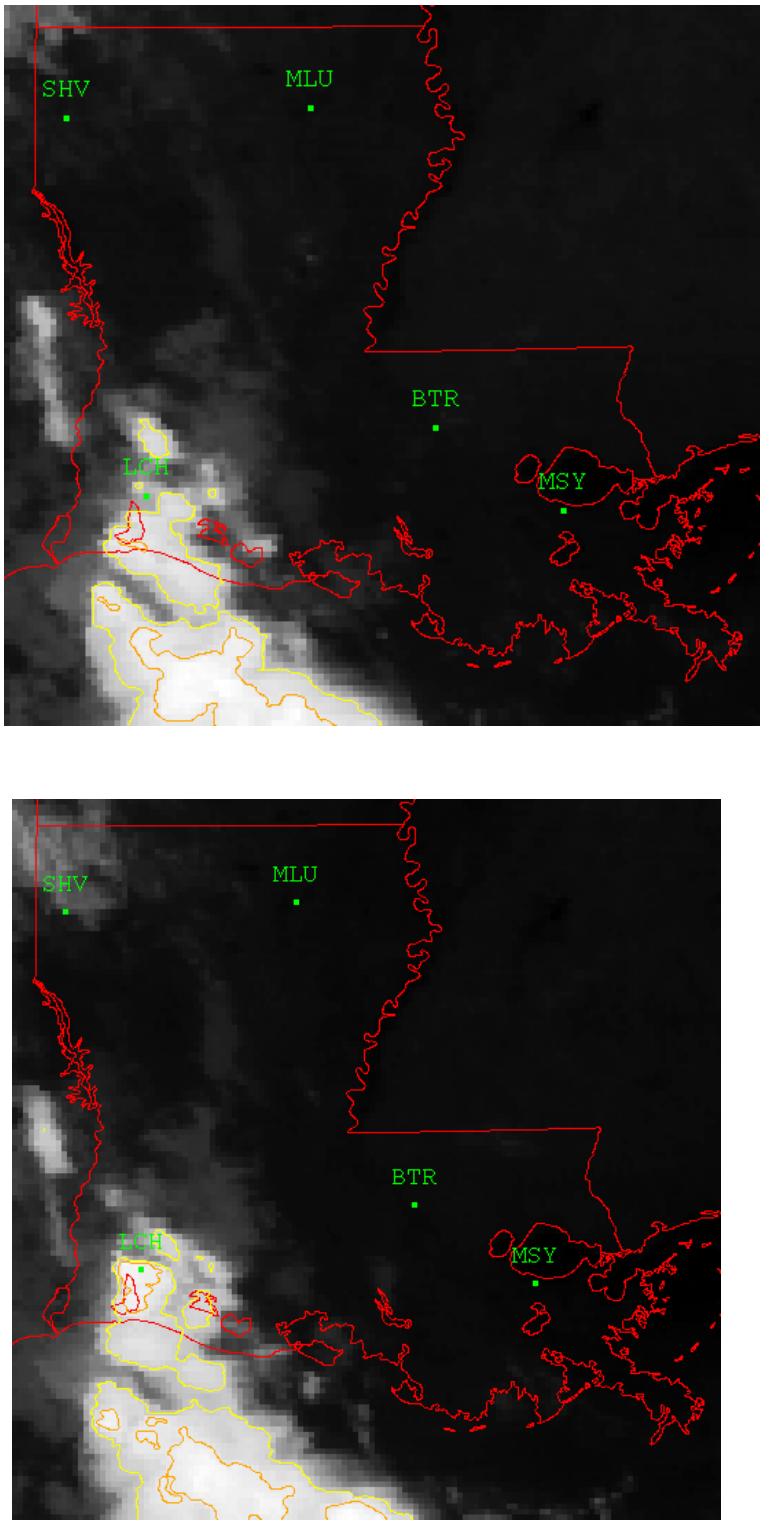

Figure 44
GOES IR image for 1215 UTC (0615 CST) (top) and 1245 UTC (0645 CST) (bottom) on July 15, 2008

August 11, Monroe (MLU) (Table 11, Figures 45 – 47)

North Louisiana is between two frontal zones, stationary to the south and a dissipating cold front to the north through Arkansas and Mississippi. The northern front washes out; the stationary front moves north as warm, Frontal Gulf Return. A large cloud mass was present over northeastern Louisiana with embedded very cold MCSs. Heavy thunderstorms were reported. In Figure 47, note the very distinct MCS near to the MLU station at 2315 UTC; however, no rain was recorded at this time. Estimated totals for the morning rain were much greater than measured.

Table 11
Selected surface observations from MLU on August 11, 2008 CST (coded as in Table 2)

Time	Sky Conditions	Visibility	Weather Type
53	FEW070 OVC100	5	BR
153	FEW024 BKN065 OVC090	5	BR
228	FEW005 BKN020 OVC060	2.5	-RA BR
243	BKN005 BKN020 OVC049	2	+TSRA BR
253	OVC005	4	VCTS –RA BR
342	BKN005 BKN013 OVC018	1.75	+TSRA BR
353	FEW005 BKN013 OVC055	2.5	TSRA BR
425	SCT003 BKN015 OVC065	4	TSRA BR
453	FEW003 SCT015 OVC020	2.5	VCTS +RA BR
553	OVC005	1.75	+TSRA BR
612	SCT005 OVC011	1.25	+RA BR
653	SCT003 OVC021	4	VCTS +RA BR
718	BKN003 OVC023	1.75	+RA BR
753	FEW005 SCT014 OVC021	2	+RA BR
820	FEW005 BKN018 OVC028	2	+RA BR
853	OVC020	6	RA BR
953	FEW018	6	-RA BR

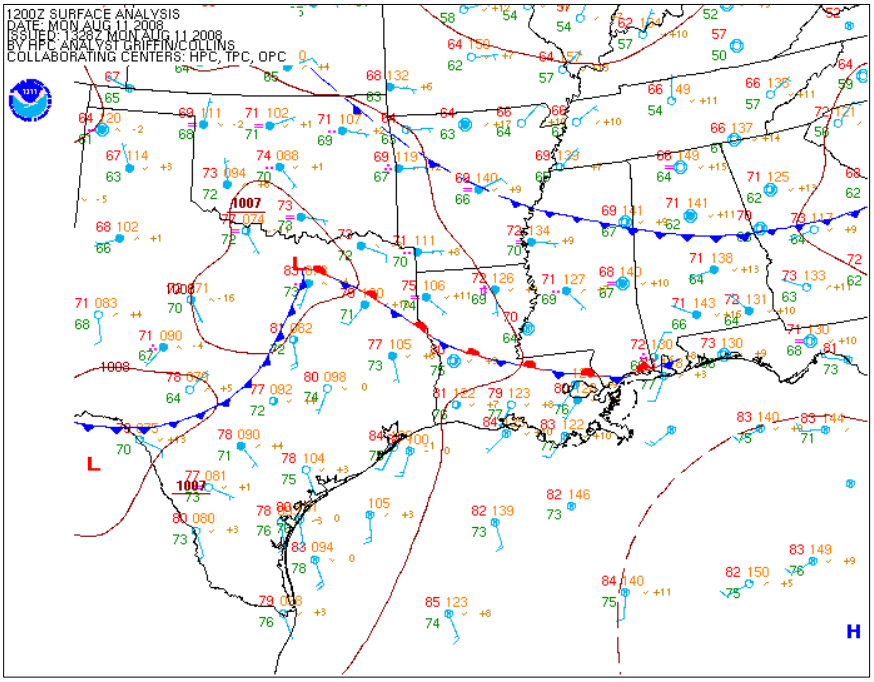

Figure 45
August 11, 2008 1200 UTC (0600 CST) surface weather map

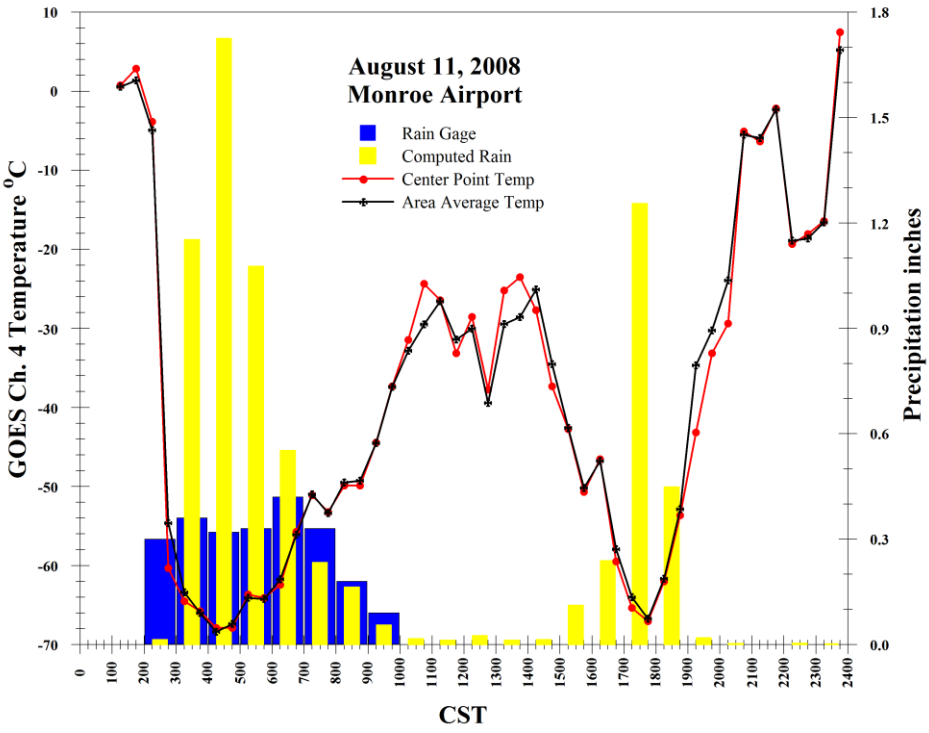

Figure 46
Time series of IR temperature along with measured and estimated rainfall on August 11, 2008 at MLU

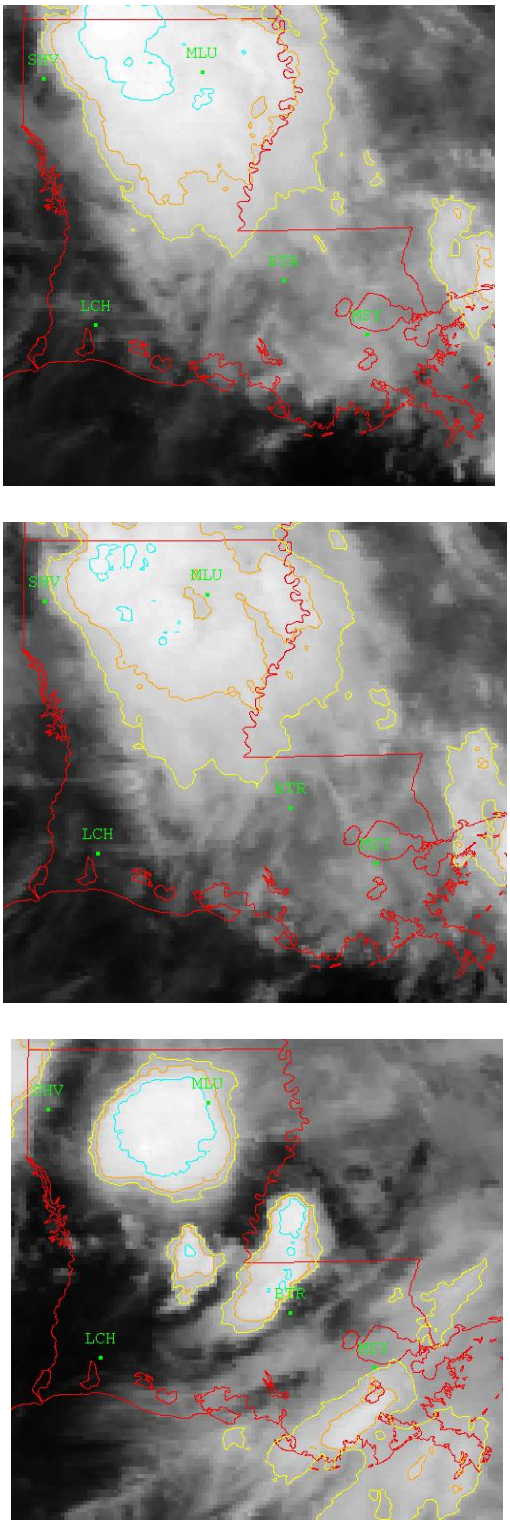

Figure 47
GOES IR image for 1215 UTC (0615 CST) (top), 1245 UTC (0645 CST) (middle), and 2315 UTC (1715 CST) (bottom) on August 11, 2008

August 13, New Orleans (MSY) (Table 12, Figures 48 – 51)

A frontal zone extends across southern Louisiana with weak Continental High to the north and stronger Coastal Return to the south. Unstable air mass south of the front with multiple very cold MCSs observed along the coast. CBs and thunder were reported. Note that a heavy shower was recorded near noon CST (Figure 49); however, the IR imagery only shows a small cell over the station (Figure 51). Estimated values for the event were much lower than recorded.

Table 12
Selected surface observations from MSY on August 13, 2008 CST (coded as in Table 2)

Time	Sky Conditions	Visibility	Weather Type
317	BKN026 BKN090 OVC250	10	-RA
353	BKN010 BKN013 OVC021	3	+RA BR
453	SCT014 SCT042 BKN120	5	BR
653	FEW005CB SCT020	10	-RA
1130	SCT023CB OVC055	8	-RA
1153	SCT020 SCT026CB	7	RA
1212	SCT017CB BKN024 OVC060	1.5	TSRA BR
1248	BKN007CB BKN011 OVC017	2	TSRA BR
1317	FEW002 BKN007CB OVC020	2	TSRA BR
1346	SCT010 BKN014CB OVC020	10	TS
1453	FEW018 BKN030CB BKN120	8	-RA
1537	FEW025 SCT060 BKN150	10	-RA

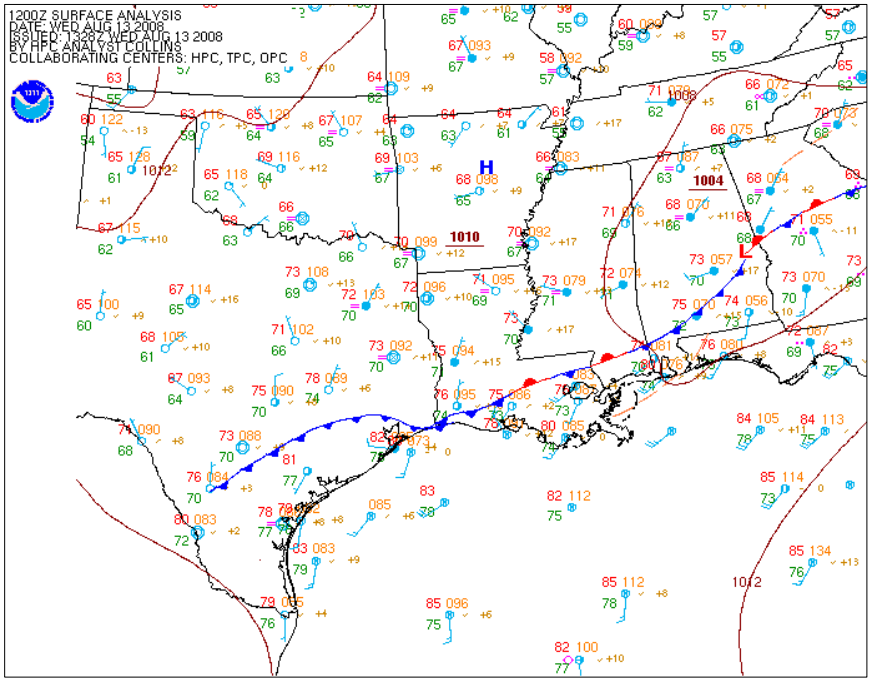

Figure 48
August 13, 2008 1200 UTC (0600 CST) surface weather map

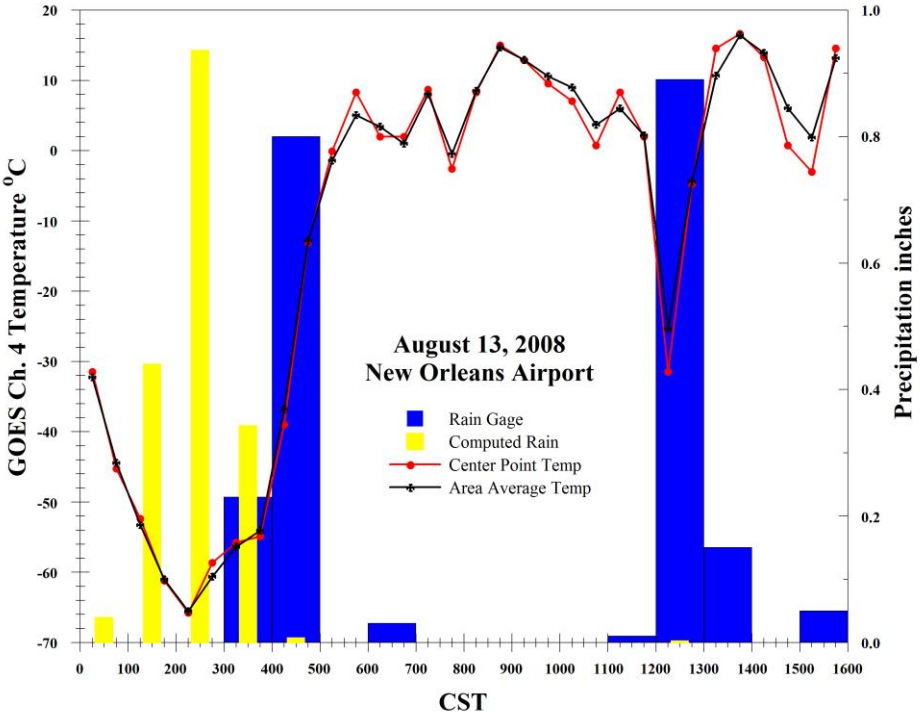

Figure 49
Time series of IR temperature along with measured and estimated rainfall on August 13, 2008 at MSY

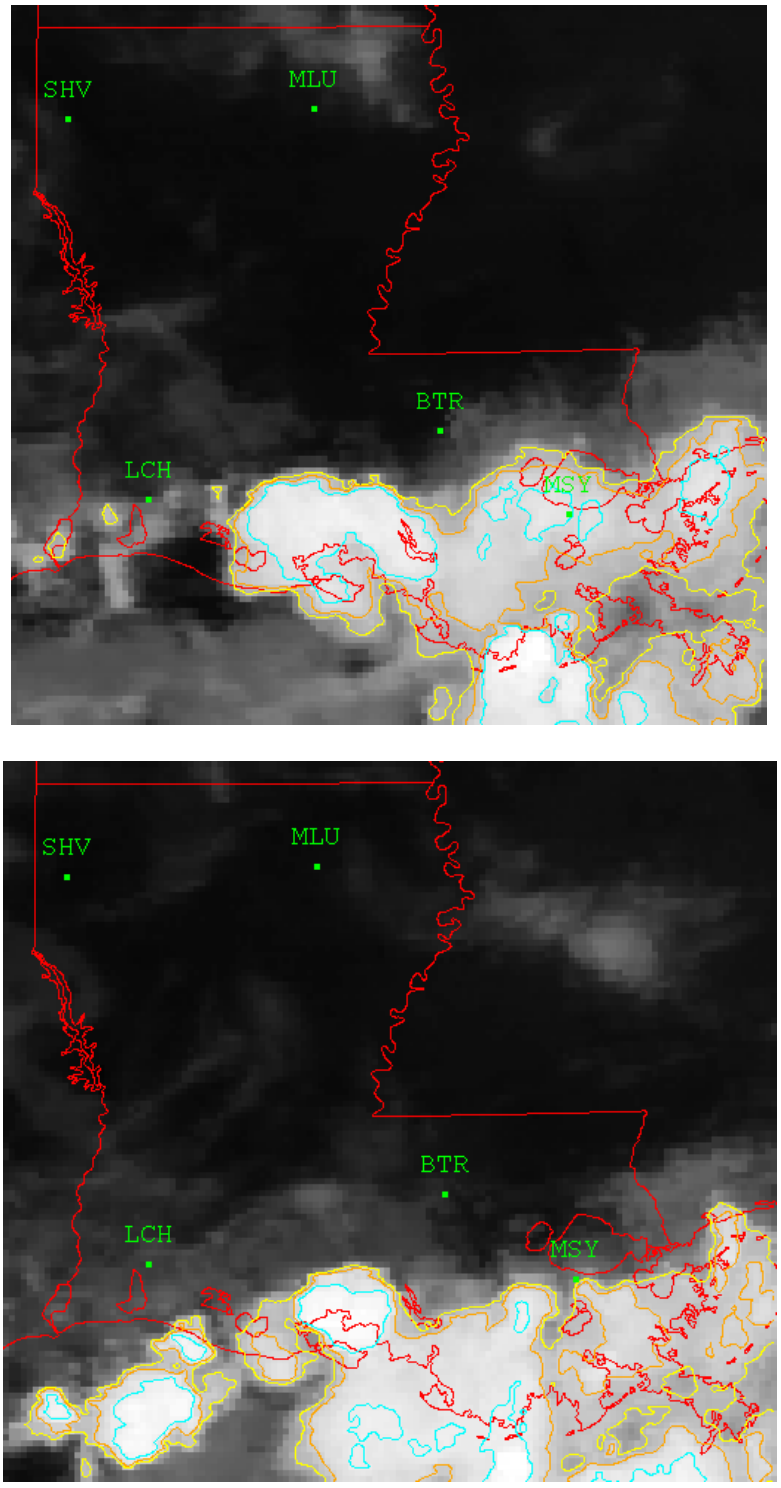

Figure 50
GOES IR image for 0815 UTC (0215 CST) (top) and 1015 UTC (0415 CST) (bottom) on August 13, 2008

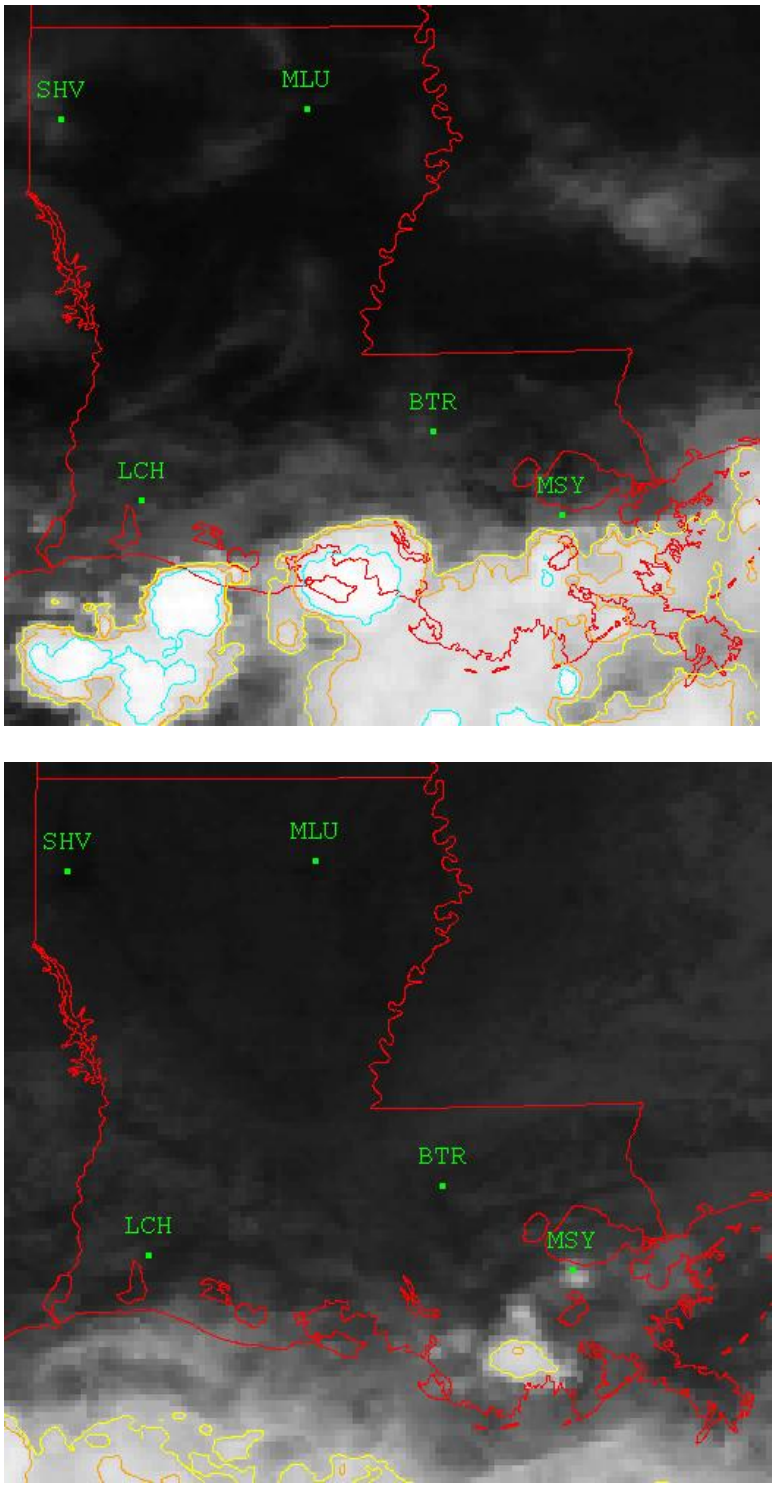

Figure 51
GOES IR image for 1045 UTC (0445 CST) (top) and 1815 UTC (1215 CST) (bottom) on August 13, 2008

September 2, Baton Rouge (BTR) (Table 13, Figures 52 – 54)

The remnants of Tropical Depression Gustav were centered near the Shreveport area; a feeder band extended through south-central Louisiana, Gulf Tropical Disturbance. Figure 54 shows a very cold cell moving west to east over the reporting station. CB and thunder were reported. Good agreement existed between measured rain and CTTs. The event's estimated total by equation (1) was very low, while the derived estimate [equation (2)] was within 0.7 in.

Table 13
Selected surface observations from BTR on September 2, 2008 CST
(coded as in Table 2)

Time	Sky Conditions	Visibility	Weather Type
6	FEW014 BKN019 OVC110	10	RA
48	BKN019 OVC024	1.5	RA BR
153	FEW060 SCT075 OVC100	10	RA
253	SCT015 BKN020 OVC050	10	RA
353	BKN017 BKN110	10	RA
453	FEW015 BKN023 OVC090	10	RA
553	FEW033 OVC085	10	RA
653	FEW018 BKN028 OVC060	3	RA BR
753	SCT013 BKN022 OVC050	1.5	RA BR
853	SCT013 BKN024 OVC038	3	RA BR
953	FEW007 BKN014 OVC021	2.5	RA BR
1053	FEW018 OVC060	5	RA BR
1153	FEW012 BKN030 OVC035	3	RA BR
1233	BKN010CB OVC030	1.25	TSRA BR
1329	SCT010 SCT020CB BKN030	2	-TSRA BR
1353	SCT010CB BKN020 BKN030	3	-TSRA BR
1453	SCT020 SCT040 BKN060	8	-RA
1542	FEW018 SCT040CB BKN120	6	-TSRA BR
1553	FEW018 SCT040CB BKN120	6	-TSRA BR
1606	FEW014 SCT040 BKN150	6	-RA BR

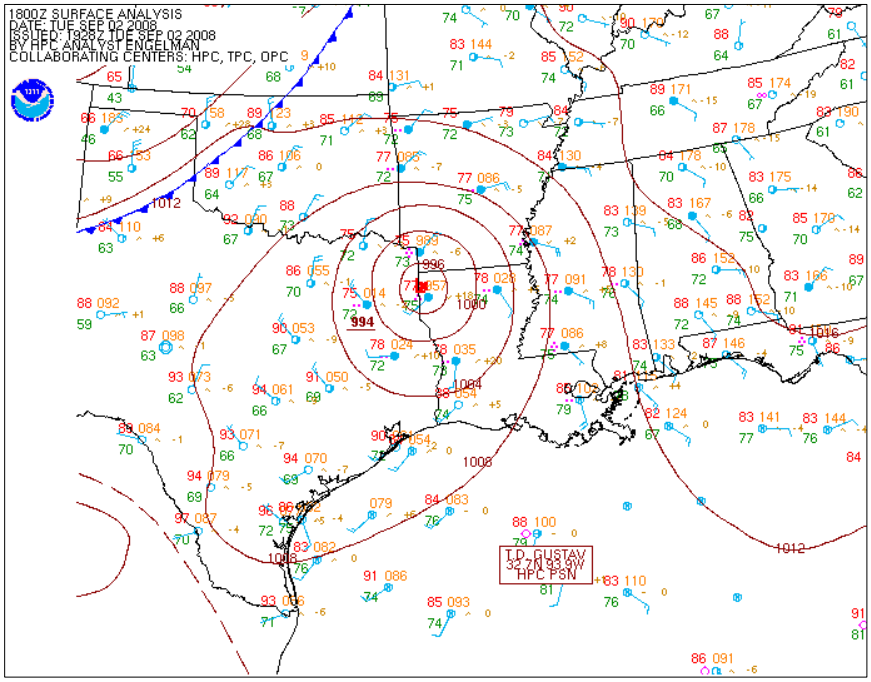

Figure 52
September 2, 2008 1800 UTC (1200 CST) surface weather map

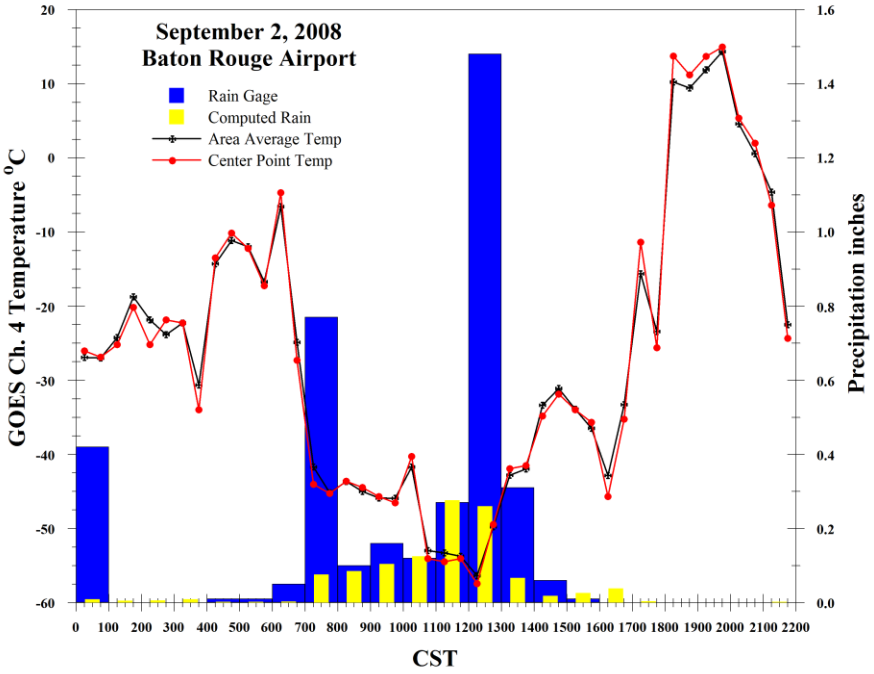

Figure 53
Time series of IR temperature along with measured and estimated rainfall on September 2, 2008 at BTR

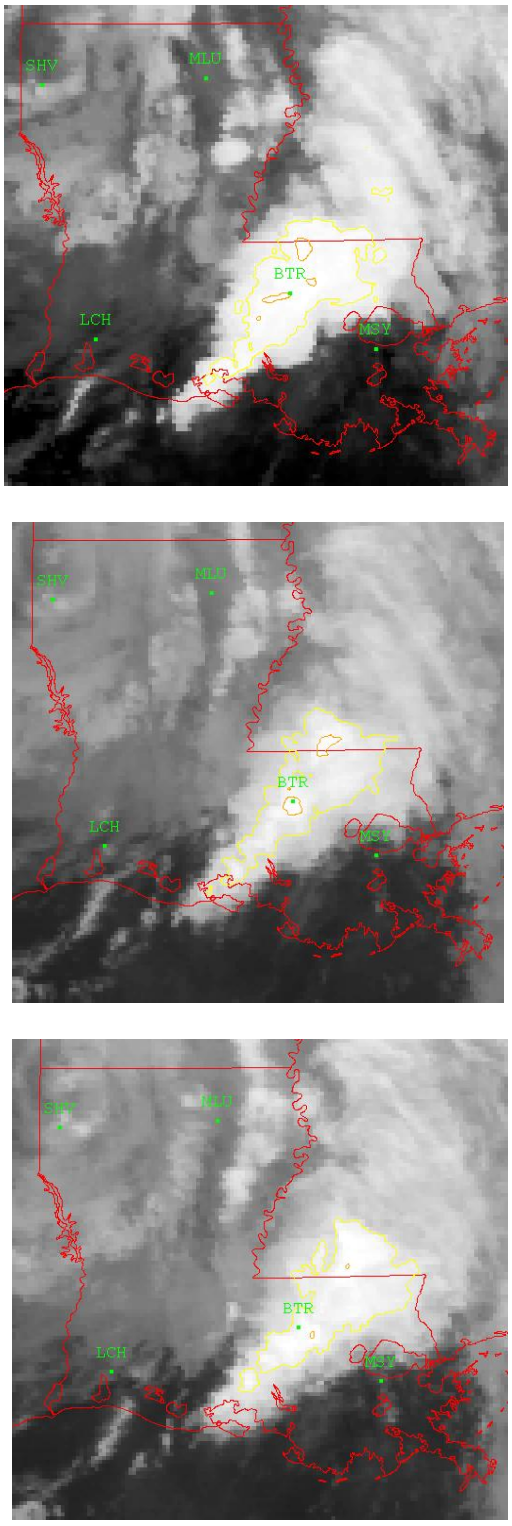

Figure 54
GOES IR image for 1745 UTC (1145 CST) (top), 1815 UTC (1215 CST) (middle), and 1845 UTC (1245 CST) (bottom) on September 2, 2008

September 20, New Orleans (MSY) (Table 14, Figures 55 – 57)

A weak Coastal Return pattern prevailed. Broken cloudiness appeared over southeastern Louisiana and offshore, but no significant MCSs. Nevertheless, TCU, CBs, and thunder were reported and heavy rain was recorded near noon CST. Poor agreement existed between estimated and measured rain.

Table 14
Selected surface observations from MSY on September 20, 2008 CST
(coded as in Table 2)

Time	Sky Conditions	Visibility	Weather Type
1053	BKN034TCU BKN150 BKN250	10	
1153	BKN030CB BKN150 OVC250	6	-RA BR
1228	BKN030CB BKN150 OVC250	4	RA BR
1253	SCT016 BKN033 OVC041	2.5	RA BR
1319	FEW011 SCT022 OVC039	1.75	RA BR
1338	BKN009 BKN021CB OVC035	1.25	+TSRA BR
1353	BKN009 BKN019CB OVC032	1.25	+TSRA BR
1429	SCT018 BKN025 OVC035	3	-RA BR
1453	FEW015 BKN022 OVC040	4	-RA BR
1553	FEW026 SCT095 OVC130	7	-RA
1653	FEW025 BKN055 OVC100	9	-RA
1711	SCT017TCU BKN036 OVC050	10	-RA
1753	SCT010 OVC032	10	-RA
1853	FEW012 OVC060	7	-RA
1953	BKN013 BKN080 OVC110	7	-RA
2053	FEW013 SCT070 OVC085	7	-RA
2153	FEW060 BKN075 OVC100	9	-RA
2253	FEW030 BKN060 OVC100	10	-RA

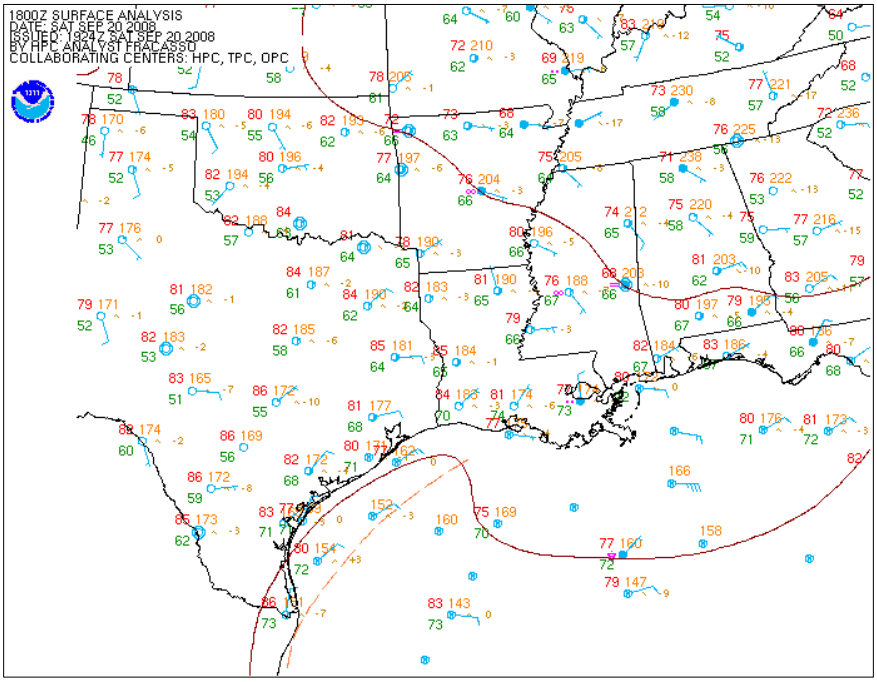

Figure 55
September 20, 2008 1800 UTC (1200 CST) surface weather map

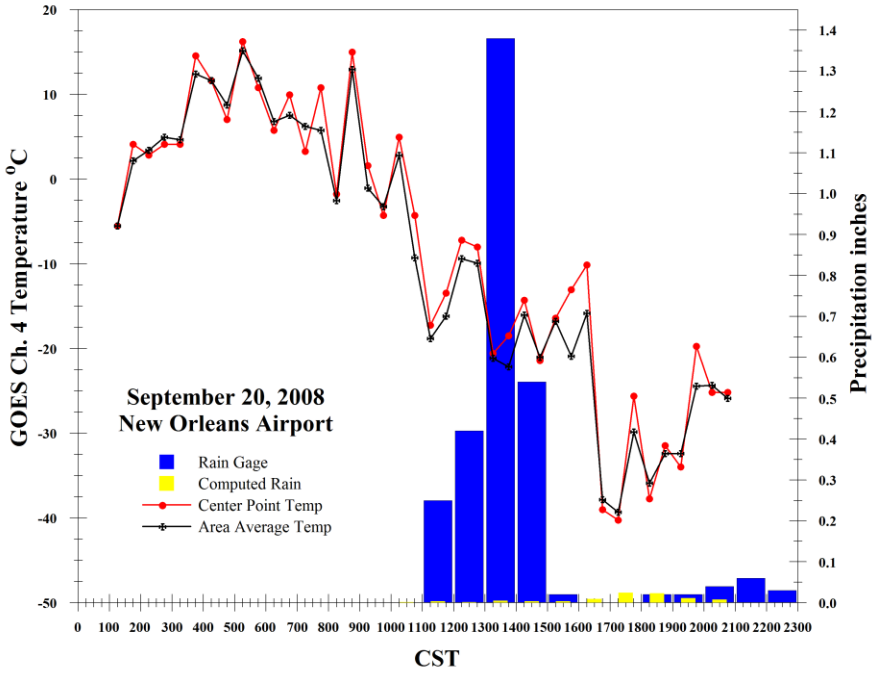

Figure 56
Time series of IR temperature along with measured and estimated rainfall on September 20, 2008 at MSY

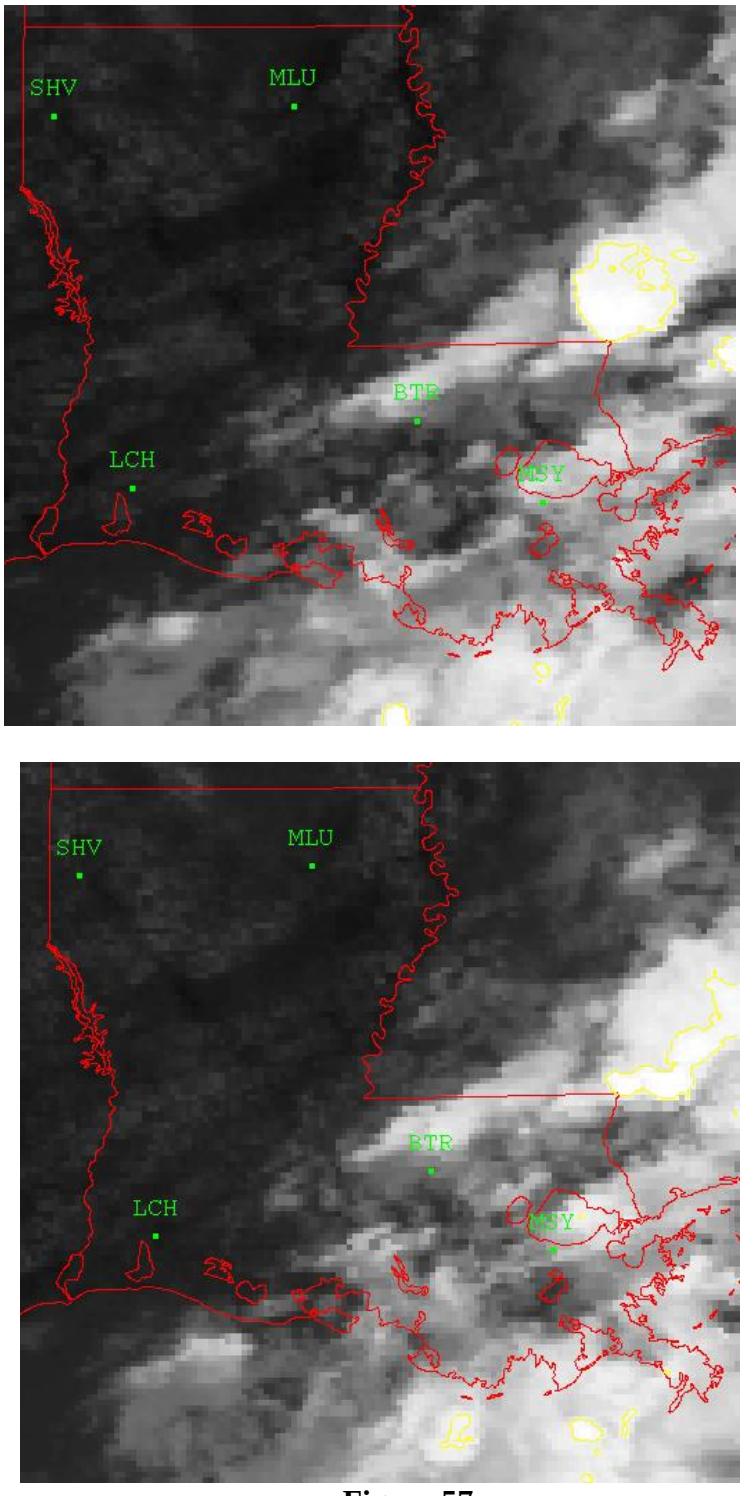

Figure 57
GOES IR image for 1915 UTC (1315 CST) (top) and 1945 UTC (1345 CST) (bottom) on September 20, 2008

October 7, New Orleans (MSY) (Table 15, Figures 58 – 60)

A slow moving cold front approaching western Louisiana became nearly stationary. Outflow boundaries occurred east of the front in the Coastal Return air mass. A cloud mass associated with these boundaries moved eastward and weakened. CBs and thunder were reported. Main recorded rain occurred prior to coldest CTTs. Estimated rain values were lower than measured.

Table 15
Selected surface observations from MSY on October 7, 2008 CST (coded as in Table 2)

Time	Sky Conditions	Visibility	Weather Type
340	SCT010 BKN028 OVC065	7	-RA
405	BKN018CB BKN060 BKN085	6	+RA BR
439	SCT009 BKN027CB BKN095	10	-RA
453	FEW009 BKN044 BKN090	10	-RA
1036	FEW012 BKN024CB OVC060	1	-RA BR
1120	SCT005 BKN017CB OVC033	3	-RA BR
1353	BKN020 BKN027CB BKN039	10	-RA
1623	FEW004 SCT013CB	10	-TSRA
1636	FEW004 SCT013CB	2	+TSRA BR
1653	SCT011CB BKN045	5	-RA BR

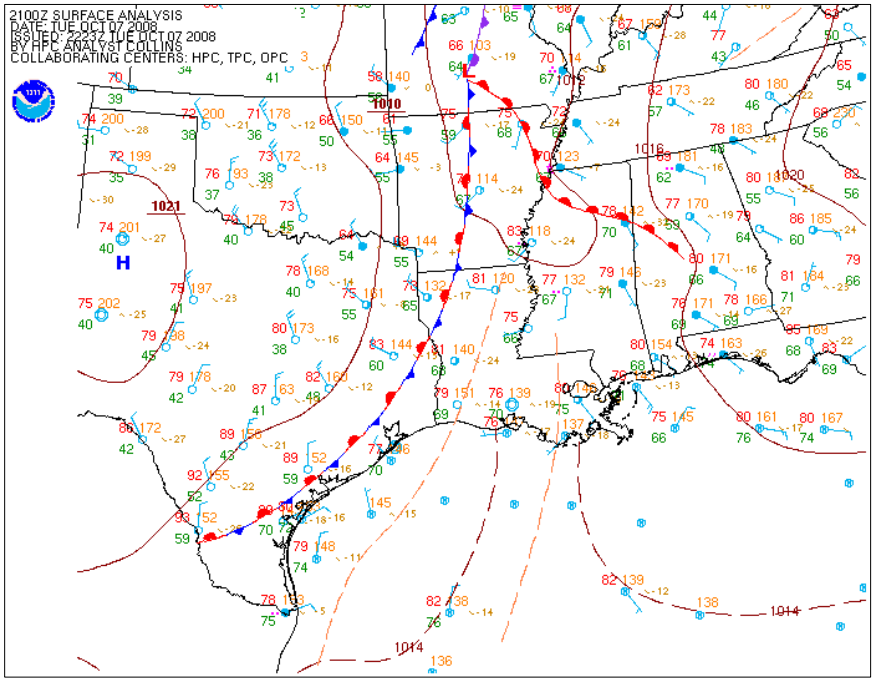

Figure 58
October 7, 2008 2100 UTC (1500 CST) surface weather map

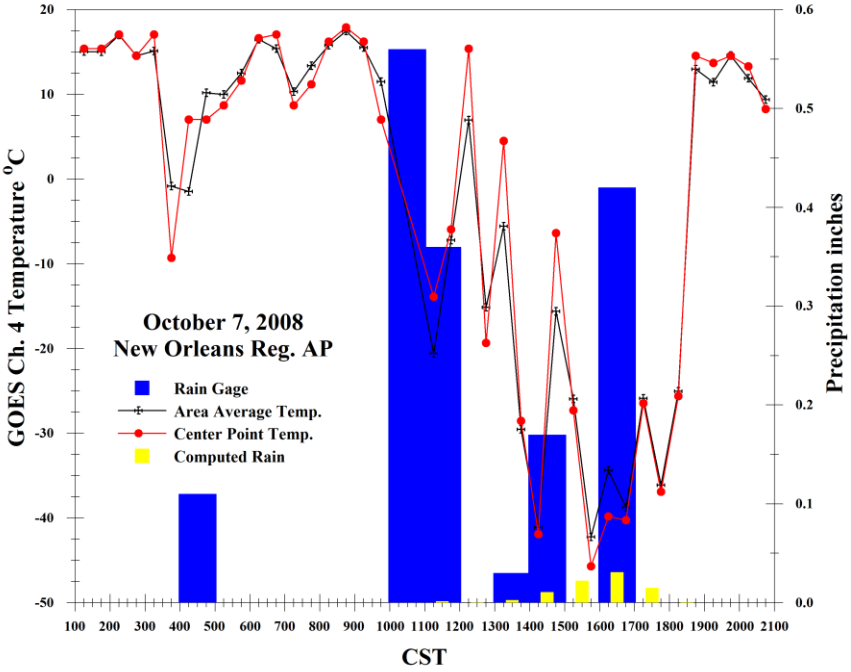

Figure 59
Time series of IR temperature along with measured and estimated rainfall on October 7, 2008 at MSY

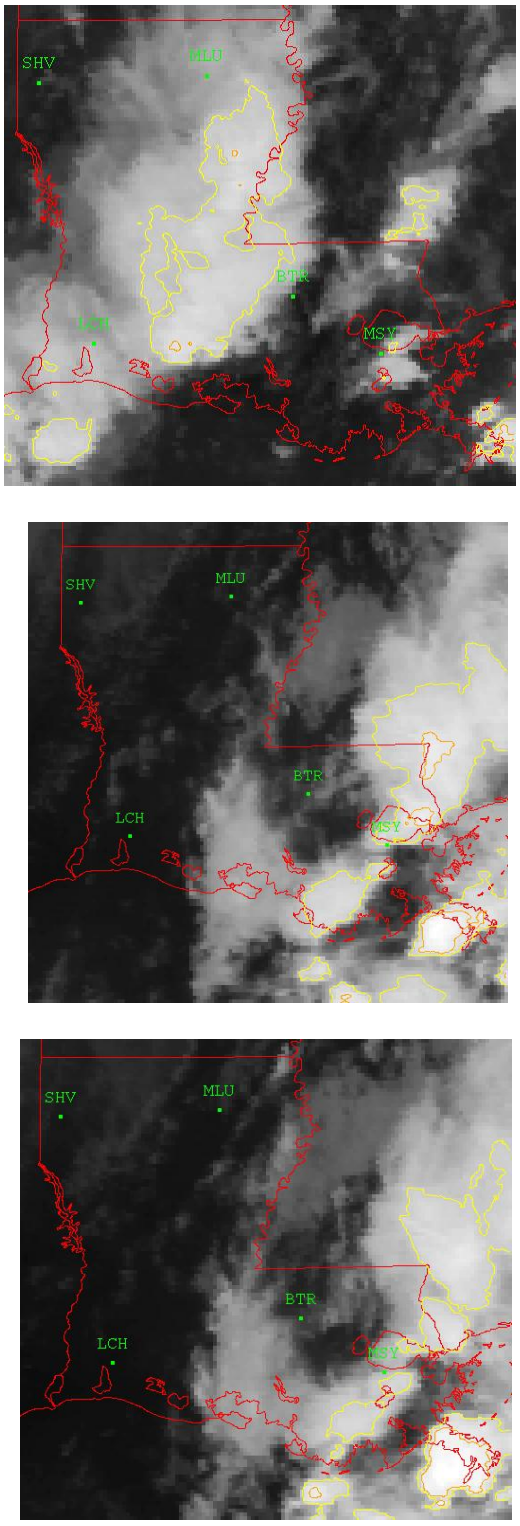

Figure 60
GOES IR image for 1715 UTC (1115 CST) (top), 2215 UTC (1615 CST) (middle), and 2245 CST (1645 CST) (bottom) on October 7, 2008

November 11, Shreveport (SHV) (Table 16, Figures 61 – 63)

Coastal Return became Frontal Gulf Return as a low and cold frontal system developed over central Texas. Thick cloud cover was moving into northwest Louisiana, but CTTs were not very cold. Reasonable agreement existed between measured rain and CTT time series, but estimated amounts were below measured.

Table 16
Selected surface observations from SHV on November 11, 2008 CST
(coded as in Table 2)

Time	Sky Conditions	Visibility	Weather Type
456	OVC012	4	-RA BR
537	FEW006 BKN023 OVC028	4	RA BR
556	FEW016 BKN037 OVC044	4	+RA BR
621	FEW003 BKN041 OVC050	2.5	+RA BR
656	FEW002 OVC038	2.5	+RA BR
756	FEW004 BKN039 OVC047	4	RA BR
856	OVC004	3	+RA BR
956	OVC004	3	-RA BR
1009	BKN006 BKN009 OVC020CB	1.5	+TSRA BR
1029	FEW006 BKN015 OVC020CB	1.5	+TSRA BR
1056	FEW006 BKN015 OVC020CB	1.5	+TSRA BR
1125	BKN004 OVC027CB	1.5	+TSRA BR
1156	FEW004 OVC025	2	RA BR
1256	OVC002	3	-RA BR
1356	BKN004 BKN085	4	-RA BR
1456	FEW006 BKN050 BKN100	4	-RA BR
2232	OVC003	10	-RA
2256	OVC003	8	-RA
2327	OVC005	2	+RA BR
2356	OVC017	2	+RA BR

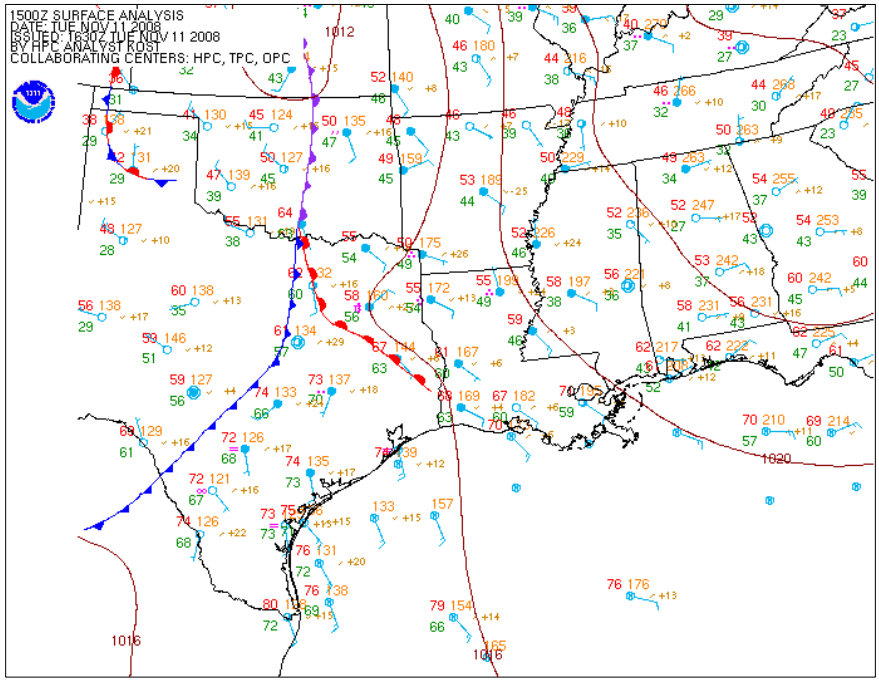

Figure 61
November 11, 2008 1500 UTC (0900 CST) surface weather map

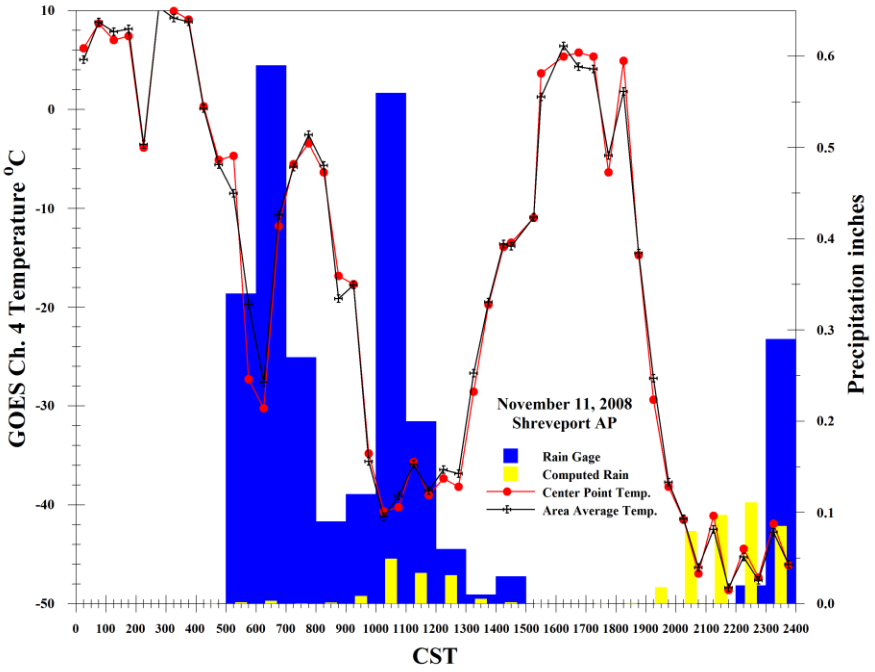

Figure 62
Time series of IR temperature along with measured and estimated rainfall on November 11, 2008 at SHV

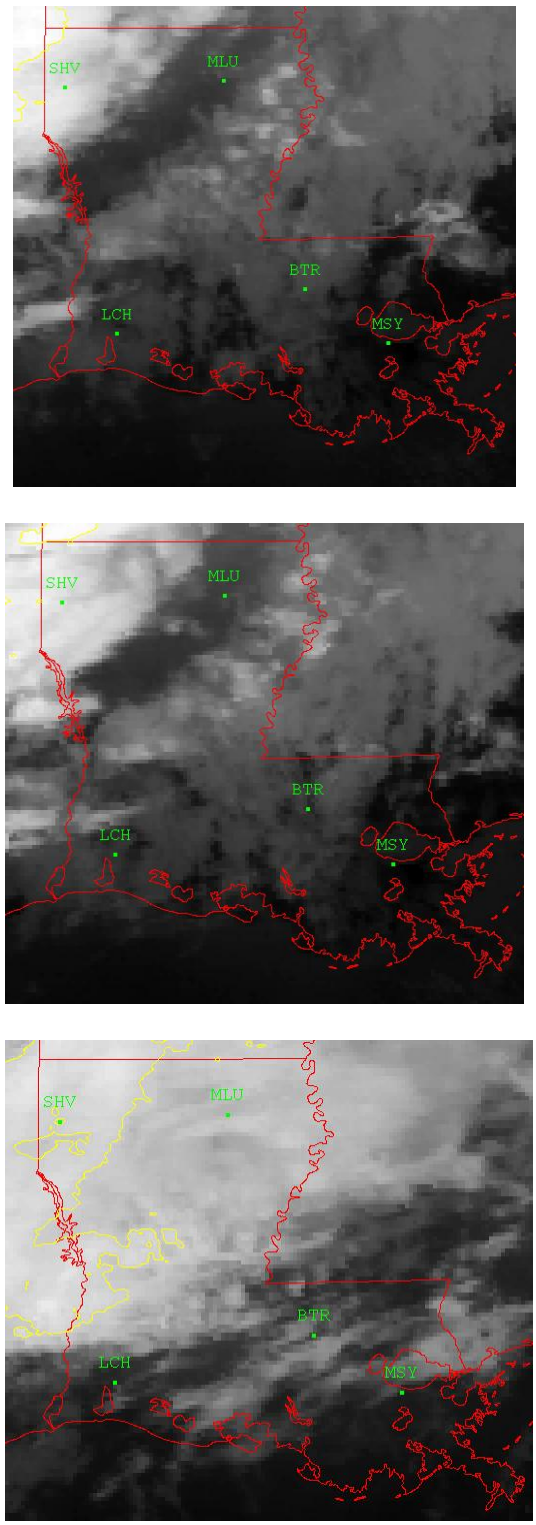

Figure 63
GOES IR image for 1615 UTC (1015 CST) (top) and 1645 UTC (1045 CST) (middle) on November 11, 2008. Bottom image is 0415 UTC November 12 (2215 CST November 11)

December 9, Monroe (MLU) (Table 17, Figures 64 – 66)

A low and warm front moved northeast away from the Arkansas-Louisiana-Mississippi border, while a cold front approached the northwest corner of the state. Outflow boundaries were noted in the Frontal Gulf Return air mass over Louisiana. An extremely cold cloud mass covered the northern half of the state ahead of the front, but there were no reports of CB or thunder. The very cold CTTs resulted in a large overestimation of rain as compared to the actual measured amount.

Table 17
Selected surface observations from MLU on December 9, 2008 CST
(coded as in Table 2)

Time	Sky Conditions	Visibility	Weather Type
253	OVC023	10	-RA
453	OVC019	10	-RA
745	OVC013	10	-RA
951	BKN013 BKN018 OVC095	7	-RA
953	BKN015 OVC095	7	-RA
1013	BKN013 OVC070	1.75	+RA BR
1035	SCT008 BKN016 OVC100	8	-RA
1153	OVC036	7	-RA
1235	FEW006 OVC018	1.75	+RA BR
1253	BKN016 OVC024	5	RA BR
1353	FEW011 BKN038 OVC080	10	-RA BR
1427	BKN008 BKN014 OVC031	1	+RA BR
1453	BKN010 BKN033 OVC042	1.75	+RA BR
1526	SCT008 BKN017 OVC035	2.5	+RA BR
1553	FEW012 BKN049 OVC060	3	+RA BR
1633	BKN009 BKN049 OVC060	2.5	+RA BR
1653	BKN009 BKN049 OVC060	4	+RA BR
1753	FEW027 BKN048 OVC065	6	+RA BR
1853	OVC055	10	-RA
2207	SCT005 BKN015 OVC038	10	-RA
2253	OVC007	7	-RA
2353	OVC007	3	BR

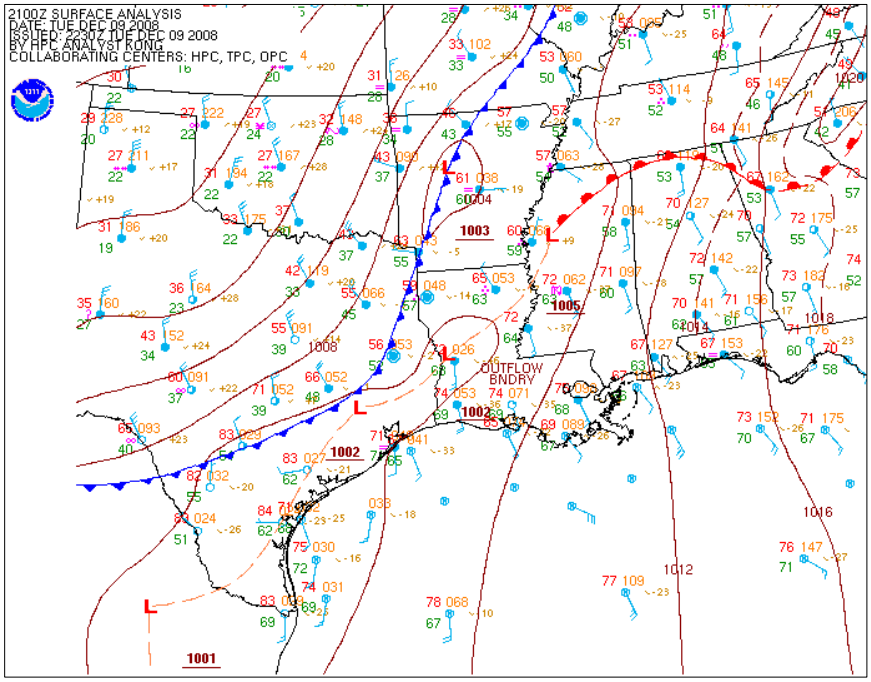

Figure 64
December 9, 2008 2100 UTC (1500 CST) surface weather map

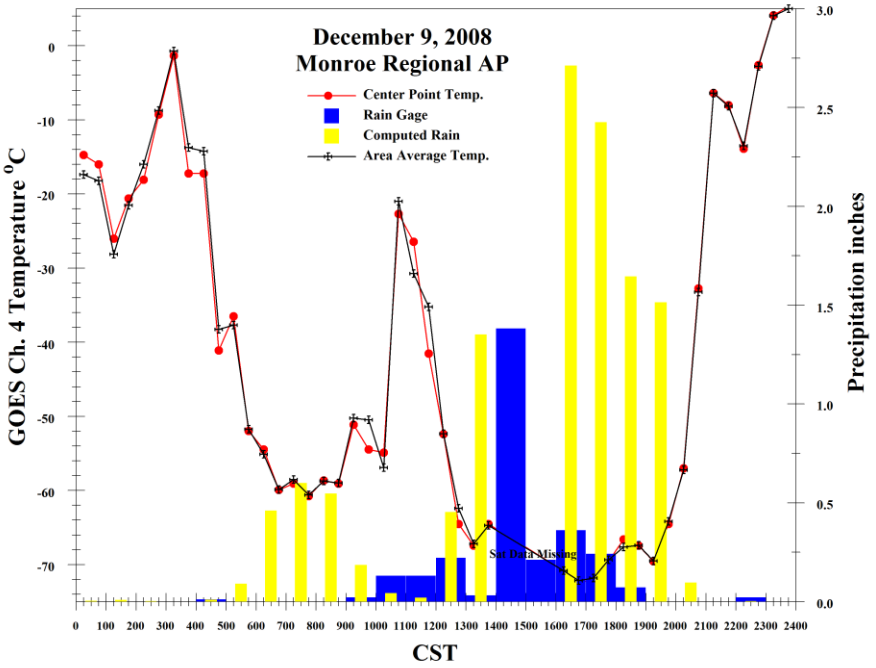

Figure 65
Time series of IR temperature along with measured and estimated rainfall on December 9, 2008 at MLU

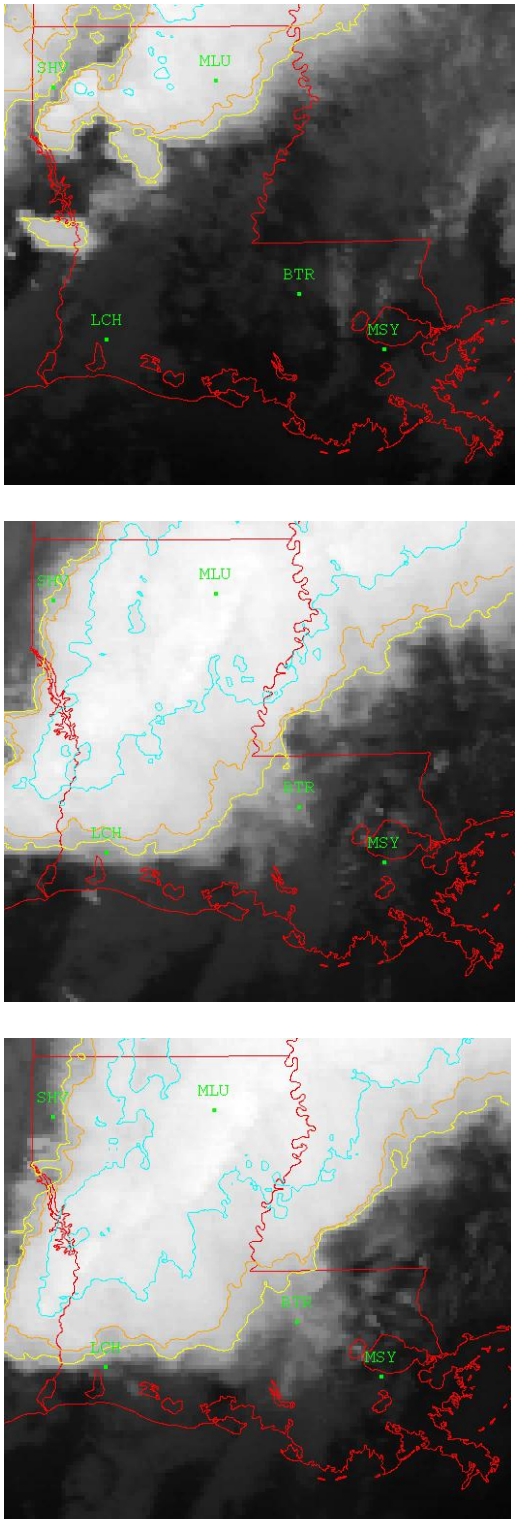

Figure 66
GOES IR image for 1315 UTC (0715 CST) (top), 2215 UTC (1615 CST) (middle), and 2245 UTC (1645 CST) (bottom) on December 9, 2008

The time series of IR temperatures for each case displays both a point value (station location) and an area average. The average is over a 3 x 3 pixel (12 x 12 km) space with the station as center. Agreement is typically within a few degrees; however, it should be noted that even within this small grid temperatures can vary significantly (> 30°C).

The hourly rain values for all case studies are summarized and compared in Figure 67. Although the scatter is large, neither formulation exhibits a bias. For this sample, the derived formula [equation (2)] performed only slightly better than Vincente's [equation (1)].

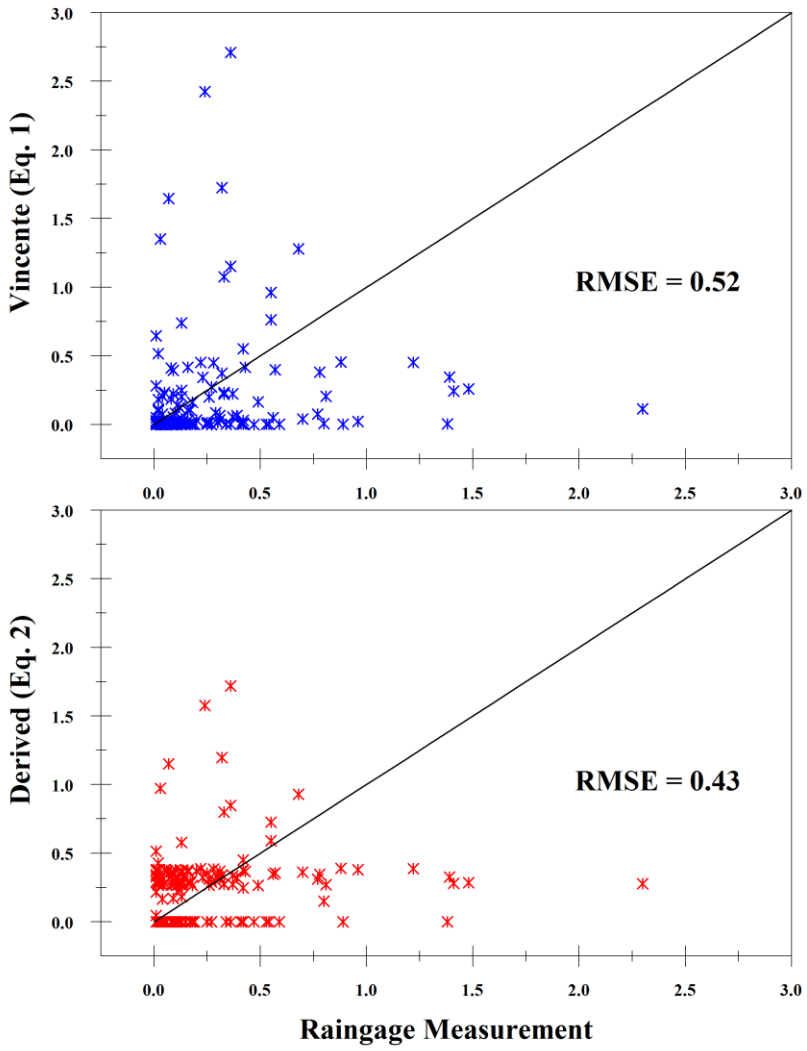

Figure 67
One-to-one distribution of forecast and observed hourly rain values from all case studies with root mean square error (RMSE)

Monthly Rain Estimates

GOES IR imagery recorded every 30 minutes was averaged hourly and processed into one-month time series. Equation (1) was applied to compute rain totals at individual stations. The results are provided in Figures 68 – 73. Most of the more significant rain events (of multiple hour duration) are identified by the IR imagery. On the other hand, poorer performance is demonstrated in total rain estimates, with computed rain totals being lower than those measured in five of the six months run. The exception (July 2008) is due to a MCS that developed over the observing station on July 23. This system produced very cold (< -60°C) CTTs for several hours, leading to an overestimated rain total.

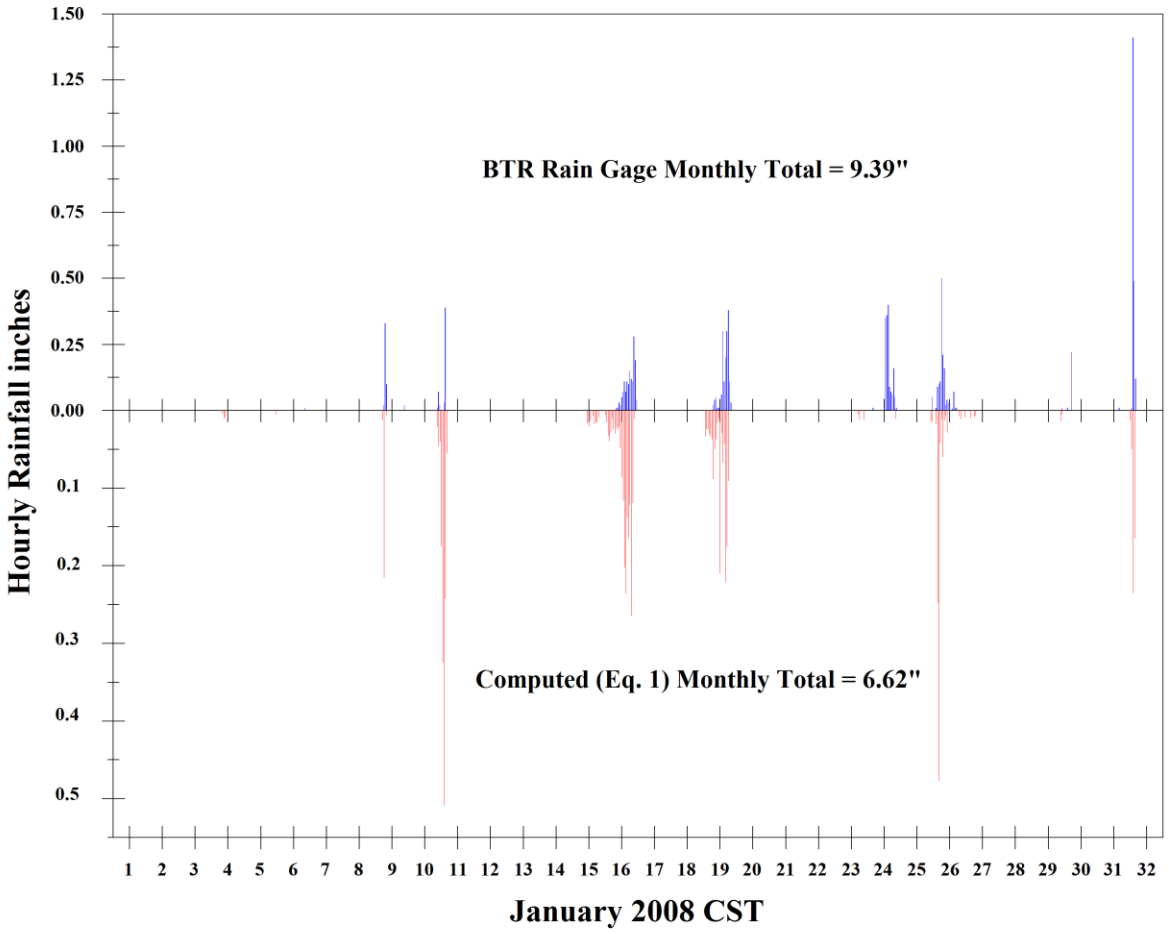

Figure 68
Time series of hourly measured (blue) and estimated [equation (1), red] rain totals for January 2008

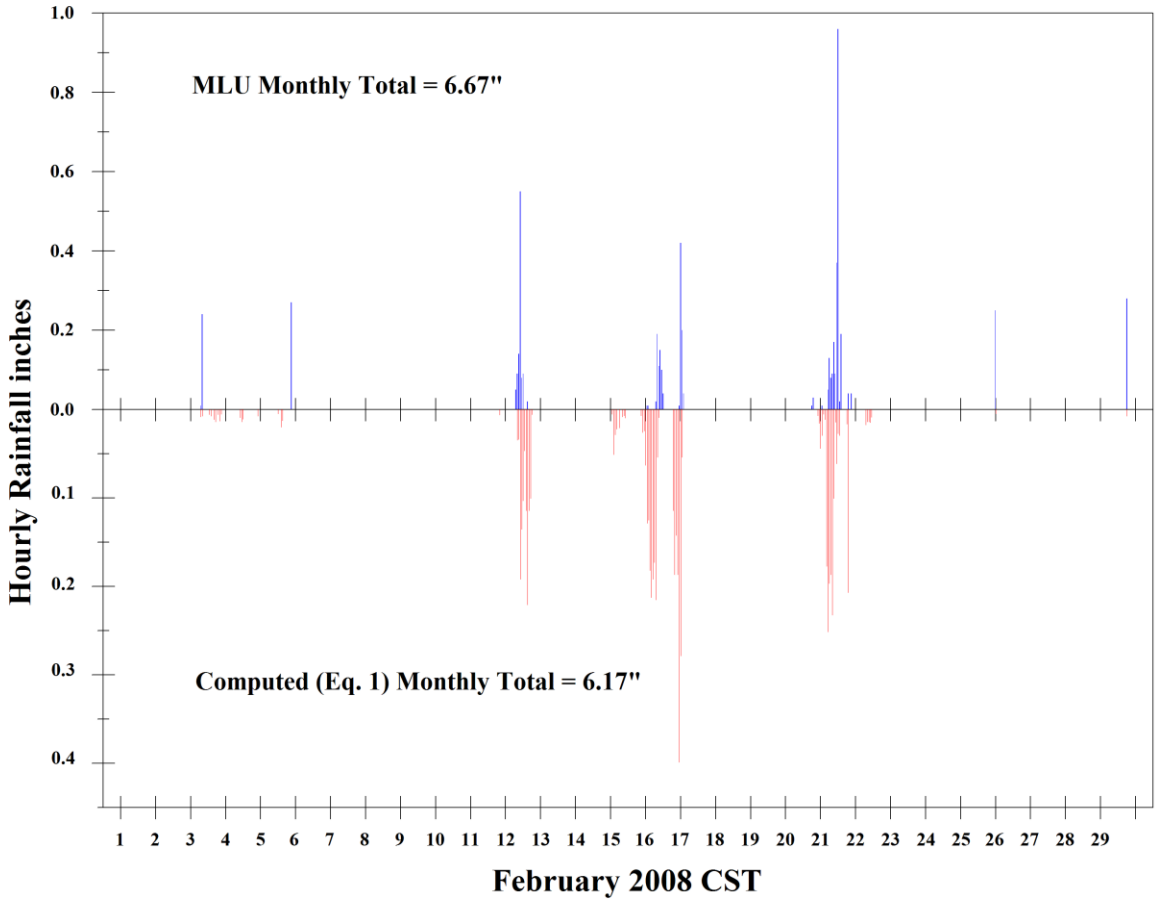

Figure 69
Time series of hourly measured (blue) and estimated [equation (1), red] rain totals for February 2008

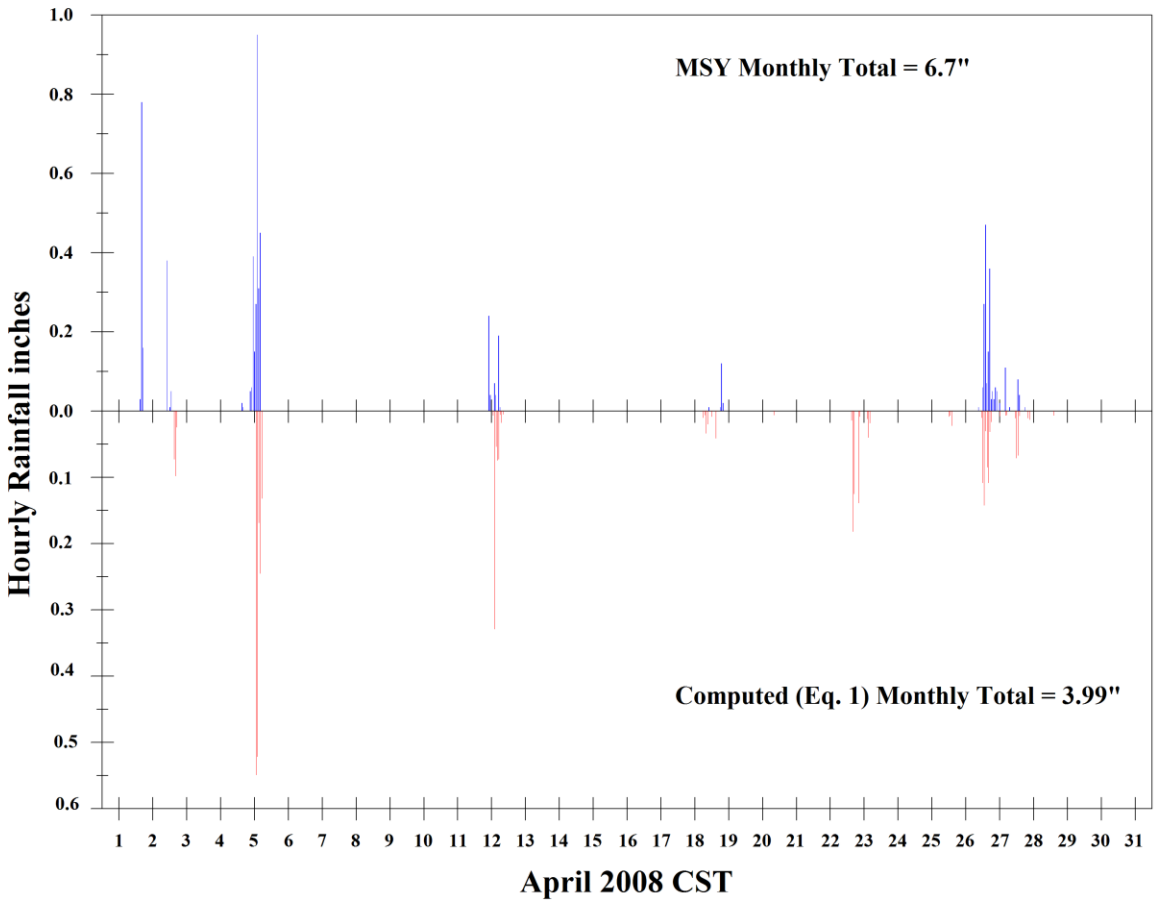

Figure 70
Time series of hourly measured (blue) and estimated [equation (1), red] rain totals for April 2008

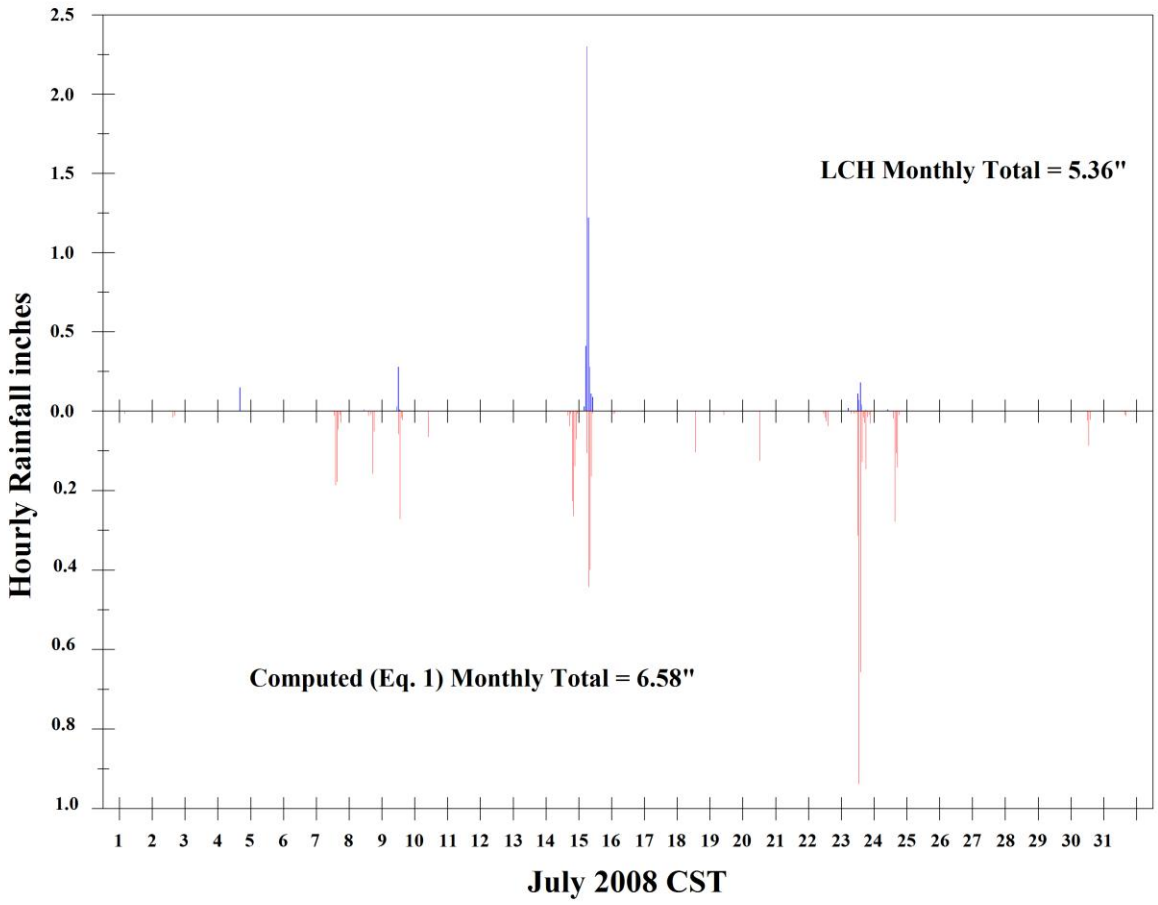

Figure 71
Time series of hourly measured (blue) and estimated [equation (1), red] rain totals for July 2008

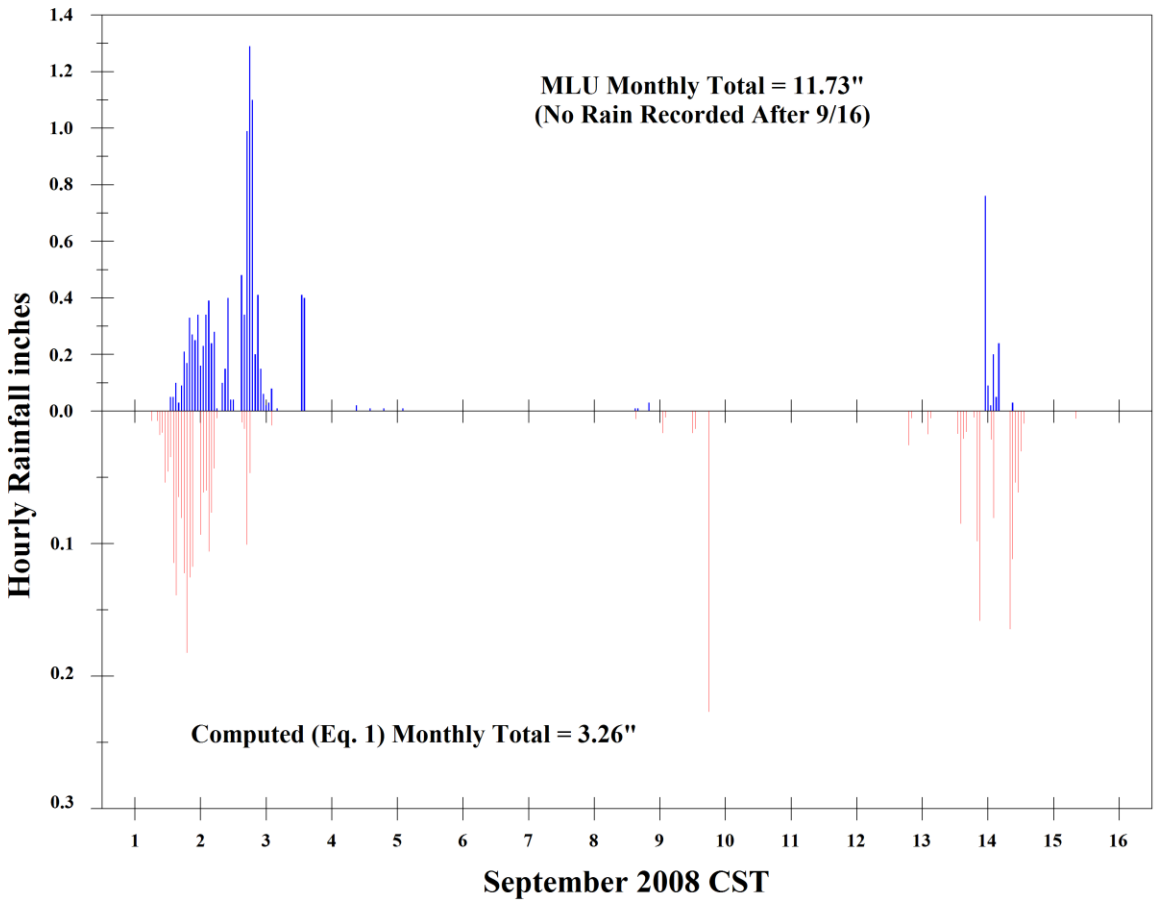

Figure 72
Time series of hourly measured (blue) and estimated [equation (1), red] rain totals for September 2008

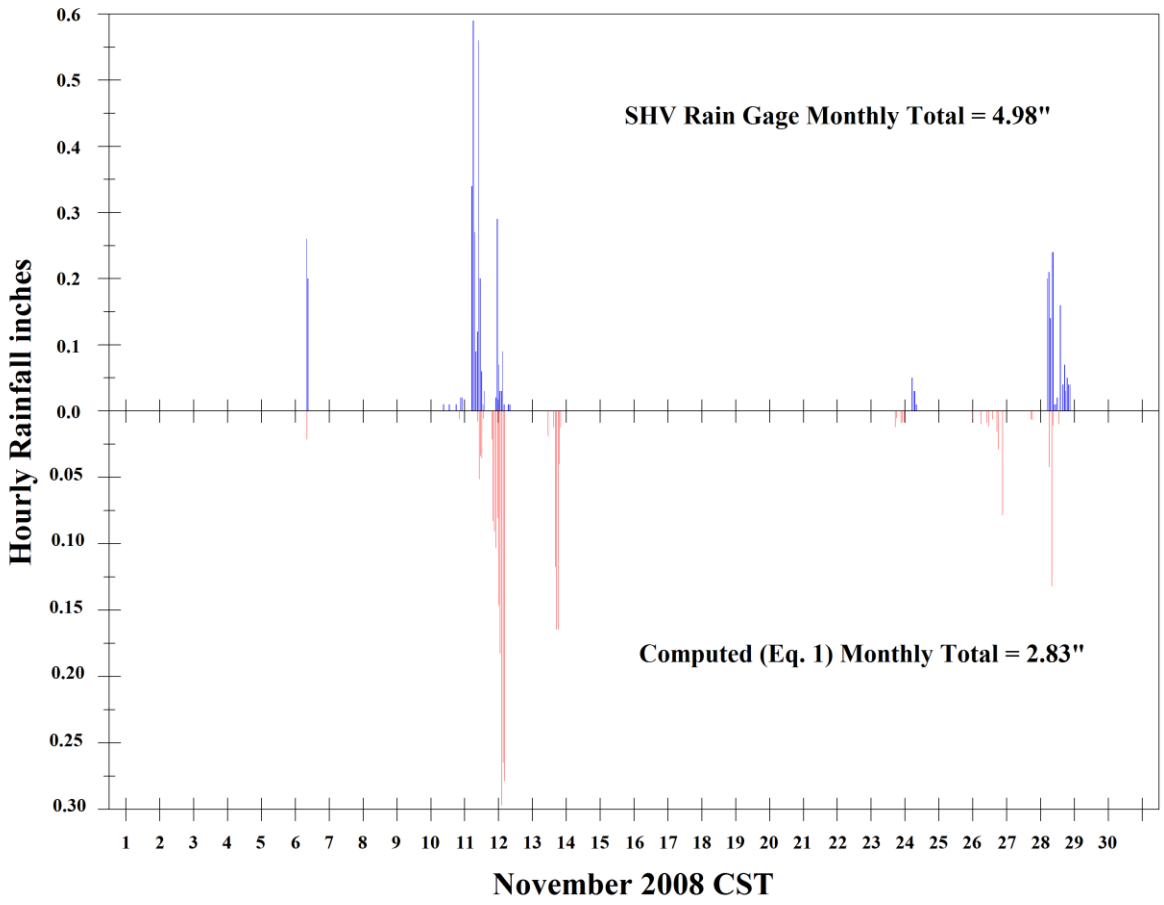

Figure 73
Time series of hourly measured (blue) and estimated [equation (1), red] rain totals for November 2008

CONCLUSIONS

GOES IR values observed over Louisiana during 2008 were analyzed with respect to surface measured rain totals, and a rain-rate relationship was derived. Within the IR temperature range of approximately -45°C to -61°C, both the derived formula [equation (2)] and an existing algorithm [equation (1)] developed by Vincente et al. fall between the first and third quartile of the measured rain data *[1]*. The IR imagery was shown to identify most rain events of multiple hour duration, but the computed estimates often varied significantly from the actual measured amount. There are many contributing factors to this error. As discussed, cirrus outflow from a convective system can mask the area of a precipitating cloud beneath. Location errors can occur in regions of wind shear as clouds move in one direction and the rain they produce in another *[15]*. Heavy rain may only fall from a small portion of an MCS *[17]*. With thin or smaller clouds that do not fill the field of view, IR from lower levels or surface can reach the sensor, making the clouds appear warmer than they actually are *[14]*. Many computational techniques exist that endeavor to improve the estimated rain rate by adjusting the satellite IR data for atmospheric (sub-cloud) conditions, cloud growth characteristics, and cloud particle size. This study's results suggest that such corrective actions are necessary for a more accurate estimation. Although the technology continues to be developed and tested, satellite rain-rate estimation is an accepted method currently being applied operationally by many agencies. In those regions without an official rain gage station or adequate radar coverage, even direct use of the algorithm as performed here can yield useful estimates, at least as a first approximation. Averaging over a larger spatial domain to capture more of the cloud characteristics may help reduce the errors associated with a single point measurement.

RECOMMENDATIONS

Surface rain accumulations can be estimated from satellite IR information. Direct application of the Vincente or derived formulas [equations (1) and (2)] provide an initial estimation, which is essential for locations without a rain gage or radar coverage. Larger spatial and temporal averages should be tested during specific events and compared to measured and/or modeled data. Since GOES is the only platform currently providing near continuous data over the contiguous U.S., it remains the sensor of choice. As more data from other satellites (such as the Tropical Rainfall Measuring Mission or TRMM) become routinely available, further comparative analyses should be performed.

ACRONYMS, ABBREVIATIONS, AND SYMBOLS

BKN	Broken cloud cover
BR	Mist
BTR	Baton Rouge Regional Airport
CB	Cumulonimbus cloud
CH	Continental High synoptic type
CR	Coastal Return synoptic type
CST	Central Standard Time
CTT	Cloud Top Temperature
FEW	Few cloud cover
FGR	Frontal Gulf Return synoptic type
FOR	Front Overrunning synoptic type
GH	Gulf High synoptic type
GOES	Geostationary Operational Environmental Satellite
GR	Gulf Return synoptic type
GTD	Gulf Tropical Disturbance synoptic type
IR	Infrared
LCH	Lake Charles Regional Airport
LOSC	Louisiana Office of State Climatology
LSU	Louisiana State University
MCS	Mesoscale Convective System
MLU	Monroe Regional Airport
MSY	New Orleans International Airport (Moisant)
OVC	Overcast cloud cover
PH	Pacific High synoptic type
R	Rain rate
RA	Rain
RMSE	Root Mean Square Error
SCT	Scattered cloud cover
SHV	Shreveport Regional Airport
SRCC	Southern Regional Climate Center
T	Temperature
TCU	Towering cumulus cloud
TIRE	Transportation Innovation For Research Exploration
TRMM	Tropical Rainfall Measuring Mission
TS	Thunderstorm

TSRA	Thunderstorm/Rain
UTC	Coordinated Universal Time
VC	Vicinity
VV	Vertical Visibility
WV	Water Vapor
XVU	Software package for analysis and visualization of digital satellite data

REFERENCES

1. Vincente, G.A., Scofield, R.A., and Menzel, W.P. "The Operational GOES Infrared Rainfall Estimation Technique." Bull. Amer. Meteor. Soc., Vol. 79, No. 9, 1998, pp. 1883-1898.

2. Ba, M. B., and Gruber, A. "GOES Multispectral Rainfall Algorithm." J. Applied Meteor., Vol. 40, No. 8, August 2001, pp. 1500-1504.

3. Kuligowski, R.J. "A Self-Calibrating Real-Time GOES Rainfall Algorithm for Short-Term Rainfall Estimates." J. Hydrometeor., Vol. 3, No. 4, April 2002, pp. 112-130.

4. National Oceanographic and Atmospheric Administration (NOAA). "Hourly Precipitation Data Louisiana." Vol. 58, Nos. 1-12, 2008.

5. American Meteorological Society (AMS): Glossary of Meteorology, 2nd Edition. Todd S. Glickman, Editor. American Meteorological Society, Boston, 2000.

6. Louisiana Office of State Climatology (LOSC). http://www.losc.lsu.edu/. Accessed March 2010.

7. Southern Region Climate Center (SRCC). http://www.srcc.lsu.edu/. Accessed March 2010.

8. Burroughs, W.J., Crowder, B., Robertson, T., Vallier-Talbot, E., and Whitaker, R. A Guide to Weather. Fog City Press, San Francisco, 1996.

9. Muller, R.A. "A Synoptic Climatology for Environmental Baseline Analysis: New Orleans." J. Applied Meteor., Vol. 16, 1977, pp. 20-33.

10. Muller, R.A. and Willis, J.E. "New Orleans Weather 1961-1980: A Climatology by Means of Synoptic Weather Types." Misc. Pub. 83-1, School of Geoscience, Louisiana State University, Baton Rouge, LA, 1983.

11. Hsu, S. A. "Characteristics of Marine Meteorology and Climatology in the Gulf of Mexico." In The Gulf of Mexico Large Marine Ecosystem, H. Kumpf, K. Steidinger,

and K. Sherman (Editors). Blackwell Science, Malden, MA, pp. 113-131, 1999.

12. Muller, R.A., and Wax, C.L. "A Comparative Synoptic Climatic Baseline for Coastal Louisiana." Geosci. Man., Vol. 18, 1977, pp. 121-129.

13. Faires, G. E., Keim, B.D., and Muller, R.A. "Rainfall Frequency/Magnitude Atlas for the South/Central United States." SRCC Technical Report 97-1, Geoscience Publications, Department of Geography and Anthropology, Louisiana State University, Baton Rouge, LA, 1997.

14. Bader, M.J., Forbes, G. S., Grant, J.R., Lilley, R.B.E., and Waters, A.J. Images in Weather Forecasting. Press Syndicate of Cambridge University, 1995.

15. Vasiloff, S.V., Seo, D.J., Howard, K.W., Zhang, J., Kitzmiller, D.H., Mullusky, M.G., Krajewski, W.F., Brandes, E.A., Rubin, R.M., Berkowitz, D.S., Brooks, H.E., McGinley, J.A., Kuligowski, R.J., and Brown, B.G. "Improving QPE and Very Short Term QPF." Bull. Amer. Meteor. Soc., Vol. 88, No. 12, 2007, pp. 1899-1911.

16. Vasquez, T. Weather Map Handbook. Weather Graphics Technologies, Austin, TX, 2003.

17. Woodley, W.L., and Sancho, B. "A First Step Towards Rainfall Estimation From Satellite Cloud Photographs." Weather, July, 1971, pp. 279-289.